UNIVERSITAT POLITÈCNICA DE VALÈNCIA

CENTRO DE TECNOLOGÍAS FÍSICAS

DISEÑO, CARACTERIZACIÓN Y APLICACIONES CLÍNICAS DE LENTES DE CONTACTO MULTIFOCALES APERIÓDICAS

TESIS DOCTORAL

PRESENTADA POR: D. MANUEL RODRÍGUEZ VALLEJO

DIRIGIDA POR: DR. JUAN A. MONSORIU SERRA

DR. WALTER D. FURLAN

Valencia, Noviembre de 2016

A mis padres,

por darme la vida y la libertad para vivirla.

A Beatriz,

porque todo mejoró cuando ella apareció.

Agradecimientos

Las primeras personas a las que quiero agradecer su apoyo durante todos estos años de trabajo son a mis directores de tesis, los Doctores Walter Furlan y Juan A. Monsoriu, por haberme dado la oportunidad de dar un giro a mi carrera profesional dedicándome a lo que más me apasiona. En segundo lugar, a los compañeros con quienes he compartido años de laboratorio. Especialmente a Arnau Calatayud y Vicente Ferrando, por cambiar las letras por números para que todo fuese más fácilmente comprensible, a Clara Llorens por hacerme ver las cosas cuando tenía los ojos cerrados y a Laura Remón por inundar de alegría cada día de trabajo con su forma de ser y ver la vida.

Me gustaría también acordarme de todos aquellos que han participado en mi formación hasta llegar a esta meta, pues colocaron los cimientos que me han posicionado cada día un escalón más alto. A todos los que me pusieron las cosas difíciles, en especial a quienes no me ayudaron a resolver los problemas, pues me otorgaron la habilidad de la autonomía, con la que se puede conseguir todo lo que te propongas en la vida. Al arbitraje, mi mayor beca, porque aunque suene raro creo que ha sido una de las experiencias más positivas en mi educación regalándome recuerdos inolvidables con gente maravillosa, a ellos también va dedicado este trabajo.

Por último y más importante, a mi familia, mis padres, hermanos y abuelos. Gracias por haber respetado mis opiniones a lo largo de toda una vida, aunque soy consciente de ser atípicas y en ocasiones difíciles de entender. Nunca les he dicho lo mucho que les quiero y que les debo por llegar a ser quien soy, necesitaría muchos siglos para ello, que mejor oportunidad que dejarlo escrito para que nunca se olvide.

Beatriz y Liam, gracias por haber hecho que todo fuese más fácil permitiendo ocupar un tiempo que era para vosotros en el desarrollo de este proyecto personal. Sois la pieza más importante para que mi cerebro siga creando, esta es vuestra tesis.

"Más allá de lo que el ojo ve, el cerebro crea"

Índice general

Listado de Abreviaturas

Add	Addition
AL	Axial Length
APPs	Applications
ATS	Amblyopia Treatment Study
AV	Agudeza Visual
AVAC	Agudeza Visual de Alto Contraste
AVBC	Agudeza Visual de Bajo Contraste
BVP	Back Vertex Power
C	Correction Zones or Contrast
CD	Curva de Desenfoque
CPD	Cycles per Degree
CR	Corneal Radius
CS	Contrast Sensitivity
CSF	Contrast Sensitivity Function
D	Distance Zones
DF	Dual Focus
DOF	Depth of Focus
ERN	Escala de Reconocimiento Numérico
ERP	Error Relativo Periférico
EST	Estereopsis
ETDRS	Early Treatment Diabetic Retinopathy Study
FACT	Functional Acuity Contrast Test
FCL	Fractal Contact Lens
FSC	Función de Sensibilidad al Contraste
FSCS	Fast Screening Contrast Sensitivity
FSVA	Fast Screening Visual Acuity
HD	Howard Dolman
JCR	Journal Citation Rank
LCs	Lentes de Contacto
LCMs	Lentes de Contacto Multifocales

LIOMs	Lentes Intraoculares Multifocales
logC	Logarithm of the Contrast
lp	Line Pairs
LuT	Look up Table
MCL	Multifocal Contact Lens
MD	Mean Difference
N	Near Zones
OTF	Optical Transfer Function
LuT	Look-up Table
MCL	Multifocal Contact Lens
MD	Mean Difference
N	Near Zones
OTF	Optical Transfer Function
PD	Pupil diameter
PPI	Points per Inch
PRE	Peripheral Refractive Error
Q	Asphericity
RPRE	Relative Peripheral Refractive Error
RVN	Rango de Visión Nítida
SC	Sensibilidad al Contraste
SCI	Science Citation Index
SD	Standard Deviation
SF	Spatial Frequency
SPD	Screen's pixels density
ST	Estereopsis measured with iPad Stereotest
T	Treatment Zones
TF-MTF	Trough-Focus Modulation Transfer Function
TFR	Through Focus Response
TFR-C	Through Focus Response for Contrast
TFR-VA	Through Focus Response for Visual Acuity
TNO	Test for stereopsis at near
TP	Treatment Power
VA	Visual Acuity

Resúmenes en español, valenciano e inglés

Resumen

La miopía es el error refractivo de mayor prevalencia a partir de los 20 años de edad e impide la visión nítida a distancia lejana. La presbicia, por otra parte, es una anomalía de la función visual que aparece a partir de los 45 años, que impide la visión nítida a distancia próxima, y que afecta a toda la población por ser un defecto natural asociado a la edad. Las lentes de contacto multifocales representan una solución para facilitar que los pacientes présbitas puedan ver de forma simultánea a múltiples distancias. Además, podrían ser utilizadas, según recientes teorías sobre las señales ópticas que modulan el crecimiento ocular, para ralentizar la progresión de la miopía en niños en etapas de desarrollo.

En esta Tesis se proponen dos nuevos diseños de lentes de contacto aperiódicas para ralentizar el desarrollo miópico o compensar la presbicia. El primero de ellos posee como principal ventaja inducir un mayor error relativo periférico con una menor afectación de la visión central en comparativa con la primera lente comercializada con el fin de ralentizar la progresión de la miopía. Este diseño ha sido fabricado, caracterizado y medida su eficiencia real en una muestra de sujetos miopes demostrando un buen acuerdo con su base teórica.

El segundo de los diseños, enfocado a la compensación de la presbicia, también ha sido fabricado, caracterizado y adaptado en una serie de sujetos présbitas con el fin de evaluar el rendimiento visual alcanzado con los prototipos. No obstante, para cumplir esta tarea era necesario disponer de una amplia batería de test visuales para medir el rendimiento visual a múltiples distancias. Es por ello que otro de los objetivos dentro de esta Tesis fue analizar la capacidad de los iPad para ser utilizados como sistemas de reproducción de aplicaciones para la medida del rendimiento visual. Se han desarrollado y validado nuevas aplicaciones de medida de agudeza visual, sensibilidad al contraste y estereopsis. Con las nuevas aplicaciones disponibles, se midió el rendimiento visual en los sujetos présbitas adaptados con la lente aperiódica, mejorando significativamente el rendimiento visual a distancia próxima y mostrando como ventaja principal la baja pupilo-dependencia y buena tolerancia al descentramiento pese a tratarse de un diseño zonal.

Resum

La miopia és l'error refractiu amb major prevalença a partir dels 20 anys d'edat i impedeix la visió nítida a distància llunyana. La presbícia, d'altra banda, és una anomalia de la funció visual que apareix a partir dels 45 anys, que impedeix la visió nítida a distancia pròxima, i que afecta a tota la població per ser un defecte natural associat a l'edat. Les lents de contacte multifocals representen una solució per facilitar que els pacients prèsbites puguen veure de forma simultània a múltiples distancies. A més, podrien ser utilitzades, segons recents teories sobre les senyals òptiques que modulen el creixement ocular, per a ralentitzar la progressió de la miopia en xiquets en etapes de desenvolupament.

En aquesta Tesis es proposen dos nous dissenys de lents de contacte aperiòdiques per a ralentitzar el desenvolupament miòpic o compensar la presbícia. El primer d'ells té com a principal avantatje induir un major error relatiu perifèric amb una menor afectació de la visió central en comparació amb la primera lent comercialitzada amb la finalitat de ralentitzar la progressió de la miopia. Aquest disseny ha sigut fabricat, caracteritzat y s'ha mesurat la seua eficiència real en una mostra de subjectes miops demostrant un bon acord amb la seua base teòrica.

El segon dels dissenys enfocat a la compensació de la presbícia, també ha sigut fabricat, caracteritzat y adaptat en una sèrie de subjectes prèsbites amb la finalitat d'avaluar el rendiment visual obtingut amb els prototips. No obstant, per complir aquesta feina era necessari disposar d'una àmplia bateria de test visuals per mesurar el rendiment visual a múltiples distàncies. És per açò que un altre dels objectius dins d'aquesta Tesis fou analitzar la capacitat dels iPad per a ser utilitzats com sistemes de reproducció d'aplicacions per a la mesura del rendiment visual. Han sigut dissenyades y validades noves aplicacions de mesura de l'agudesa visual, sensibilitat al contrast y estereòpsis. Amb les noves aplicacions disponibles, es va medir el rendiment visual en els subjectes prèsbites adaptats amb la lent aperiòdica, millorant significativament el rendiment visual a distancia pròxima i mostrant com avantatje principal la baixa pupilo-dependència i bona tolerància al descentrament a pesar de tractar-se d'un disseny zonal.

Abstract

Myopia is the most prevalent refractive error from the age of 20 and impairs clear vision at far distance. Presbyopia, on the other hand, is an anomaly of the visual function that appears from the age of 45, impairs clear vision at near distance, and affects all people for being a natural age associated defect. Multifocal contact lenses represent a solution by which presbyopic patients can see simultaneously at multiple distances. Furthermore, they can be used, according to the last theories about optical signals that modulate the ocular growth, to slow down myopia progression in growing children.

This Thesis proposes two new aperiodic contact lens designs for slowing down myopia progression or for presbyopia compensation. The first design has the main advantage of inducing greater relative peripheral refractive error with less impairment of central vision in comparison with the first lens commercialized in order to slow down myopia progression. This design has been manufactured, characterized, and the real efficiency has been measured in a sample of myopic subjects, offering a good agreement with its theoretical basis.

The second design, for compensating presbyopia, has been also manufactured, characterized and tested in a sample of presbyopic subjects for measuring the visual performance achieved with the prototypes. Moreover, to accomplish this task, it was required to have a wide amount of different tests for testing vision at multiple distances. Therefore, another aim of this Thesis was to analyze the capabilities of the iPad for the reproduction of apps for measuring visual performance. New apps for measuring visual acuity, contrast sensitivity and stereopsis have been designed and validated for this purpose. With these new apps available, the visual performance was measured in the presbyopic subjects wearing the aperiodic contact lenses. Visual performance at near distance was significantly improved and the main advantage of the lens was the low pupil-dependence and good decentration tolerance despite of being a multizonal design.

Capítulo 1
Introducción General

1.1. Antecedentes y Objetivos de la Investigación.

Desde el punto de vista anatómico, el ojo se compone de múltiples estructuras que aportan diferentes funcionalidades al sistema en su conjunto. De manera sencilla, podemos diferenciar dos tipos de componentes: ópticas y neuronales. La principal función de las componentes ópticas es formar imágenes en el plano de la retina. La retina, primera estructura de las componentes neuronales, tiene como función transformar las señales ópticas en impulsos nerviosos que viajan desde ésta hasta el cerebro para completar el procesado de la información visual. Alteraciones en la parte óptica o neuronal pueden derivar en una disminución del rendimiento visual del paciente. Por ejemplo, diversas patologías oculares que afectan a las componentes neuronales cursan con una disminución del rendimiento visual de la misma forma que lo pueden hacer alteraciones en las componentes ópticas (Woods et al. 1998). Las Lentes de Contacto (LCs) tienen como objetivo mejorar el rendimiento visual del paciente cuando no existe ningún tipo de patología ocular que pueda ser motivo de la pérdida visual, o lo que es lo mismo, cuando la pérdida de visión pueda ser explicada exclusivamente por una pérdida de equilibrio entre las componentes ópticas y la longitud axial del ojo. De aquí en adelante descartaremos la componente neuronal del sistema visual para centrarnos exclusivamente en su parte óptica y consideraremos estas alteraciones neuronales como un factor de exclusión para todos los estudios llevados a cabo en esta investigación.

La principal causa de pérdida de rendimiento visual es la presencia de errores refractivos clasificados como miopía, hipermetropía y astigmatismo. El origen de estos errores refractivos se debe a una descompensación del equilibrio entre la refracción de la luz a través de los componentes ópticos y su focalización con respecto a la posición de la retina. En el caso de la miopía (Fig. 1A), la luz focaliza por delante de la retina debido a una excesiva potencia dióptrica de los medios ópticos, a un tamaño ocular más grande de lo normal o una combinación de ambos motivos. En la hipermetropía (Fig. 1B) ocurre lo contrario, la potencia dióptrica es menor a la normal, el tamaño del ojo es más pequeño o una combinación de ambos.

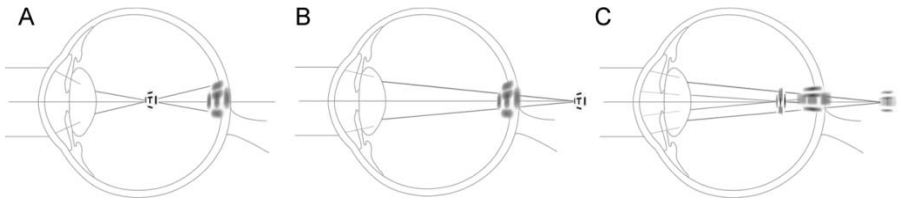

Figura 1. Esquema de errores refractivos (A) miopía, (B) hipermetropía y (C) astigmatismo mixto con una focal miópica y otra hipermetrópica.

El astigmatismo (Fig. 1C) suele estar presente de manera mixta con los dos errores refractivos anteriores y se origina cuando la potencia dióptrica no es rotacionalmente uniforme a lo largo de la óptica ocular, dando origen a dos focos principales que podrán ser miópicos cuando estén por delante de la retina, hipermetrópicos cuando estén por detrás, o mixtos cuando cada uno de los dos ocupa una de las dos posiciones anteriores.

El error refractivo de mayor prevalencia a partir de los 20 años es la miopía. Estudios epidemiológicos en los EEUU exponen que, con independencia del valor de miopía, el porcentaje medio de miopes es de 36.2% (20-39 años), 37.6% (40-59 años) y 20.5% (> 60 años). Entre los 40-49 años disminuye el número de personas con errores refractivos entre ±0.50D con una tendencia a la hipermetropía que convierte a este error refractivo en el más prevalente para edades superiores a 60 años (Vitale et al. 2014).

La alta prevalencia del error refractivo fomenta que un gran porcentaje de la población de EEUU utilice gafas o LCs. Aunque las gafas son el medio de compensación óptica principal (64%), un 11% del total utilizan LCs, lo que resulta un retorno económico de 6.1 billones de dólares tan solo en EEUU (National Eye Institute 2014). Los porcentajes de usuarios de gafas y LCs son similares a los de otros países europeos como Holanda (Statistics Netherlands [CBS] 2013). En el caso de España, inclusive se ha incrementado el porcentaje de adaptaciones (55%) con respecto al resto del mundo (36%) (Santodomingo and Morgan 2014).

Entre los 40-45 años, se origina otro defecto funcional del sistema óptico ocula: la presbicia. Este defecto es un fenómeno natural asociado al envejecimiento ocular que afecta al 100% de la población con edad superior a los

45 años. Se estima que cerca de 209 millones de personas sufren presbicia en Europa (44% de la población) y se prevé que en el 2030 afectará a la mitad de la población Europea (Marcos 2010). El mecanismo de la presbicia puede explicarse de la siguiente manera. Si considerásemos el ojo como un sistema óptico estático diseñado para ver a una distancia determinada, por ejemplo más allá de una distancia de 6 metros (Fig. 2A), nos encontraríamos con la imposibilidad de mantener en la retina las imágenes nítidas para aquellos objetos que se encuentran más cerca de la distancia óptima de enfoque (Fig. 2B). Sin embargo, el ojo es un sistema óptico dinámico capaz de enfocar objetos a múltiples distancias gracias a la acomodación, que consiste en el incremento de la potencia dióptrica del cristalino, devolviendo la imagen de un objeto cercano formado detrás de la retina (Fig. 2B) al plano de la misma (Fig. 2C).

La acomodación es una habilidad del sistema óptico ocular cuya funcionalidad se encuentra mermada con el envejecimiento. Al valor dióptrico máximo que el ojo puede acomodar se le denomina amplitud de acomodación (Furlan et al. 2009). Fue Tomas Young en 1804 quien clarificó por primera vez la naturaleza de los procesos asociados a la acomodación, mientras que Donders en 1864 realizó la primera presentación de cómo la amplitud de acomodación disminuye con la edad (Charman 2014). Esta disminución está asociada una pérdida progresiva de la elasticidad del cristalino y con ello, la imposibilidad de que éste modifique su forma e incremente su poder dióptrico para enfocar objetos a distancias cercanas.

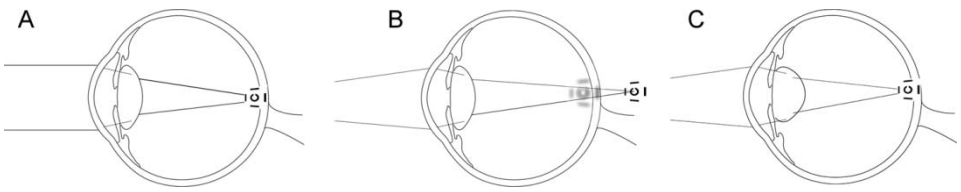

Figura 2. (A) Ojo emétrope que forma la imagen de un objeto en infinito en el plano de la retina, (B) ante un objeto cercano la imagen se desplaza más allá de la retina permaneciendo en ésta una imagen desenfocada, (C) al ponerse en marcha el mecanismo de la acomodación la potencia del cristalino se incrementa devolviendo la imagen al plano de la retina.

La amplitud de acomodación disminuye de manera lineal a lo largo de la vida hasta que a los 40-45 años alcanza un valor tal que se hace necesario el uso de una compensación óptica para poder enfocar objetos cercanos, o lo que es lo mismo, la compensación de la presbicia.

Por otro lado, los errores refractivos anteriormente descritos, miopía, hipermetropía y astigmatismo pueden corregirse a través de una lente que modifique la vergencia de los rayos que atraviesan la pupila. La óptica fisiológica utiliza el término punto remoto para definir el lugar más lejano en el que puede situarse un objeto para que pueda verse con nitidez (Cinta Puell Marín 2006). En el ojo emétrope, este punto se encuentra situado en infinito. Sin embargo, la posición del punto remoto de un ojo amétrope se define como la inversa del error refractivo en metros. Por ejemplo, el punto remoto de un miope de -3.00 D se encuentra situado a -0.33 m, o lo que es lo mismo, a 33 cm por delante del ojo. Si tomamos como punto de inicio la retina de este ojo miope nos encontraremos que los rayos salen del ojo con una vergencia tal que convergen en el punto remoto (Fig. 3B). Tanto la vergencia de los rayos al atravesar la lente en la Fig. 3A como los rayos que salen del ojo en dirección opuesta Fig. 3B coinciden de forma que al colocar una lente de -3.00 D en un ojo miope de -3.00 D lo que obtenemos es que los rayos que provienen de infinito se formen en la retina Fig. 3C (Douthwaite 2006).

En Fig. 3C se muestra como la lente empleada por el sujeto miope de -3.00 D tiene como finalidad llevar a la retina la imagen de un objeto situado en infinito. Sin embargo, si el objeto deja de estar en infinito y se aproxima al ojo, la imagen se desplazará hacia una posición posterior a la retina como mostramos en la Fig. 2B y por lo tanto para seguir manteniendo la imagen nítida deberemos actuar de alguna de las siguiente dos formas: (1) retirar la lente de -3.00 D para mantener nítida la imagen del objeto situado a 33 cm (Fig. 3B) o (2) activar el mecanismo de la acomodación para devolver la imagen a retina sin necesidad de retirar la lente. En el caso de un sujeto présbita que no pueda acomodar lo suficiente como mantener nítida la imagen del objeto a 33 cm, la segunda opción quedaría descartada aunque podría continuar viendo el objeto retirando la lente.

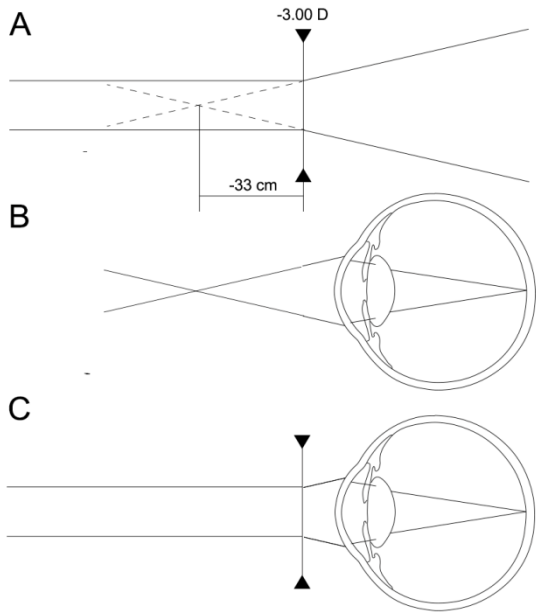

Figura 3. Esquema que muestra cómo se compensa un error refractivo modificando la vergencia de la luz. (A) Vergencia originada por una lente negativa (B) el conjugado de la imagen de la retina de un miope de -3D se forma a 33 cm por delante del ojo (C) la lente que compensa la ametropía es la que induce una vergencia igual a la que emerge del ojo miope.

Nos encontramos entonces con el problema de que sujetos présbitas necesitan una compensación óptica múltiple que les permita aproximar de forma variable su punto próximo (punto más cercano en el que se mantiene la imagen nítida), que se encuentra alejado debido a una disminución de la amplitud de acomodación, y a la vez corregir la posición de su punto remoto para llevarlo a infinito (Furlan et al. 2009). En el mundo clínico de la óptica, muchos sujetos miopes recurren a la opción de retirar sus gafas de lejos para poder ver de cerca o utilizan unas lentes bifocales o progresivas cuya potencia varía a lo largo de las regiones superior e inferior de la lente puesta en gafa. Pero, ¿qué ocurre cuando el paciente utiliza LCs que no pueden retirarse para seguir viendo de cerca?

En el caso de las LCs existen tres alternativas claramente reconocidas desde hace más de 50 años (Charman 2014):

1. Utilizar las LCs para corregir el error refractivo de lejos y una gafa con la adición en el caso de desear ver nítido algún objeto cercano.
2. Monovisión con LCs: Compensar el error refractivo de un ojo para visión de lejos (punto remoto) y otro para visión de cerca (punto próximo). Sin embargo, esta técnica tiene como principal inconveniente la pérdida de estereopsis y una menor profundidad de campo (Fernandes et al. 2013).
3. Uso de LCs bifocales y multifocales basadas en los principios de visión simultánea o alternante.

En la compensación de la presbicia encontramos por lo tanto la primera aplicación clínica de las lentes de contacto multifocales (LCMs) aperiódicas desarrolladas en esta Tesis con el objetivo de optimizar el rendimiento visual a múltiples distancias de manera simultánea. No obstante, en los últimos años, una nueva aplicación de las LCMs está alcanzando un mayor interés con un objetivo totalmente diferente, el de controlar la progresión del crecimiento del globo ocular y con ello del desarrollo de la miopía. Esta segunda aplicación se basa en que el crecimiento axial del ojo se encuentra gobernado por las señales ópticas que llegan a la retina (Flitcroft 2013).

Multitud de estudios desde los desarrollados en los años 30 (Ferree et al. 1931) han demostrado que la formación de imágenes en la periferia de la retina difiere entre sujetos que comparten la característica de presentar una imagen foveal enfocada. En sujetos emétropes, en los que la imagen más nítida se encuentra sobre la fóvea, los rayos que focalizan conforme nos alejamos hacia posiciones excéntricas de la retina lo hacen por delante de la misma (desenfoque periférico miópico). Esto se debe principalmente a que las distintas superficies que conforman el globo ocular no son perfectamente esféricas. Esta imagen por delante de la retina sería la señal óptica que indicaría al globo ocular la no necesidad de seguir creciendo, puesto que su crecimiento llevaría a un mayor desarrollo miópico. En algunos casos, de ma-

nera general en ojos miopes, se ha visto que las imágenes formadas en la periferia de la retina no ocupan una posición por delante de la misma, sino por detrás (desenfoque periférico hipermetrópico). En este caso la señal óptica transmitida indicaría al globo ocular la necesidad de seguir creciendo para llevar de nuevo la imagen a la retina. Se cree por tanto que la inducción de un desenfoque miópico periférico similar al de los sujetos emétropes sería la señal óptica necesaria para evitar el desarrollo de la miopía (Mutti et al. 2000) (Véase Fig. 4).

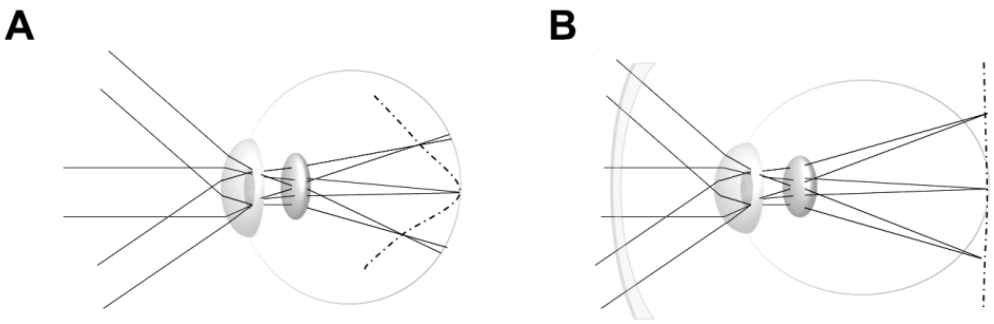

Figura 4. (A) Ojo emétrope en fóvea y miope en la periferia. (B) Ojo miope compensado con gafas con la imagen foveal sobre la retina y con defecto refractivo hipermetrópico en la periferia.

Esta teoría basada en señales ópticas se puede resumir de la siguiente manera. Si las imágenes se forman por delante de la fóvea y el crecimiento del ojo se encuentra modulado por señales ópticas, cabría esperar que una imagen miópica en fóvea terminase frenando el crecimiento ocular. Sin embargo, se ha demostrado que la miopización foveal no solo no frena la miopía sino que puede favorecer su desarrollo (Chung et al. 2002). La respuesta a la inhibición del crecimiento ocular a través del desenfoque miópico podría encontrarse más allá de la zona foveal. Esto tiene su explicación en que, aunque existe una mayor densidad neuronal en retina central respecto a la misma área en retina periférica, el área ocupada por la retina central es muy pequeña comparada con la extensión total de la retina, por lo que la suma-

ción espacial de las señales foveales será mucho menor que las provenientes de la periferia (Wallman and Winawer 2004).

Algunas preguntas surgen acerca de si el crecimiento ocular está modulado por la retina o por el contrario se debe a una etapa posterior en el procesado de la información visual. El desarrollo del error refractivo miópico tras la sección del nervio óptico en animales (Troilo et al. 1987) apoya la teoría de que el crecimiento ocular debe estar mediado por señales que se producen en la propia retina. Esta hipótesis está respaldada por el hecho de el globo ocular crece de manera local dependiendo de las zonas de la retina estimuladas (Wallman et al. 1987). Sin embargo, aunque la retina ha demostrado responder de diferente forma dependiendo del tipo de desenfoque inducido (Ho et al. 2012), todavía quedan muchas cuestiones que resolver en torno al tipo de estímulos que median el crecimiento ocular (Diether and Wildsoet 2005), regiones de la retina que deben ser estimuladas (Smith 2013), cantidad de desenfoque provocado (Benavente-Pérez et al. 2014), etc.

En resumen, nuevos prototipos de LCs basados en diseños aperiódicos pueden ser desarrollados para las dos aplicaciones clínicas que hemos mencionado: (1) Compensación de la presbicia para la mejora del rendimiento visual a múltiples distancias en sujetos présbitas (uso en sujetos a partir de 40 años) y (2) Tratamiento de la miopía a través de la inducción de un error relativo periférico miópico (uso en niños). Para desarrollar nuevos prototipos con la aplicabilidad citada anteriormente necesitamos cumplir con tres fases de innovación y desarrollo: (1) Análisis teórico de los nuevos diseños; (2) Fabricación y caracterización de los prototipos; y (3) Evaluación del rendimiento visual (LCMs para la presbicia) o del error periférico inducido (LCMs para ralentizar la progresión de la miopía).

Para la realización de la primera de las fases "*Análisis teórico de los nuevos diseños*" se puede recurrir a software especializado basado en el trazado de rayos como puede ser Zemax (Zemax Development Corporation, Bellevue, WA, USA). Dentro de este software se pueden implementar modelos de ojo

reportados en la literatura científica sobre los cuales se evalúa el rendimiento óptico del nuevo diseño. Para seleccionar uno u otro modelo de los actualmente disponibles se ha de tener en cuenta la precisión (debe ser lo suficientemente exacto a la hora de predecir la calidad óptica del sistema) y la sencillez (no tiene que ser más complejo de lo estrictamente necesario para reducir los tiempos de cálculo) (Schwiegerling 1995). La principal utilidad de un modelo de ojo teórico reside en la capacidad de valorar como un sistema óptico funciona en conjunción con el sistema óptico ocular. De manera particular, muchos de los sistemas ópticos que deseamos valorar son a su vez empleados para compensar un error refractivo. Ante tal necesidad, la gran mayoría de los modelos de ojo actuales quedan obsoletos por el gran número de cambios que se producen en los diferentes elementos del sistema (Liou and Brennan 1997).

Cuando trabajamos con modelos de ojo emétropes podemos optar por variar aquellos elementos en los que cambios leves proporcionan significativos saltos en el error refractivo. Estos cambios se basarían principalmente en la longitud axial (AL del inglés *Axial Length*) y la curvatura de la córnea (CR del inglés *Corneal Radius*). Investigaciones previas para el estudio del efecto del descentramiento de una lente de contacto blanda sobre una córnea asférica se basan en la modificación de la curvatura de la córnea para generar una ametropía (Schwiegerling 1995). Sin embargo, se ha demostrado que la relación entre ametropía, AL y CR, conlleva un mayor peso en el cambio de la longitud axial que en la curvatura de la córnea, siendo el mejor predictor del error refractivo el ratio AL/CR (Ip et al. 2007; Gonza et al. 2008). Durante el desarrollo de esta Tesis, tan solo el modelo de ojo miope de Atchison ha sido propuesto para evaluar cambios en la calidad óptica de ojos amétropes teniendo en cuenta variaciones de gradiente de índice, asfericidad de la córnea, cristalino y retina (Atchison 2006). Sobre el modelo de ojo miope de Atchison se pueden simular en Zemax cada uno de los nuevos diseños aperiódicos incluyendo esta estructura en la superficie anterior de la lente de contacto.

La aperiodicidad en oftalmología se encuentra presente principalmente en el diseño de Lentes Intraoculares Multifocales (LIOMs) refractivas y difractivas. L. Remón en su trabajo de Tesis Doctoral presentó resultados teóricos e in-vitro de la primera LIOM Fractal (Remón 2012). Esta lente catalogada como híbrido refractiva-difractiva se comporta como una lente bifocal con una mayor profundidad de foco y una menor aberración cromática con respecto a otras lentes comerciales. Posteriormente, A. Calatayud realizó un análisis teórico de diseños puramente difractivos cuya aplicación se encontraba dirigida a solventar algunas de las limitaciones de los diseños fractal (Calatayud et al. 2013). Sin embargo, ninguno de los diseños previos de LIOMs han sido estudiados por el momento en ojos reales debido a que la implantación de una LIOM es un proceso quirúrgico invasivo que requiere complejos mecanismos de producción así como exigencias burocráticas que hacen que se extienda considerablemente el tiempo desde el diseño hasta la implantación en ojos reales.

El tamaño de zonas de los diseños aperiódicos empleados en este trabajo de Tesis se basan en el conjunto de Cantor triádico. Esta función consiste en la división de una estructura unidad llamada *iniciador* (S=0) en tres partes cuyo tamaño viene definido por γ_1 para el primer segmento y γ_2 para el tercero, siendo el tamaño del segmento intermedio 1-γ_1-γ_2 (S=1). En la siguiente etapa (S=2) se vuelve a repetir la misma iteración en tres partes siguiendo la misma escala y resultando en un total de 7 zonas alternantes. Los tamaños de cada una de estas zonas se resumen en la Tabla 1, mientras que el procedimiento de iteraciones anteriormente descrito se representa gráficamente en la Fig. 5A (Furlan et al. 2013).

Tabla 1. Expresión analítica de las zonas del conjunto de Cantor de orden S=2 expresado en la variable radial cuadrática $(r/a)^2$, donde a es la extensión radial máxima de la lente. La zona i-esima está limitada entre una posición radial inicial r_{i-1} y final r_i.

Zona (i)	$(r_{i-1}/a)^2$	$(r_i/a)^2$
1	*0*	γ_1^2
2	γ_1^2	$\gamma_1(1-\gamma_2)$
3	$\gamma_1(1-\gamma_2)$	γ_1
4	γ_1	$1-\gamma_2$
5	$1-\gamma_2$	$1-\gamma_2+\gamma_1\gamma_2$
6	$1-\gamma_2+\gamma_1\gamma_2$	$1-\gamma_2^2$
7	$1-\gamma_2^2$	1

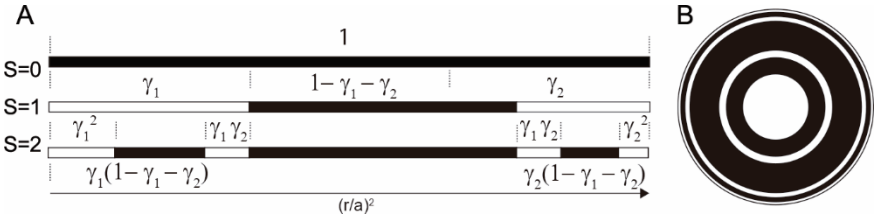

Figura 5. (A) Procedimiento de obtención de una estructura aperiódica Fractal de orden S=2 en r^2. (B) Representación de las zonas anulares de esta estructura a través de la rotación del segmento en $r_0=0$.

Tras la segunda iteración se origina una estructura fractal que representa la aperiodicidad de las zonas en la variable radial cuadrática normalizada $(r/a)^2$, donde los gaps se corresponden con zonas cuya potencia base se encuentra enfocada a la compensación del error refractivo y los segmentos negros, con zonas de potencia terapéutica (control de la miopía) o zonas de adición (presbicia). Las zonas se obtienen sobre la superficie de la lente rotando la estructura alrededor de la posición inicial $r_0=0$ (véase Fig. 5B).

A partir del desarrollo analítico anterior podemos diseñar infinidad de casos particulares asignando diferentes valores a γ_1 y γ_2. Para converger en dise-

ños aplicables a LCMs se ha de pensar en la aplicación específica de la lente y en el diámetro pupilar del paciente ya que estos serán los factores que regularán la eficiencia de la lente. En esta Tesis estudiaremos dos casos particulares optimizados en los que $\gamma_1 = \gamma_2 = 0.333$ en lentes de aplicación para la presbicia y $\gamma_1 = \gamma_2 = 0.324$ para lentes de control de la miopía.

La segunda fase comprende la "*Fabricación y caracterización de los prototipos*". Los dos métodos utilizados con mayor frecuencia de manera aislada o combinada en la fabricación de LCs son el *moldeo* y el *torneado*, aunque existe un tercer método por *fundición centrifuga* que apenas se utiliza (Maldonado-Codina and Efron 2003). El *moldeo* se lleva a cabo a través de la inyección de un material plástico en un molde. Con este proceso se fabrican las LCs de reemplazo frecuente (diarias, quincenales o mensuales). Posee como principal ventaja la posibilidad de realizar un gran número de lentes de manera simultánea reduciendo considerablemente los costes de fabricación. Sin embargo, el principal inconveniente reside en que es necesario sustituir el molde cuando se busca cambiar algún parámetro de la lente.

Si es necesaria una mayor personalización de la lente se recurre a un segundo método denominado de *torneado.* Con este procedimiento se tallan cada una de las caras de la LC a partir de los datos introducidos en un software informático. A diferencia del método de *moldeo*, los parámetros de la LC pueden ser fácilmente modificados aunque el tiempo de fabricación es más largo. Es por este segundo motivo que las lentes torneadas suelen ser fabricadas con el fin de soportar periodos de reemplazo más largos en el tiempo. Todos los prototipos fabricados a lo largo de este trabajo de investigación han sido llevados a cabo mediante el sistema de torneado, con el torno Optoform 40 mostrado en la Fig. 6 (AMETEK Ultra Precision Technologies 2016), por las ventajas que anteriormente han sido descritas.

Figura 6. Imagen del torno Optoform 40 empleado en la fabricación de las LCs objeto de estudio.

Cuando diseñamos un sistema óptico que posteriormente debe ser fabricado hemos de ser conscientes que existirán ciertos errores ligados al proceso de fabricación que no podemos controlar. Estos errores pueden ser clasificados en forma de "*tolerancias*" (Remón et al. 2012; Furlan et al. 2016), con las

cuales proporcionamos un margen de error a cada parámetro de la lente en función de la calidad óptica final y la dificultad en el proceso de fabricación (Fischer and Tadic 2000).

En la actualidad las tolerancias requeridas por la normativa internacional tan solo hacen referencia a LCs monofocales (UNE-EN ISO 18369-2 2013) debido a que los instrumentos de caracterización de LCMs todavía no se encuentran ampliamente aceptados y validados. Es por ello, que a lo largo de este trabajo de investigación no se han establecido unas tolerancias de fabricación determinadas sino que se ha evaluado la influencia en el efecto clínico deseado de cualquier tipo de sesgo en la fabricación.

En la última década, han surgido nuevos instrumentos con los cuales podemos medir los denominados perfiles de potencia**,** que representan la variación de potencia a lo largo de la posición radial respecto al centro geométrico de la LC (Plainis et al. 2013a). Se han empleado diversas técnicas para la valoración de los perfiles de potencia con lentes hidrófilas multifocales. Sin embargo, en la actualidad tan solo existen cuatro instrumentos comerciales basados en distintas tecnologías (véase Fig. 7):

A. ClearWave: sensor Hartman-Shack con resolución espacial de 0.104 mm (AMO-Wavefront Sciences 2014).
B. SHSOphtalmic: sensor Hartman-Shack con resolución espacial de 0.069 mm (Optocraft 2014).
C. NIMO TR1504: ajuste de fase principio de Schlieren con resolución de 0.018 mm (Lambda-X 2014)
D. Phase Phocus Lens Profiler: reconstrucción de patrones de difracción con resolución 0.007 mm (PhasePhocus 2014).

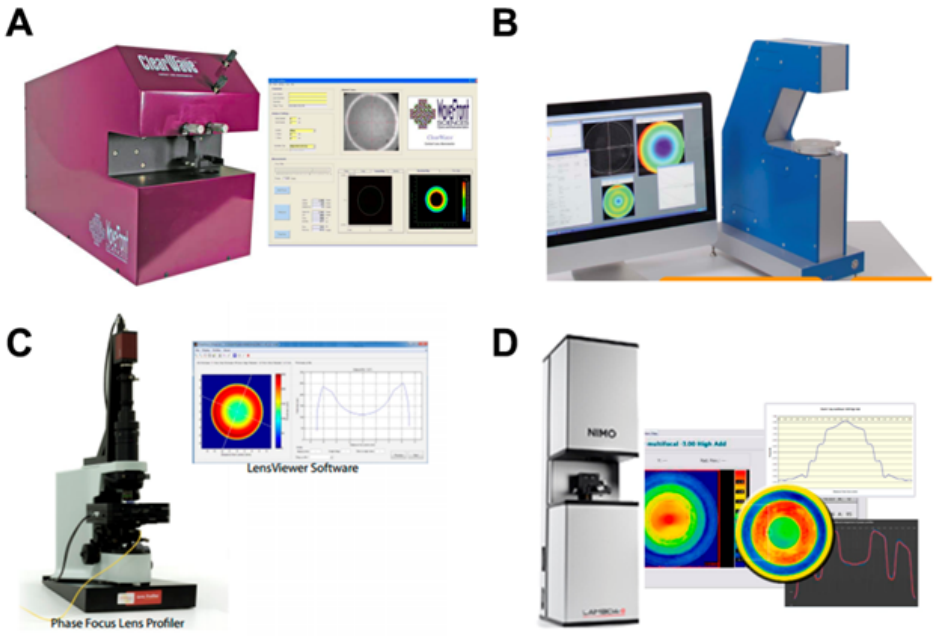

Figura 7. Instrumentos de caracterización de LCMs. (A) Clear Wave, (B) SHSOphtalmic, (C) Phase Phocus Lens Profiler y (D) NIMO TR1504. (Imágenes obtenidas de las páginas web de los fabricantes).

Estos instrumentos nos permiten conocer si el prototipo que hemos mandado fabricar posee la potencia que debería tener a lo largo de toda su superficie óptica, detectando las diferencias entre los diseños teóricos y los prototipos experimentales. Esto es algo fundamental para interpretar posteriormente el rendimiento visual y el error relativo periférico con los nuevos diseños aperiódicos.

La tercera y última fase supone la *"Evaluación del rendimiento visual (LCMs para la presbicia) o del error periférico inducido (LCMs para ralentizar la progresión de la miopía)"* con el fin de validar el efecto esperado de las simulaciones ópticas de la primera fase. En el caso del diseño específico de la LCM para el control de la miopía se debe cotejar el Error Relativo Periférico (ERP) inducido. Las primeras referencias de medida del ERP datan del año 1931 a través de un optómetro manual (Ferree 1931). Posteriormente, alternativas más o menos complejas han surgido hasta las dispo-

nibles en el nuevo siglo: retinoscopía periférica (Rempt et al. 1971), sistemas de doble paso (Jennings and Charman 1978), refracción subjetiva periférica por detección de contraste (Wang et al. 1996), fotorrefractores (Seidemann et al. 2002), auto-refractómetros (Atchison et al. 2005) y aberrometría periférica (Atchison et al. 2007).

Pese a la variedad de técnicas disponibles, las dos más utilizadas en la actualidad son la aberrometría y los auto-refractómetros (Fedtke et al. 2009) (Fig. 8). Sin embargo, todos los instrumentos utilizados hasta la fecha representan modificaciones de aparatos cuyo propósito inicial no era la medida del ERP, por lo que el instrumento ideal para la medida todavía está por llegar. Entro los propuestos más recientes cabe destacar el EyeMapper que permite la rápida medida del ERP y las aberraciones de alto orden en ± 50º a distancia lejana y diferentes condiciones de acomodación manteniendo el ojo estático (Fedtke et al. 2014).

Figura 8. Autorrefractómetro de campo abierto WAM-5500 utilizado en este trabajo de investigación para llevar a cabo las medidas de error relativo periférico.

En el diseño de LCMs para la compensación de la presbicia es necesario conocer el estado del rendimiento visual sin y con la LCM con el fin de

comprobar si la lente cumple el objetivo de mejorar la visión del paciente présbita (Rodríguez-Vallejo 2009b). Es importante resaltar que las necesidades del paciente pueden estar asociadas a una mejora del rendimiento a más de una distancia, por lo que, con independencia del estímulo empleado, debemos realizar mediciones en lejos (> 3 m), distancia intermedia (~ 67 cm) o cerca (< 50 cm) lo que nos obliga a disponer de test especialmente diseñados para trabajar a todas estas distancias. Ejemplo de ello es un reciente estudio con LCMs que incluía una completa batería de pruebas de evaluación del rendimiento visual (Vasudevan et al. 2014):

1. Agudeza Visual (AV) (logMAR) de alto (94%) y bajo (36%) contraste a 6 m y 33 cm.
2. Función de Sensibilidad al Contraste (FSC) a 2.5 m para frecuencias de 3, 6, 12 y 18 cpg con el CSV-1000 (Precision Vision, La Salle, Illinois).
3. Curva de desenfoque de AV (bajo contraste) de 0 a -3 D en pasos de 0.50D.
4. Estereoagudeza medida a 40 cm y 3 m con dos test de estereopsis, (Randot Dot para cerca y Random Dot para lejos).

Las 3 primeras pruebas hacen referencia a habilidades relacionadas con la capacidad de resolver detalles de los objetos (AV de Alto Contraste, AV_{AC}), de detectar patrones de contraste variable (FSC) (Rodríguez-Vallejo et al. 2010b), o una combinación de ambas (AV de Bajo Contraste, AV_{BC}). Sin embargo, la estereoagudeza global se basa en la capacidad de percibir imágenes en 3 dimensiones a partir de la disparidad retiniana formada por puntos aleatorios ligeramente dispares visibles de manera independiente con cada uno de los dos ojos. Además, otras habilidades pueden ser de interés para ciertas condiciones específicas como el deporte (Rodríguez-Vallejo and Martínez Verdú 2008; Rodríguez-Vallejo 2009a; Rodríguez-Vallejo et al. 2010a; Rodríguez-Vallejo and Jiménez Jiménez 2010; Quevedo et al. 2012; Fernández et al. 2016). Un resumen de las principales pruebas realizadas en diferentes estudios se muestra en la Tabla 3.

Tabla 3. Resumen de pruebas de evaluación del rendimiento visual con lentes de contacto multifocales incluidas en algunos estudios.

Autor	AV_{AC}	AV_{BC}	EST	CD	FSC	RVN
(Vasudevan et al. 2014)	C: 94% 6 m y 33 cm	C: 36% 6 m y 33 cm	RD 40 cm y 3 m	BC de 0 a -3D	2.5m	0.66
(Plainis et al. 2013b)	-	-	-	AC +3 a -3D	-	-
(Papas et al. 2009)	C: 90% 6 m, 1 m y 40 cm	C: 10% 6 m, 1 m y 40 cm	RD 40 cm	-	-	?
	Otros: Diferentes condiciones de iluminación, deslumbramiento, ERN, imágenes fantasma, velocidad de lectura, halos, etc.					
(Rajagopalan et al. 2006)	C: 95% lejos	C: 18% lejos	-	-	2.5m	-
	Otros: Deslumbramiento, cuenta letras en cerca.					
(Guillon et al. 2002)	C: 90% Lejos y cerca	C: 10% Lejos y cerca	-	-	-	-
	Otros: Diferentes condiciones de iluminación					

AV_{AC} = AV de alto contraste. C = % Contraste optotipo / fondo
AV_{BC} = AV de bajo contraste.
EST = Estereopsis. RD, Random Dot o estereopsis global.
CD = Curva de desenfoque; BC realizada a bajo contraste y AC para alto contraste.
FSC = Función de sensibilidad al contraste.
RVN = Rango de visión nítida para un optotipo de AV decimal determinado.
ERN = Escala de reconocimiento numérico.
? = Test realizado pero no especificado.

La evaluación del rendimiento con LCMs multifocales posee por tanto como principal inconveniente el tener que disponer de múltiples test para múltiples distancias. La aparición de las tabletas o iPads puede suponer una solución a este inconveniente ya que, al ser dispositivos portátiles sobre los cuales podemos programar cualquier test visual, tan solo necesitaríamos un dispositivo para todo el conjunto de pruebas (Rodríguez-Vallejo et al. 2014b). No obstante, como ocurre con cualquier otra pantalla, no se encuentran exentos de ciertas limitaciones que deben ser estudiadas en torno a la representación de optotipos de AV de alto y bajo contraste (Rodríguez-Vallejo 2015; Rodríguez-Vallejo 2016).

Tras esta introducción del estado actual sobre el diseño, caracterización y posibles aplicaciones clínicas de diseños aperiódicos en LCMs, esta Tesis Doctoral pretende cumplir los siguientes objetivos.

1. Diseñar LCs aperiódicas que puedan ser aplicables a la compensación de la presbicia, mejorando el rendimiento visual, o para el control de la progresión de la miopía, induciendo un error relativo periférico miópico.
2. Control de calidad de los prototipos fabricados con el fin de determinar el sesgo existente con los diseños teóricos.
3. Evaluar el error relativo periférico inducido en sujetos adaptados con LCs para el control de la miopía.
4. Analizar las capacidades del iPad (hardware) para el desarrollo de test que puedan servir para la medición del rendimiento visual a múltiples distancias con LCs aperiódicas.
5. Programar y validar aplicaciones para iPad que puedan ser utilizadas para la medida de las siguientes habilidades visuales: AV, sensibilidad al contraste (SC) y estereopsis.
6. Evaluar el rendimiento visual en pacientes présbitas adaptados con LCs para la compensación de la presbicia mediante un estudio clínico previo.

1.2. Estructura de la tesis.

En primer lugar, cabe destacar que se trata de una Tesis por compilación de artículos científicos. Cada uno de ellos puede ser leído autónomamente al tener los aspectos necesarios para su comprensión (introducción, métodos, resultados, discusión y bibliografía), pero es importante recalcar que la unión de todos ellos constituye un solo trabajo con un claro hilo argumental.

Así pues la tesis se estructura en 4 capítulos:

1. Introducción general.
2. Publicaciones.
   - 2.1. The effect of Fractal Contact Lenses on peripheral refraction in myopic model eyes.
   - 2.2. Two-dimensional relative peripheral refractive error induced by Fractal Contact Lenses for myopia control.
   - 2.3. Inter-display reproducibility of contrast Sensitivity measurement with iPad
   - 2.4. Designing a new test for contrast sensitivity function measurement with iPad.
   - 2.5. Visual acuity and contrast sensitivity screening with a new iPad application.
   - 2.6. Fast and reliable stereopsis measurement at multiple distances with iPad.
   - 2.7. Design, characterization and visual performance of a new multizone contact lens.
3. Discusión de los resultados.
4. Conclusiones.

El cuerpo principal de la tesis está compuesto por el **Capítulo 2**, que recoge cuatro artículos publicados por revistas científicas de prestigio y tres en estado de revisión editorial que pueden ser consultados en el repositorio arxiv.org.

El **primer artículo** se titula "*The effect of Fractal Contact Lenses on peripheral refraction in myopic model eyes*" (Rodríguez-Vallejo et al. 2014a). Los resultados preliminares se presentaron en el XXIII Congreso OPTOM (Remón et al. 2014) y, posteriormente, este artículo se ha publicado en la revista "Current Eye Research". Esta revista está soportada por Thomson-Reuters en el Science Citation Index (SCI). En el año 2014 su Factor de Impacto ha sido de 1,639, ocupando una posición relativa de 30/57 (Q3) en la categoría "Ophthalmology" del Journal Citation Rank (JCR). Esta revista cubre todas las áreas relacionadas con la investigación en Ciencias de la Visión: investigación clínica, anatomía, fisiología, biofísica, bioquímica, farmacología, biología del desarrollo, microbiología y inmunología. Todos los artículos de esta revista se han sometido a una rigurosa revisión por pares, basado en el cribado inicial y arbitraje de doble ciego de dos evaluadores anónimos internacionales.

En este primer artículo se presenta un diseño particular de LCM aperiódica cuyo tamaño y distribución de zonas se encuentra basado en el conjunto de Cantor triádico. El rendimiento de este diseño se evaluó en términos de calidad óptica y ERP para dos diámetros de pupila particulares a través del software de trazado de rayos Zemax. Ambas variables fueron evaluadas considerando la aplicación clínica futura de este diseño aperiódico centrado en la ralentización de la progresión de la miopía. Por este motivo, los resultados fueron comparados con los correspondientes a otro diseño recogido en la literatura el cual se encuentra, en la actualidad, comercializado como LC para el tratamiento de la progresión de la miopía. Este nuevo diseño se presenta como una alternativa a esta lente comercial con la ventaja principal de inducir un mayor ERP miópico y afectar en menor medida a la visión central.

El **segundo artículo** se titula "*Two-dimensional relative peripheral refractive error induced by Fractal Contact Lenses for myopia control*" (Rodríguez-Vallejo et al. 2016a). Los resultados preliminares se presentaron en el Congreso SIYO 2014 (Rodríguez-Vallejo 2014). Este artículo se encuentra en proceso de revisión editorial en una revista internacional impactada y la versión del autor está alojada en el repositorio arxiv.org. En este segundo artículo se llevó a cabo la medida del ERP con prototipos de la LC aperiódica para el control de la miopía realizando una caracterización previa

de los mismos a través del NIMO TR1504. El ERP fue medido con el WAM 5500 en los ojos derechos de 26 sujetos miopes sin la lente de contacto y nuevamente con la lente de contacto adaptada. La lente demostró una inducción de ERP miópico máximo en la misma medida que la potencia promedio experimental de las zonas terapéuticas. Además, se obtuvo un desplazamiento del pico con mayor potencia negativa fue obtenido en comparación con los resultados teóricos, el cual fue explicable por el descentramiento generalizado que experimenta la LC sobre la córnea hacia el lado temporal. Una nueva representación a través de un mapa bidimensional permitió valorar los cambios producidos en las componentes astigmáticas J_0 y J_{45}. Estos mapas demostraron que para la componente M, la medida exclusiva de la sección horizontal sería suficiente para extrapolar el comportamiento de la lente a lo largo de la región vertical. No obstante, para analizar las componentes astigmáticas, el mapa bidimensional ofrece información más completa en posiciones extremas del campo que difiere de la descrita a través una única sección horizontal.

El **tercer artículo** se titula "*Inter-display Reproducibility of Contrast Sensitivity Measurement with iPad*" (Rodríguez-Vallejo et al. 2016g). Los resultados preliminares se presentaron en el XXIV Congreso OPTOM (Rodríguez-Vallejo et al. 2016d) y, posteriormente, este artículo se ha publicado en la revista "Optometry and Vision Science". Esta revista está soportada por ThomsonReuters en el SCI. En el año 2015 su Factor de Impacto ha sido de 1,442, ocupando una posición relativa de 37/56 (Q3) en la categoría "Ophthalmology" del JCR. Esta revista cubre los desarrollos actuales en optometría, óptica fisiológica y ciencias de la visión. Todos los artículos de esta revista se han sometido a una rigurosa revisión por pares, basado en el cribado inicial y arbitraje de doble ciego de dos evaluadores anónimos internacionales.

En este artículo se muestra una evaluación de la fiabilidad en la reproducción de optotipos de contraste variable para iPads previamente no calibrados. Se midieron seis iPads retina con un colorímetro obteniendo la relación entre niveles digitales y respuesta de luminancia para cada uno de los canales R,G,B. Se aplicó el método bitStealing con el fin de expandir los niveles de luminancia de 255 hasta 2540 y se determinó el promedio y el intervalo de confianza al 95% para el conjunto de los seis iPads. Considerando la lu-

minancia máxima (fondo) como el nivel 2540, se calcularon las luminancias correspondientes a niveles de contraste espaciados 0.05 o 0.1 unidades logarítmicas de contraste del optotipo. Los resultados mostraron que para un test diseñado en pasos de 0.1 unidades logarítmicas la variabilidad entre iPads es lo suficientemente pequeña como para garantizar la fiabilidad en la reproducción de contrastes. Este trabajo pone de manifiesto que aplicaciones correctamente diseñadas pueden ser utilizadas para medir la SC sin requerir un calibrado previo del iPad. De esta forma, podemos desarrollar de manera fiable un test de SC que sirva para evaluar el rendimiento visual con LCMs aperiódicas.

El **cuarto artículo** se titula "*Designing a new test for contrast sensitivity function measurement with iPad*" (Rodríguez-Vallejo et al. 2015). Los resultados preliminares se presentaron en el Congreso SIYO 2013 (Rodríguez-Vallejo et al. 2013b) y, posteriormente, este artículo se ha publicado en la revista "Journal of Optometry". En la actualidad se encuentra posicionado como el artículo con más lecturas en la historia de esta revista. Aunque de momento esta revista no está soportada por ThomsonReuters en el SCI, se encuentra indexada en PMC (US National Library of Medicine National Institutes of Health), en Medline (US National Library of Medicine) y en el Índice Bibliográfico Español en Ciencias de la Salud. Además, está incluida en Scopus y ocupa la posición relativa 6/9 en la categoría "Optometry" de SCImago Journal Rank con Factor de Impacto de 0,344. Esta revista cubre investigación clínica y experimental en el campo de la optometría, óptica oftálmica, superficie ocular y ciencias de la visión básica y aplicada. Todos los artículos de esta revista se han sometido a una rigurosa revisión por pares, basado en el cribado inicial y arbitraje de doble ciego de dos evaluadores anónimos internacionales.

En el cuarto artículo se llevó a cabo la validación de dos variantes de una nueva aplicación desarrollada para medir la SC con redes sinusoidales. En concreto, se compararon dos versiones de la aplicación que diferían en el método psicofísico empleado para obtener el umbral y en los niveles de SC con el Functional Acuity Contrast Test (FACT) contenido en el analizador de visión Optec6500. Este test se emplea con frecuencia en la evaluación del rendimiento visual en procedimientos multifocales. Los resultados mostraron que de las dos versiones de la aplicación, aquella con mayor similitud en

método de medida y niveles de contraste fue la que guardaba un mejor acuerdo con el FACT, no existiendo diferencias significativas entre ambos tests. Los resultados de este estudio demuestran que podemos utilizar esta aplicación de manera fiable puesto que obtenemos resultados comparables a los instrumentos comercializados en la actualidad.

El **quinto artículo** se titula "*Visual acuity and contrast sensitivity screening with a new iPad application*" (Rodríguez-Vallejo et al. 2016b). Los resultados preliminares se presentaron en el V Congreso de Metrología (Rodríguez-Vallejo et al. 2013a) y, posteriormente, este artículo se ha publicado en la revista "Displays". Esta revista está soportada por Thomson-Reuters en el SCI. En el año 2015 su Factor de Impacto ha sido de 1,903, ocupando una posición relativa de 9/51 (Q1) en la categoría "Computer Science, Hardware & Architecture" del JCR. Esta revista cubre la investigación y desarrollo actual en tecnologías de visualización, su presentación efectiva y percepción de la información, además de aplicaciones y sistemas incluyendo interfaces de visualización humana. Todos los artículos de esta revista se han sometido a una rigurosa revisión por pares, basado en el cribado inicial y arbitraje de doble ciego de dos evaluadores anónimos internacionales.

En el quinto artículo se validaron dos métodos rápidos para la medición de la AV y la SC a través de aplicaciones para iPad. En el caso de la AV se empleó como instrumento de comparación el Early Treatment Diabetic Retinopathy Study (ETDRS) considerado como el Gold Estándar actual en la medida de la AV. La aplicación sobreestimó en 0.06 logMAR la AV. No obstante, su repetibilidad fue mejor que la del gold estándar demostrando ser un test con mejor reproducibilidad. En el caso de la SC, la aplicación demostró una baja reproducibilidad comparable a la del FACT, lo que supone que futuros estudios deberían ir encaminados a desarrollar aplicaciones que mejoren la reproducibilidad de los test de SC actuales. Los resultados obtenidos en este estudio sirven como muestra de que se puede medir la AV y la SC con un iPad. En el segundo de los casos, la reproducibilidad no es por el momento lo excesivamente buena, aunque es comparable a la de los test convencionales.

El **sexto artículo** se titula "*Fast and reliable stereopsis measurement at multiple distances with iPad*" (Rodríguez-Vallejo et al. 2016f). Los resultados preliminares se presentaron en el congreso SIYO 2014 (Llorens-Quintana et al. 2014). Este artículo se encuentra en proceso de revisión en una revista internacional impactada y la versión del autor está alojada en el repositorio arxiv.org. En el artículo se describen las bases de diseño de una nueva aplicación para la medida de estereopsis global a múltiples distancias mediante un iPad retina. Una muestra de sujetos fue evaluada con la aplicación en cerca y lejos en tres días diferentes. Los resultados obtenidos fueron comparados con el TNO en cerca y el Howard Dolman en lejos, pruebas que se llevaron a cabo en los mismos sujetos durante las tres sesiones. La aplicación para iPad mostró una muy buena concordancia con el TNO en cerca y una mayor reproducibilidad que el test convencional. No obstante, los resultados en lejos no pueden ser comparables a los del Howard Dolman, algo esperable en teoría teniendo en cuenta las bases en las que se fundamentan cada uno de los tests, la aplicación en estereopsis global y el Howard Dolman en estereopsis local, respectivamente.

El **séptimo artículo** se titula "*Design, characterization and visual performance of a new multizone contact lens*" (Rodríguez-Vallejo et al. 2016c). Los resultados preliminares se presentaron en el XXIV Congreso OPTOM (Rodríguez-Vallejo et al. 2016e). Este artículo se encuentra en proceso de revisión en una revista internacional impactada y la versión del autor está alojada en el repositorio arxiv.org. En este trabajo se simuló el comportamiento de un diseño aperiódico para el control de la miopía a través de Zemax para dos tamaños de pupila y en estado de la lente centrada y descentrada. Los prototipos fueron posteriormente fabricados y caracterizados detectando una infraestimación de la potencia en las zonas efectivas de adición. Se adaptaron los prototipos en 9 ojos hipermétropes de 5 sujetos présbitas y el rendimiento visual se midió a través de las aplicaciones descritas en los trabajos anteriores. Los pacientes adaptados con los prototipos mostraron una ligera pérdida de la calidad visual en lejos, manifestada por una ligera caída de la SC en lejos. En contrapartida, la visión de cerca mejoró considerablemente con hasta dos líneas de mejora en la AV. Las curvas de desenfoque mostraron que la lente se comporta como una lente de profundidad de foco extendida con un pico máximo energético próximo al valor de la adición, algo que ya mostraron las simulaciones en Zemax.

En el **Capítulo 3** se presenta una breve discusión acerca de los principales resultados mientras que el **Capítulo 4** muestra las conclusiones finales de la Tesis así como el cumplimiento de los objetivos planteados. Por último, se muestra la bibliografía general utilizada a lo largo de toda la Tesis.

Capítulo 2
Publicaciones

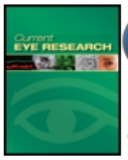

Research Article

The Effect of Fractal Contact Lenses on Peripheral Refraction in Myopic Model Eyes

DOI: 10.3109/02713683.2014.903498
Manuel Rodriguez-Vallejo[*ab], Josefa Benlloch[b], Amparo Pons[b], Juan A. Monsoriu[a] & Walter D. Furlan[b]
pages 1151-1160

Publishing models and article dates explained

Received: 7 Oct 2013
Accepted: 4 Mar 2014
Published online: 21 Apr 2014

Abstract

Purpose: To test multizone contact lenses in model eyes: Fractal Contact Lenses (FCLs), designed to induce myopic peripheral refractive error (PRE).

Methods: Zemax ray-tracing software was employed to simulate myopic and accommodation-dependent model eyes fitted with FCLs. PRE, defined in terms of mean sphere *M* and 90°–180° astigmatism J_{180}, was computed at different peripheral positions, ranging from 0 to 35° in steps of 5°, and for different pupil diameters (PDs). Simulated visual performance and changes in the PRE were also analyzed for contact lens decentration and model eye accommodation. For comparison purposes, the same simulations were performed with another commercially available contact lens designed for the same intended use: the Dual Focus (DF).

Results: PRE was greater with FCL than with DF when both designs were tested for a 3.5 mm PD, and with and without decentration of the lenses. However, PRE depended on PD with both multizone lenses, with a remarkable reduction of the myopic relative effect for a PD of 5.5 mm. The myopic PRE with contact lenses decreased as the myopic refractive error increased, but this could be compensated by increasing the power of treatment zones. A peripheral myopic shift was also induced by the FCLs in the accommodated model eye. In regard to visual performance, a myopia under-correction with reference to the circle of least confusion was obtained in all cases for a 5.5 mm PD. The ghost images, generated by treatment zones of FCL, were dimmer than the ones produced with DF lens of the same power.

Conclusions: FCLs produce a peripheral myopic defocus without compromising central vision in photopic conditions. FCLs have several design parameters that can be varied to obtain optimum results: lens diameter, number of zones, addition and asphericity; resulting in a very promising customized lens for the treatment of myopia progression.

2.1. The Effect of Fractal Contact Lenses on Peripheral Refraction in Myopic Model Eyes

Manuel Rodriguez-Vallejo[1*], Josefa Benlloch[2], Amparo Pons [2], Juan A. Monsoriu[1] and Walter D. Furlan[2]

[1] *Centro de Tecnologías Físicas, Universitat Politècnica de València, 46022 Valencia, Spain*

[2] *Departamento de Óptica, Universitat de València, 46100 Burjassot, Spain*
[*] *Corresponding author: mrvallejo2004@hotmail.com*

2.1.1. Abstract

Purpose: To test multizone contact lenses in model eyes: Fractal Contact Lenses (FCLs), designed to induce myopic peripheral refractive error (PRE).

Methods: Zemax ray-tracing software was employed to simulate myopic and accommodationdependent model eyes fitted with FCLs. PRE, defined in terms of mean sphere *M* and 90º-180º astigmatism J_{180}, was computed at different peripheral positions, ranging from 0 to 35º in steps of 5º, and for different pupil diameters (PDs). Simulated visual performance and changes in the PRE were also analyzed for contact lens decentration and model eye accommodation. For comparison purposes, the same simulations were performed with another commercially available contact lens designed for the same intended use: the Dual Focus (DF).

Results: PRE was greater with FCL than with DF when both designs were tested for a 3.5 mm PD, and with and without decentration of the lenses. However, PRE depended on PD with both multizone lenses, with a remarkable reduction of the myopic relative effect for a PD of 5.5mm. The myopic PRE with contact lenses decreased as the myopic refractive error increased,

but this could be compensated by increasing the power of treatment zones. A peripheral myopic shift was also induced by the FCLs in the accommodated model eye. In regard to visual performance, a myopia undercorrection with reference to the circle of least confusion was obtained in all cases for a 5.5 mm PD. The ghost images generated by treatment zones of FCL, was dimmer than the ones produced with DF lens of the same power.

Conclusions: FCLs produce a peripheral myopic defocus without compromising central vision in photopic conditions. FCLs have several design parameters that can be varied to obtain optimum results: lens diameter, number of zones, addition, and asphericity; resulting in a very promising customized lens for the treatment of myopia progression.

Keywords: myopia, peripheral refraction, myopia progression, contact lenses, fractal lenses, model eyes.

2.1.2. Introduction

The treatment of myopia progression deserves the attention of ophthalmologists and optometrists mainly because of the high risk of serious ophthalmic diseases associated with it (Gwiazda 2009; Tarutta et al. 2011). Experimental studies in animals (Smith et al. 2005; Smith 2012) found that refractive error in the peripheral retina can regulate the eye growth, in particular, relative peripheral hyperopia has been suggested as a possible factor that could cause the progression of myopia (see (Smith 2012) for a review). Consequently, the induction of a myopic peripheral refractive error (PRE) could be considered as a myopia progression treatment in humans, taking into consideration that retina (Troilo et al. 1987) is able to identify positive and negative defocus, and paracentral retina reacts more vigorously than central retina to optical defocus (Ho et al. 2012). This finding may be related to sign-dependent sensitivity to peripheral defocus for myopes (Rosén et al. 2012b), which could be due to specific combinations of eye aberrations at peripheral retina (Buehren et al. 2007; Thibos et al. 2013; Yamaguchi et al. 2013).

Based on this theory, different optical treatment strategies have been proposed and tested (Tabernero et al. 2009; Santodomingo-Rubido et al. 2012;

Ticak and Walline 2013). With regard to soft contact lenses, the effect on peripheral refraction (Rosén et al. 2012a; Kang et al. 2013) and on myopia progression (Walline et al. 2013) of several designs for presbyopia have also been investigated, but these lenses showed a negative impact on foveal vision because of the nature of their designs (Kollbaum et al. 2013). Consequently, new contact lenses have been proposed specifically for myopia treatment (Sankaridurg et al. 2011; Anstice and Phillips 2011). Unfortunately, little information is available concerning the impact on peripheral refraction of different variables such as pupil diameter (PD), refractive error, lens decentration and therapeutic power. In this sense, we think that some improvements could be obtained by making ray-tracing simulations on model eyes with a careful optimization of several lens design parameters.

Different human model eyes can be used to perform such simulations. For instance, the Model 1 proposed by Atchison (Atchison 2006), derived from experimental data, reflects the refraction related changes of the eye. It has been demonstrated that this model gives good predictions of the hyperopic peripheral shift in the mean sphere along the nasal visual field in myopic eyes (Atchison et al. 2006; Bakaraju et al. 2008), and it has also been employed to study the effect on PRE of contact lenses with different degrees of asphericity (Atchison 2006). Nevertheless, this model does not predict changes in the eye power with accommodation. The accommodation-dependent model eye proposed by Navarro & Santamaria represents an alternative to Atchison's model to simulate the relative effect of the accommodation on the PRE of an emmetropic eye (Navarro and Santamaria 1985).

In this work, a new contact lens design is presented as a potential therapeutic method for the treatment of myopia progression. These lenses have been specifically designed to correct the foveal refractive error of the eye and simultaneously to generate a myopic refractive error along the peripheral retina. Our design, named Fractal Contact Lens (FCL)(Furlan et al. 2012a), is inspired on Fractal Zone Plates, which are multifocal diffractive lenses characterized by a fractal focal structure (i.e. self-replicating pattern at different scales) along the optical axis (Saavedra et al. 2003). Under white-light illumination, this property optimizes their performance as image forming devices, because it makes them with an extended depth of field and a reduced chromatic aberration (Furlan et al. 2007). Different ophthalmic optical elements in the form of multifocal intraocular lenses and multifocal

contact lenses have been proposed based on Fractal zone plates (Furlan et al. 2012a). In particular, the FCLs for myopia treatment (Furlan et al. 2012b) are multi-zone contact lenses with a larger central zone than those intended for presbyopia correction, previously developed (Furlan et al. 2012a). The outer zones of the FCLs are designed to obtain a myopic PRE without producing a secondary image at the central fovea in normal photopic vision and to not interfere with the normal functioning of the accommodation system in myopic young subjects. Simulations of the FCLs performance in model eyes are simulated with Zemax ray tracing software and compared with those calculated by the use of another contact lens specifically proposed for the treatment of myopia progression: The Dual Focus (DF) (Anstice and Phillips 2011). Our purpose is to show that FCLs can improve the optical performance of the DF lenses, producing a higher myopic PRE without compromising the foveal image quality over a wide range of viewing conditions.

2.1.3. Methods

2.1.3.1 Contact Lenses

FCL design for myopia treatment consists of six refractive zones, (three correction (C) zones and three treatment (T) zones). The radii of the zones are distributed from center to periphery according to the triadic fractal Cantor set (Saavedra et al. 2003; Monsoriu et al. 2004) along of the squared radial coordinate. As illustrated in Fig. 1A, the diameters of the FCL zones are C1 = 4.50 mm, T1 = 6.50 mm, C2 = 7.91 mm, T2 = 11.42 mm, C3 = 12.27 mm and T3 = 13.14 mm. The optical power of the correction zones compensates the refractive error of the eye, while the treatment zones produce simultaneously a myopic focus on the peripheral retina without affecting the foveal image, at least under photopic conditions. In this way, a FCL behaves as a multi-zone refractive lens, with negligible diffractive effects because it has a relatively low number of wide zones (Furlan et al. 2012b). The other lens chosen for comparison (Fig. 1B): The DF soft contact lens (Phillips J 2008; Anstice and Phillips 2011) has three correction (C) and two treatment (T) zones. From center to periphery, the diameter of the zones are C1 = 3.36 mm, T1 = 4.78 mm, C2 = 6.75 mm, T2 = 8.31 mm and C3 = 11.66 mm (Fig. 1B).

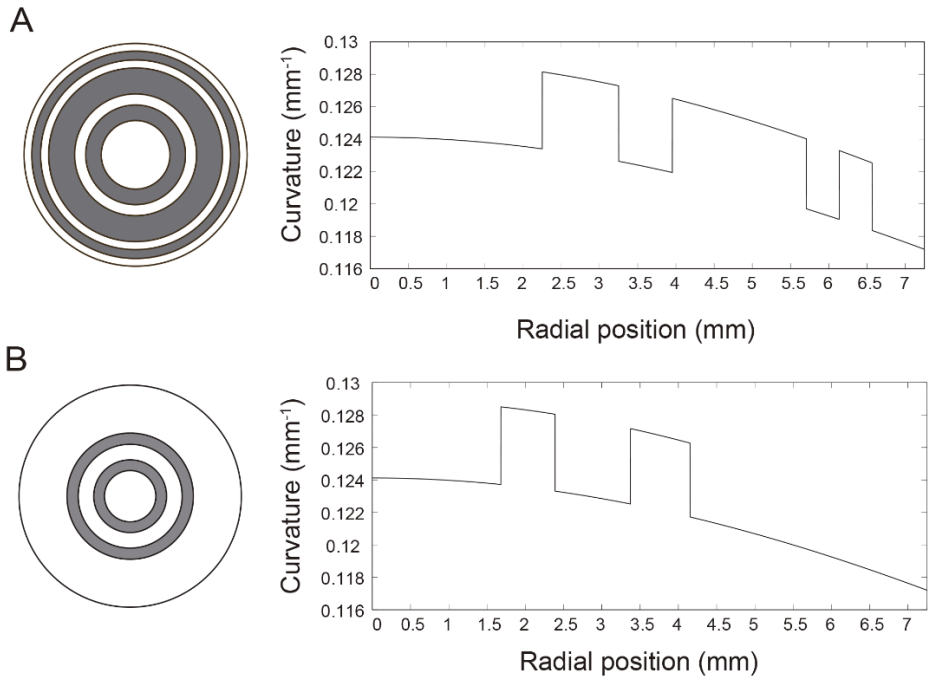

Figure 1 Graphical sketch of (A) FCL and (B) DF lens. Front view with zone sizes in gray for treatment zones and white for correction zones (left), and a section view with the curvature along the radial position (right).

2.1.3.2 Ray Tracing

The performance of our designs was tested by raytracing simulations using a commercially available software package (Zemax 13 SE; Zemax Development Corporation, Bellevue, WA). Myopic eyes were simulated with the model eye proposed and tested by Atchison (Model 1) because this model includes spectacle refraction-related changes of the anterior corneal radius, vitreous length and retinal shape, and accurately predicts the hyperopic peripheral shift in the mean sphere measured in myopic eyes along the nasal visual field (Atchison 2006). However, this model eye does not allow different levels of accommodation. Therefore, instead of the myopic Model 1, the Navarro (Navarro and Santamaria 1985) model eye was employed to simulate accommodated eyes. Even though Navarro model does not con-

template different refractive errors, its use in this work is justified because it has been found that the effect of accommodation on PRE (mean sphere and astigmatism) is not significantly different between emmetropic and myopic eyes (Calver et al. 2007; Davies and Mallen 2009; Tabernero and Schaeffel 2009). Tables 1 and 2 show the Zemax parameters taken from the spreadsheet program for the Model 1 and Navarro models, respectively.

Table 1. Atchison myopic model eye parameters with spectacle refraction (SR) in D.

Zemax nº:Type	**Refractive Index (Medium) (555nm)**	**Radius (mm)**	**Thickness (mm)**	**Asphericity**
1:Standard	1 (Air)			
2:Standard	1.376 (Cornea ant.)	rc	0.55	-0.15
3:Standard	1.3374 (Cornea post.)	6.4	3.15	-0.275
4 †:Standard	1.3374 (Pupil)	Inf.	0	0
5: Gradient	Grad A (Ant. Lens)	11.48	1.44	-5
6: Gradient	Grad P (Equator)	Inf.	2.16	0
7:Standard	1.336 (Post. Lens)	-5.90	vl	-2
8: Biconic	(Retina)	rx, ry		Qx,Qy

† Aperture type: Float by Stop Size
rc= 7.77+ 0.022SR
Grad A = 1.371 + 0.0652778Z - 0.0226659 Z2 - 0.0020399(X2+ Y2).
Grad P = 1.418- 0.0100737 Z2 - 0.0020399(X2 + Y2).
vl = 16.28-0.299SR
rx=-12.91-0.094SR Qx=0.27+0.026SR
ry= -12.72+0.004SR Qy=0.25+0.017SR

As the model eyes are rotationally symmetric, PREs were computed only across one horizontal semimeridian of the eye in steps of 5º, from 0º to 35º. To determine the PREs, we followed a similar procedure as the one described in Ref. [20], i.e. for each angle of eccentricity, a thin lens (a paraxialXY (Zemax 2013) surface in Zemax) was located 0.2 mm in front of the cornea with a different value of tilt and decentration depending on the angle subtended by the chief ray. The paraxialXY surface acts as an ideal thin lens with optical power specified in two directions, (Fx) and (Fy) (Zemax 2013). Zemax Programming Language was employed to perform an optimization routine in attempt to obtain, for each angle, the values of Fx and Fy that

minimize the RMS spot radius with respect to the centroid. Decentrations and tilts were made by the Zemax coordinate break surface capability, applying decentrations before tilts and reversing the coordinate break surface before ray-tracing to the cornea.

Table 2. Escudero-Navarro model eye parameters with accommodation A in D.

Zemax nº:Type	**Refractive Index (Medium)(555nm)**	**Radius (mm)**	**Thickness (mm)**	**Asphericity**
1: Standard	1 (Air)			
2: Standard	1.376 (Cornea ant.)	7.72	0.55	-0.26
3: Standard	1.3374 (Cornea post.)	6.5	d_2	0
4†: Standard	1.3374 (Pupil)	Inf.	0	0
5: Gradient	n3 (Ant. Lens)	R_3	d_3	Q_3
6: Standard	1.336 (Post. Lens)	R_4	16.40398	Q_3
7: Biconic	(Retina)	-12		Q_4

† Aperture type: *Float by Stop Size*
R_3= 10.2-1.75 ln(A+1)
R_4= -6.0+0.2294 ln(A+1)
d_2= 3.05-0.05 ln(A+1)
d_3= 4.00+0.1 ln(A+1)
n_3= $1.42+9x10^{-5}(10A+A^2)$
Q_3= -3.1316-0.34 ln(A+1)
Q_4= -1.0-0.125 ln(A+1)

Table 3 shows the decentration and tilt values applied to paraxialXY surface and the respective position where the chief ray intersects the cornea. With the values of the parameters Fx and Fy given by the routine, the mean sphere M and the 90º–180º astigmatism J_{180} were obtained from (Atchison 2006):

$$M = (F_x + F_y)/2 \qquad (1)$$
$$J_{180} = (F_x - F_y)/2$$

Table 3. Decenter / Tilt values applied to the paraxialXY surface for each measure along the visual field.

Visual Field	Dec. X(mm)	Tilt Y(°)
40	3	-40
35	2.3	-35
30	1.95	-30
25	1.6	-25
20	1.25	-20
15	0.9	-15
10	0.6	-10
5	0.3	-5

The same Zemax procedure was performed with FCL and DF. The contact lenses were located between the paraxialXY surface and the cornea. The front surface of the contact lenses was modeled using a ZEMAX Binary Optic 4 surface, which supports a variable number of concentric radial zones of different powers with independent: radial size, conic and polynomial aspheric deformation. Although it has not been used in our simulations, all zones may also have a diffractive phase profile with independent coefficients (Zemax 2013). Despite the fact that FCLs can be fabricated in both soft and rigid gas permeable materials, in this work, we restricted the analysis to soft contact lenses in order to obtain results that could be compared with those obtained with DF. Considering soft contact lens flexure, the back surface radii (r_b) of contact lenses were considered the same of the cornea. The front radii (r) of the zones were calculated in terms of the back vertex power (BVP) as:

$$r = \frac{r_b(n_l - 1)}{n_l - 1 + (r_b BVP)} - \frac{t_c}{n_l} + t_c \qquad (2)$$

where t_c = 0.1mm is the thickness at the center of the contact lenses and n_l = 1.403 is the refractive index for the wavelength of 555 nm. We assumed that the asphericity of the contact lens surfaces matched the corresponding values of the model cornea (see Tables 1 and 2) since, as we mentioned above,

soft contact lenses conform exactly to the front corneal surface. This fact has been demonstrated in experimental studies (Garner 1977; Plainis and Charman 1998; Hong et al. 2001), and justified in previous theoretical calculations (Cox 1990). It is also important to note that model eyes do not consider changes to the curvature beyond the cornea (scleral curvature), therefore if back surface of the contact lens is considered with the same asphericity of the cornea, a perfect alignment will be obtained when r_b is similar to the cornea radius. The refractive index at the back surface of the contact lenses was set n=1 (air) and a thin tear film (n=1.336) was placed between the cornea and the contact lenses with the same curvature as both surfaces.

With the Zernike coefficients provided by Zemax, foveal images were simulated numerically using the standard Fourier techniques following the procedure detailed in Ref. Legras et al., i.e. by computing the optical transfer function (OTF) of the model eye wearing each type of lenses under different conditions (Legras et al. 2004). The image of the object was finally obtained by multiplying the computed OTF with the Fourier spectrum of the object (a set of optotypes) and doing an inverse Fourier transform. Finally, PRE was computed with and without FCL using the accommodated and unaccommodated Navarro model eye. We decided to use a PD of 3.5 mm for this analysis considering that near work is normally performed under photopic illumination. The same procedure that described previously with the myopic model was performed with two little variations. First, the soft contact lens parameters were fitted in accordance to the cornea parameters of the Navarro model. Second, the object was placed at infinity for distance vision and at 33.3cm in front the cornea (3.00 D for near vision).

2.1.4. Results

The FLC performance was first evaluated for a treatment zone power (TP) of +2.00 D in order to obtain results that could be compared with those obtained with the DF lens, which has been designed with the same TP. Figure 2 shows the PRE computed for myopic eyes along the horizontal meridian, up to 35° of visual field angle. Results for two myopic eyes are represented

in Fig. 2: -2.00 D (panels A and B), and -8.00 D (panels C and D) for two PDs, 3.5 mm and 5.5 mm. These correspond approximately to PDs of a 10-year-old child under photopic and mesopic levels of illumination, respectively (Watson and Yellott 2012). Regarding the mean sphere M, two common features of both lenses can be observed in Fig. 2A and in Fig. 2C. On the one hand, the relative peripheral myopic shift was lower for -8.00 D than for -2.00 D. We found that other values of myopia ranging between -2.00 D and -8.00 D (not shown) produced intermediate results. On the other hand, a central undercorrection was obtained in all cases, except for the FCL with a PD of 3.5mm. As can be seen, the amount of this under-correction was also dependent on the degree of myopia.

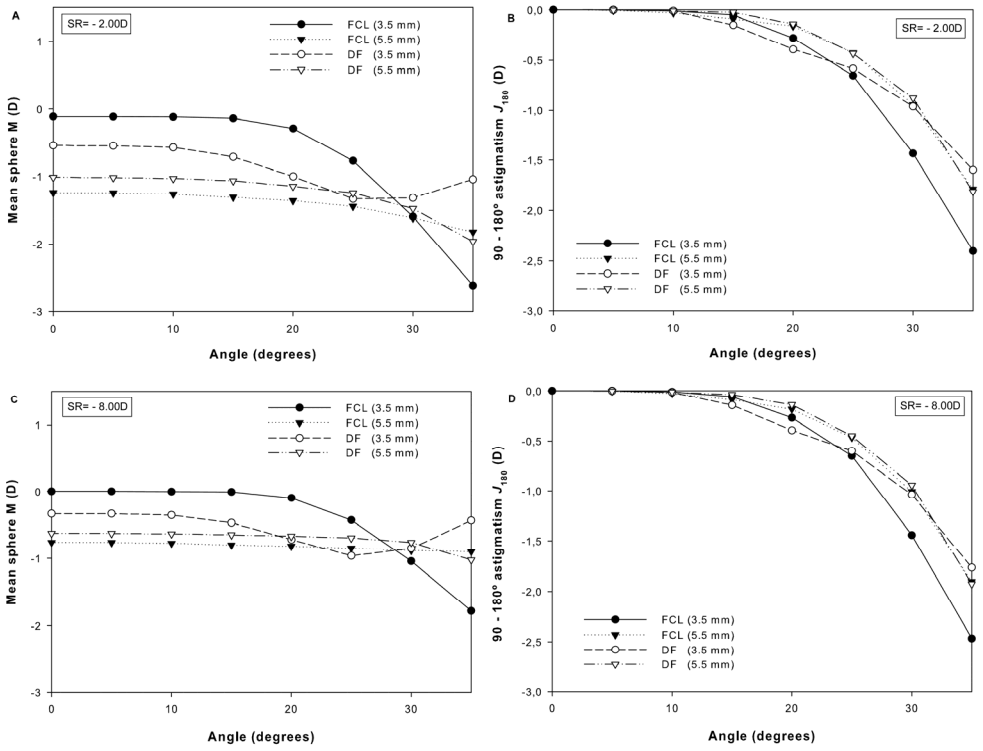

Figure 2. Mean sphere M (left) and astigmatism J180 (right) as a function of the visual field for -2D (top) and -8D (bottom) in the myopic Atchison model eye compensated with FCL and DF for pupil diameters of 3.5 and 5.5 mm.

This effect could be explained by the spherical aberration of the eye and by the relative influence of the treatment zones on central vision as PD increases. Note that, in spite of the fact that the PRE produced by both lenses was dependent on PD, the increase rate of the myopic shift with the eccentricity for a PD of 3.5 mm (circles in Fig. 2) was greater with the FCL than with the DF lens. Figs. 2 (B and D) illustrate the results obtained for 90º–180º astigmatism J_{180}. As happened with mean sphere, the peripheral astigmatism produced by both lenses was dependent on the PD but to a lower degree than M. Note that the peripheral astigmatism at 35º was higher for FCL than for DF.

Fig. 3 shows the effect of lens misalignment on PRE mean sphere. The values obtained for a FCL (Fig. 3A) and DF (Fig. 3B) centered on the eye's pupil were compared with those obtained when the lenses were decentered 0.5 mm downward and 0.5 mm to the temporal side. It can be seen that for a PD of 3.5 mm (circles), the influence of decentration was of less importance for FCL than for DF. In fact, higher values of PRE were obtained with FCL design.

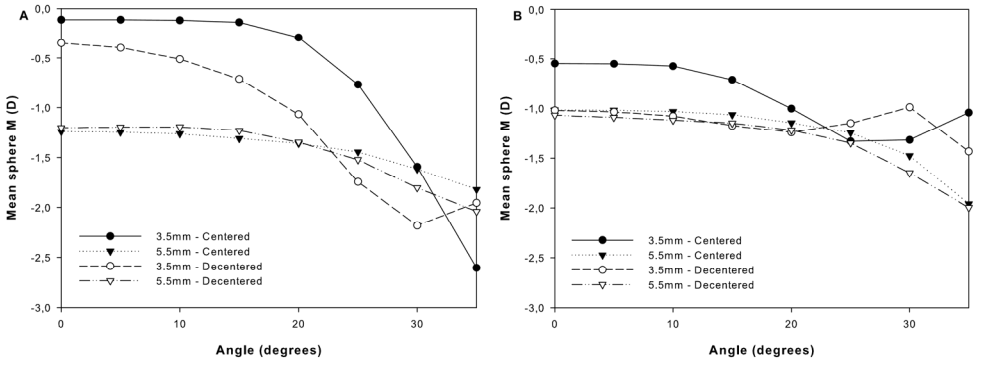

Figure 3. Impact of lens decentration on mean sphere (M) as a function of the visual field for a myopic model eye of -2D compensated with FCL (left) and DF (right). Closed symbols correspond to a centered lens. Open symbols correspond to a lens decentered 0.5 mm downward and 0.5 mm to the temporal side.

Related to the previous result, Fig. 4 shows the foveal images computed numerically. As can be seen, although both lenses have similar performance for a PD of 5.5 mm, the ghost images produced by the near focus are clearly more evident in the images corresponding to the DF lens.

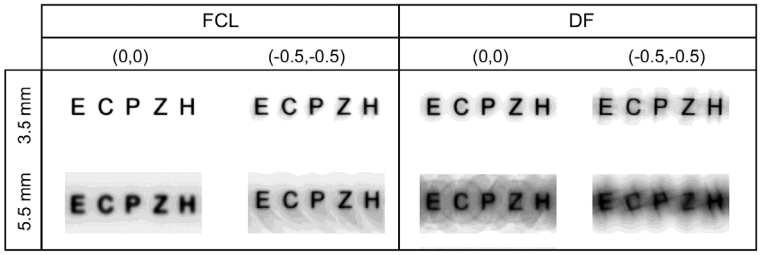

Figure 4. Images for a 20/50 set of letters at the central retina of a myopic Atchison model eye simulated for the same pupil diameters and decentration (mm) of the lenses represented in Fig. 3.

As we mentioned, FCL design admits different powers of treatment zone. The influence of this parameter on the PRE is represented in Fig. 5 for a -2.00 D myopic eye with a 3.5 mm PD. As can be observed, the effect of TP variation was more noticeable for the mean sphere, than for 90º–180º astigmatism. As TP increased, the PRE also increased in all cases, with a maximum increase for M at 35º of around 75% of the TP added, and nearly one half of this added value at 30º.

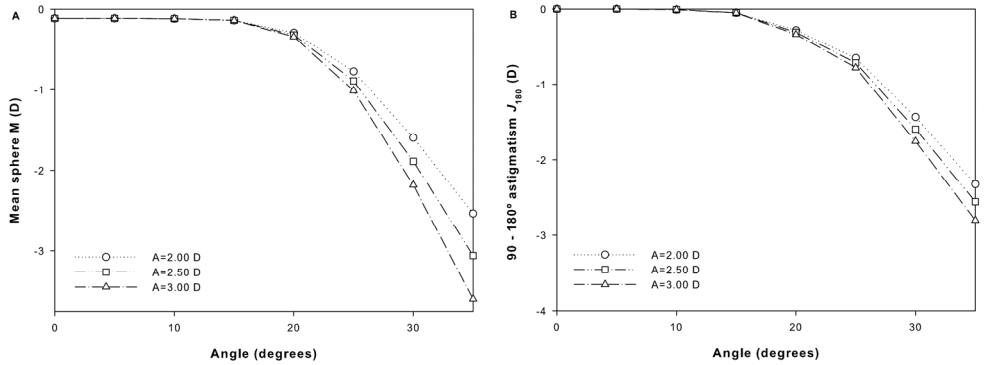

Figure 5. Mean sphere M (left) and astigmatism J180 (right) as a function of the visual field for a myopic model eye of -2D compensated with FCLs having different amount of therapeutic power.

The performance of the FCL in near vision was simulated with the Navarro model eye for a PD of 3.5 mm. The results are shown in Fig.6. As can be seen, when the accommodation was relaxed, the model eye without contact lens correction (naked eye [NE] curves in the figure) predicted that mean sphere PRE becomes more hyperopic as the peripheral angle increased. Then, a myopic shift was produced in the PRE in all cases for the accommodated eye (open symbols in the figure). Note that FCL produced a relative myopic shift, which reached its highest value at 35º for M and J_{180} in both cases, with accommodated and unaccommodated eye.

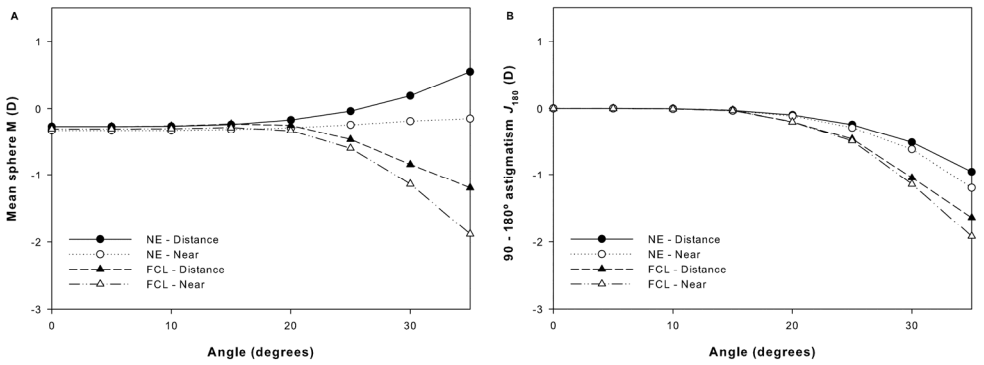

Figure 6. mean sphere M (left) and astigmatism J180 (right) as a function of the visual field for an emmetropic unaccommodated (distance) and accommodated 3D (near) Escudero-Navarro model eye; naked (NE), and fitted with a FCL with zero power at the correction zone and a therapeutic power of +2 D.

2.1.5. Discussion

2.1.5.1 Peripheral Refractive Error

We found that the PRE obtained with FCL was higher than the one produced by DF for refractive errors in the range of -2.00D to -8.00 D. However, our results seem to suggest that the effectiveness of both types of lenses with a fixed treatment power might depend on the degree of myopia, since a lesser effect was obtained for higher values of myopia. These results are explained by the increase of the hyperopic PRE with the refractive error (Atchison et al. 2006) that was properly modeled by Atchison (Atchison

2006). Therefore, as the model eye is more hyperopic in the periphery with the increase of the refractive error, the total peripheral myopic shift obtained with the contact lens was lower. In our case, we have demonstrated that this limitation could be partially solved by increasing the value of the treatment power, since this is a free parameter in FCL design that affects the PRE without compromise central vision, at least for PDs lower than 4.0mm.

Even though the impact on PRE produced by decentration of DF has not been previously reported, Sankaridurg et al. found asymmetries in the PRE with another therapeutic contact lens designed to reduce relative peripheral hyperopia (Sankaridurg et al. 2011). The authors attributed this to the fact that contact lenses were decentered from the visual axis, centering, as contact lenses actually do, on the geometric center of the cornea. In our case, we also simulated the typical decentration of the lenses. As a result, we found that the PRE and the optical quality at the fovea were less sensitive to decentrations with FCL than with DF. We also found that PD had a great impact in M at the periphery for both contact lens designs; therefore, we consider that therapeutic contact lenses should be designed to work optimally under photopic conditions. As far as the position of the first treatment zone is concerned, Anstice & Phillips measured PDs in eyes wearing DF in three different lighting conditions (Anstice and Phillips 2011). They suggested as an advantage of their design that the inner treatment zone fall inside the limits of the pupil even if miosis by accommodation is induced. Our simulations seem to contradict this assumption because we found a higher myopic shift with FCL, in which the inner zone fall outside the pupil under photopic conditions. Our results have a good agreement with those obtained with the orthokeratology technique (OK), on which the optic zone diameter of the OK lenses performs a change in the cornea curvature generally outside the pupil at photopic conditions (Kang and Swarbrick 2013). With respect to the influence of the number and extension of zones, our design has more zones that DF in order to obtain a larger therapeutic area affecting peripheral vision, since it has been hypothesized that effectiveness in myopia progression might be dependent on the extension of visual field that is manipulated (Smith 2013). In fact, Sankaridurg et al. compared myopia progression with different designs of spectacle lenses. They found that the slowest progression resulted with the spectacle lenses with the most extended treatment area (Sankaridurg et al. 2010).

Regarding to the values obtained for peripheral astigmatism, which has also been suggested as a variable involved in myopia progression (Charman and Radhakrishnan 2010; Faria-Ribeiro et al. 2013), we found that FCL and DF lenses produced a similar effect: the values of J_{180} decreased with the eccentricity and, contrary to what happened for the mean sphere, it was nearly independent of the refractive error and less sensitive to the PD. Furthermore, our results (Figs. 1, 5 and 6) allow to estimate the relative positions of the peripheral sagittal and tangential foci. In fact, from the variations of the mean sphere (M) and the astigmatic component J_{180} with the eccentricity, two features can be deduced. First, at least under photopic conditions, FCL causes that the entirety of the interval of Sturm lies in front of the peripheral retina, while the central image is positioned at the fovea. Second, the sagittal focus is more sensitive to the eccentricity than the tangential focus, because it moves away from the retina faster as the angle of incidence increases. However, our results for the mean astigmatism J_{180} should be interpreted with caution and they need to be confirmed in the future with the outcome of clinical research, since the Atchison eye Model 1 overestimates this parameter by about 50% (Atchison 2006).

2.1.5.2 Visual Performance

As we have shown, visual performance could be influenced by multizone contact lenses. DF and FCL produced an under-correction for the myopia refractive error, which was dependent on the PD. As we mentioned, this effect could be attributed to the spherical aberration and the impact on foveal vision of the treatment zones with increasing PD. In fact, this under-correction was negligible with FCLs for PDs up to around 4mm. Kollbaum et al. pointed out that patients wearing DF lenses may experience some decrease in visual performance similar to that obtained with contact lenses for presbyopia (Kollbaum et al. 2013); but in their work, it was not mentioned if lens centering and PD had been controlled. Although undercorrection has been reported as a myopiogenic stimulus (Berntsen and Kramer 2013), according to the very good clinical results reported with DF lenses (Anstice and Phillips 2011) and other multifocal contact lenses (Walline et al. 2013), it seems that this effect would be of little importance. Smith explained this fact considering that foveal myopic defocus around 0.50–0.75 D does not

create a myopic peripheral defocus under certain conditions (Smith 2013). For instance, for fixation distances inside 1m, it is likely that the foveal image will be in good focus and the eye will also experience peripheral hyperopia. However, in this situation, multifocal contact lenses also create a peripheral myopic defocus (Berntsen and Kramer 2013). This may explain the positive results in slowing myopia progression with multifocal contact lenses in contrast to those obtained with monofocal contact lenses producing an under-correction of the refractive error.

2.1.5.3 Effect of the Accommodation

Although the Navarro model eye was not designed to predict the PRE, it has been used for the analysis of the relative change of the PRE due to the accommodation (Lundström et al. 2009). Our results predicted that the peripheral hyperopic defocus generated by the NE decreased as the accommodation increased. From an optical design stand point, the change in peripheral refraction could be attributed to an increase in the curvature of field and to an increase in the amount of peripheral astigmatism of the eye on accommodation (Whatham et al. 2009). FCLs have been designed to not interfere with the normal functioning of accommodation; i.e. to avoid any additional blur at near vision under photopic lighting conditions. Therefore, the central zone of FCL covers the whole pupil area in this condition as opposed to DF on which the central zone is smaller (Anstice and Phillips 2011). According to our results, the FCL fitted to the Navarro (Navarro and Santamaria 1985) model eye produced a beneficial relative myopic shift, both with and without accommodation; i.e. the FCLs produced a relatively more myopic PRE at distance focus, which is maintained when the eye focused on a near object. Although we performed simulations with an emmetropic model eye, in our opinion these results might be extended to myopic eyes because, as we already mentioned, experimental evidence shows that the PRE profiles does not differ between emmetropes and myopes during accommodation (Calver et al. 2007; Davies and Mallen 2009; Tabernero and Schaeffel 2009).

2.1.5.4 Limitations of the Ray Tracing Simulations

Some limitations of this study are related to the model eyes employed. In spite of being the best option that we found for this purpose, these are far from being perfect models. In fact, as we mentioned above, Atchison Model 1 does not predict correctly the PRE along the vertical meridian and temporal visual field. Actually, clinical evidences of the PRE asymmetries in the visual field (Atchison 2006), and the impact of accommodation on the PRE in myopes (Lundström et al. 2009) are not fully predictable with any current model eye. In addition, we are aware of new accommodated model eyes that have been appeared (Navarro et al. 2007), but they were not considered in this study because they require special surfaces not supported by the Zemax SE version. Therefore, future improvements may be developed with the progress of the models and higher versions of Zemax.

In our simulations, we also assumed that soft contact lenses perfectly match the corneal surface. Although this assumption could be questioned, images obtained recently with ultra-high resolution OCT do support it (Wang et al. 2009) and are in agreement with findings of earlier studies obtained with a high illumination keratometer (Plainis and Charman 1998) and a Shack–Hartmann aberrometer (Hong et al. 2001). We have to recognize that we cannot directly extrapolate the results from our simulations to real efficacy of the lenses in clinic because of the above limitations. In addition, as like any other soft contact lens several variables will also influence the actual shape and performance of the contact lens on the eye: manufacturing technology (Maldonado-Codina and Efron 2005), lens materials (Tranoudis and Efron 2004), tear film (Rae and Price 2009), movement and flexure (Efron et al. 2008), etc. With regard to DF lens, we want to point out that our simulated design could not correspond exactly with the commercial lenses, since we retrieved its shape from the literature and we have not characterized the real contact lens.

2.1.6. Conclusions

In our opinion, ray tracing routines in model eyes can be considered as a versatile and fast procedure that could be very useful for predicting the outcomes of different lenses designed to slow the progression of myopia. Thus, the performance of a new design of soft contact lens for treatment of myopia progression (FCL) has been analyzed by ray tracing with Zemax 13 SE on the Atchison and Navarro model eyes. Results were compared with those provided by other soft contact lens designed for the same purpose (DF). According to our results, FCL performance was in general better than DF in terms of PRE and visual performance when contact lenses were evaluated under photopic conditions.

In spite of the previously discussed limitations, we believe that simulations performed in this work demonstrate the potentiality of the FCLs to produce a myopic relative peripheral error, which has been proposed as an optical treatment for myopia progression. In addition, we showed that the results are dependent on the PD; therefore changes in the design could be required depending on the patient. For this purpose, several design parameters can be adjusted in FCL to obtain the desired peripheral shift, such as diameter, number of zones, power of the treatment zone and asphericity. It is expected that clinical research will confirm our predictions about the PRE induced by FCLs. Finally, it is worth noting that FCL construction requires the same lathe technology employed in the fabrication of other commercial multizone contact lenses. Therefore, there are no special needs for its production. In fact, we are currently manufacturing the first prototypes of our designs intended to perform a long-term clinical study.

2.1.7. Acknowledgements

The authors wish to thank Dr. Laura Remón for her help in obtaining the simulations of retinal images. Two anonymous reviewers are also acknowledged for their comments.

2.1.8. Declaration of interest

The authors have a proprietary interest in FCLs. The author(s) have made the following disclosure(s):

J. B.: None; M. R.-V., A. P., J. A. M. and W. D. F. inventors (P) ES Patent P201330862, relating to contact lens design: assigned to Universitat Politècnica de València and Universitat de València. This research was supported by the Ministerio de Economía y Competitividad (grant FIS2011-23175), the Generalitat Valenciana (grant PROMETEO2009-077) and the Universitat Politècnica de València (grant INNOVA SP20120569), Spain.

2.1.9. References

Anstice NS, Phillips JR (2011) Effect of dual-focus soft contact lens wear on axial myopia progression in children. Ophthalmology 118:1152–61.

Atchison DA (2006) Optical models for human myopic eyes. Vis Res 46:2236–50.

Atchison DA, Pritchard N, Schmid KL (2006) Peripheral refraction along the horizontal and vertical visual fields in myopia. Vis Res 46:1450–8.

Bakaraju RC, Ehrmann K, Papas E, Ho A (2008) Finite schematic eye models and their accuracy to in-vivo data. Vis Res 48:1681–94.

Berntsen DA, Kramer CE (2013) Peripheral defocus with spherical and multifocal soft contact lenses. Optom Vis Sci 90:1215–1224.

Buehren T, Iskander DR, Collins MJ, Davis B (2007) Potential higher-order aberration cues for sphero-cylindrical refractive error development. Optom Vis Sci 84:163–174.

Calver R, Radhakrishnan H, Osuobeni E, O'Leary D (2007) Peripheral refraction for distance and near vision in emmetropes and myopes. Ophthalmic Physiol Opt 27:584–93.

Charman WN, Radhakrishnan H (2010) Peripheral refraction and the development of refractive error: a review. Ophthalmic Physiol Opt

30:321–38.

Cox I (1990) Theoretical calculation of the longitudinal spherical aberration of rigid and soft contact lenses. Optom Vis Sci 67:277–82.

Davies LN, Mallen EA (2009) Influence of accommodation and refractive status on the peripheral refractive profile. Br J Ophthalmol 93:1186–90.

Efron S, Efron N, Morgan PB (2008) Repeatability and reliability of ocular aberration measurements in contact lens wear. Cont Lens Anterior Eye 31:81–8.

Faria-Ribeiro M, Queirós A, Lopes-Ferreira D, Jorge J, González-Méijome JM (2013) Peripheral refraction and retinal contour in stable and progressive myopia. Optom Vis Sci 90:9–15.

Furlan WD, Saavedra G, Monsoriu JA (2007) White-light imaging with fractal zone plates. Opt Lett 32:2109–11.

Furlan WD, Saavedra G, Pons A, Bou PA, Monsoriu JA, Calatayud A, Remón L, Giménez F, Rojas JL, Larra E, Salazar P (2012a) Multifocal ophthalmic lens and method for obtaining same. ES Patent 070559. 2011. WO 2012/028755 A1.

Furlan WD, Saavedra G, Pons A, Bou PA, Monsoriu JA, Calatayud A, Remón L, Giménez F, Rojas JL, Larra E, Salazar P, Rodríguez-Vallejo M (2012b) Multifocal ophthalmic lens and method for obtaining same. Improvements. ES Patent P201330862.

Garner L (1977) Front surface topography of spherical flexible contact lenses on the eye. Aust J Optom 60:40–45.

Gwiazda J (2009) Treatment options for myopia. Optom Vis Sci 86:624–628.

Ho W-C, Wong O-Y, Chan Y-C, Wong S-W, Kee C-S, Chan HH-L (2012) Sign-dependent changes in retinal electrical activity with positive and negative defocus in the human eye. Vis Res 52:47–53.

Hong XIN, Himebaugh N, Thibos LN (2001) On-Eye evaluation of optical performance of rigid and soft contact lenses. Optom Vis Sci 78:872–880.

Kang P, Fan Y, Oh K, Trac K, Zhang F, Swarbrick HA (2013) The effect of

multifocal soft contact lenses on peripheral refraction. Optom Vis Sci 90:658–66.

Kang P, Swarbrick H (2013) Time course of the effects of orthokeratology on peripheral refraction and corneal topography. Ophthal Physiol Opt 33:277–82.

Kollbaum PS, Jansen ME, Tan J, Meyer DM, Rickert ME (2013) Vision performance with a contact lens designed to slow myopia progression. Optom Vis Sci 90:205–14.

Legras R, Chateau N, Charman WN (2004) A method for simulation of foveal vision during wear of corrective lenses. Optom Vis Sci 81:729–38.

Lundström L, Mira-Agudelo A, Artal P (2009) Peripheral optical errors and their change with accommodation differ between emmetropic and myopic eyes. J Vis 9:1–11.

Maldonado-Codina C, Efron N (2005) Impact of manufacturing technology and material composition on the surface characteristics of hydrogel contact lenses. Clin Exp Optom 88:396–404.

Monsoriu JA, Saavedra G, Furlan WD (2004) Fractal zone plates with variable lacunarity. Opt Express 12:4227–34.

Navarro R, Palos F, González L (2007) Adaptive model of the gradient index of the human lens. I. Formulation and model of aging ex vivo lenses. J Opt Soc Am A 24:2175–85.

Navarro R, Santamaria J (1985) Accommodation-dependent model of the human eye with aspherics. J Opt Soc Am A 2:1273–1281.

Phillips J (2008) Contact lens and method. US Patent 20080218687 A1.

Plainis S, Charman WN (1998) On-eye power characteristics of soft contact lenses. Optom Vis Sci 75:44–54.

Rae SM, Price HC (2009) The effect of soft contact lens wear and time from blink on wavefront aberration measurement variation. Clin Exp Optom 92:274–82.

Rosén R, Jaeken B, Lindskoog Petterson A, Artal P, Unsbo P, Lundström L (2012a) Evaluating the peripheral optical effect of multifocal contact lenses. Ophthalmic Physiol Opt 32:527–34.

Rosén R, Lundström L, Unsbo P (2012b) Sign-dependent sensitivity to peripheral defocus for myopes due to aberrations. Inves Opthal Vis Sci 53:7176–82.

Saavedra G, Furlan W, Monsoriu JA (2003) Fractal zone plates. Opt Lett 28:971–3.

Sankaridurg P, Donovan L, Varnas S, Ho A, Chen X, Martinez A, Fisher S, Lin Z, Smith EL, Ge J, Holden B (2010) Spectacle lenses designed to reduce progression of myopia: 12-month results. Optom Vis Sci 87:631–41.

Sankaridurg P, Holden B, Smith EL, Naduvilath T, Chen X, de la Jara PL, Martinez A, Kwan J, Ho A, Frick K, Ge J (2011) Decrease in rate of myopia progression with a contact lens designed to reduce relative peripheral hyperopia: one-year results. Invest Ophthalmol Vis Sci 52:9362–7.

Santodomingo-Rubido J, Villa-Collar C, Gilmartin B, Gutiérrez-Ortega R (2012) Myopia control with orthokeratology contact lenses in Spain: refractive and biometric changes. Invest Ophthalmol Vis Sci 53:5060–5.

Smith EL (2012) The Charles F. Prentice award lecture 2010: A case for peripheral optical treatment strategies for myopia. Optom Vis Sci 88:1029–1044.

Smith EL (2013) Optical treatment strategies to slow myopia progression: Effects of the visual extent of the optical treatment zone. Exp Eye Res 114:77–88.

Smith EL, Kee C, Ramamirtham R, Qiao-Grider Y, Hung LF (2005) Peripheral vision can influence eye growth and refractive development in infant monkeys. Invest Ophthalmol Vis Sci 46:3965–3972.

Tabernero J, Schaeffel F (2009) Fast scanning photoretinoscope for measuring peripheral refraction as a function of accommodation. J Opt Soc Am A Opt Image Sci Vis 26:2206–10.

Tabernero J, Vazquez D, Seidemann A, Uttenweiler D, Schaeffel F (2009) Effects of myopic spectacle correction and radial refractive gradient spectacles on peripheral refraction. Vis Res 49:2176–86.

Tarutta E, Chua W-H, Young T, Goldschmidt E, Saw S-M, Rose KA, Smith

EL, Mutti DO, Ashby R, Stone RA, Wildsoet C, Howland HC, Fischer AJ, Stell WK, Reichenbach A, Frost M, Gentle A, Zhu X, Summers-Rada J, Barathi V, Jiang L, McFadden S, Guggenheim JA, Hammond C, Schippert R, To C-H, Gwiazda J, Marcos S, Collins M, Charman WN, Artal P, Tabernero J, Atchison DA, Troilo D, Norton TT, Wallman J (2011) Myopia: Why study the mechanisms of myopia? Novel approaches to risk factors signalling eye growth- How could basic biology be translated into clinical insights? Where are genetic and proteomic approaches leading? How does visual function contribute to an. Optom Vis Sci 88:404–447.

Thibos LN, Bradley A, Liu T, López-Gil N (2013) Spherical aberration and the sign of defocus. Optom Vis Sci 90:1284–91.

Ticak A, Walline JJ (2013) Peripheral optics with bifocal soft and corneal reshaping contact lenses. Optom Vis Sci 90:3–8.

Tranoudis I, Efron N (2004) Parameter stability of soft contact lenses made from different materials. Cont Lens Anterior Eye 27:115–31.

Troilo D, Gottlieb MD, Wallman J (1987) Visual deprivation causes myopia in chicks with optic nerve section. Curr Eye Res 6:993–9.

Walline JJ, Greiner KL, McVey ME, Jones-Jordan LA (2013) Multifocal contact lens myopia control. Optom Vis Sci 90:1207–14.

Wang J, Jiao S, Ruggeri M, Shousha MA, Shousha MA, Chen Q (2009) In situ visualization of tears on contact lens using ultra high resolution optical coherence tomography. Eye Contact Lens 35:44–9.

Watson AB, Yellott JI (2012) A unified formula for light-adapted pupil size. J Vis 12:1–16.

Whatham A, Zimmermann F, Lazon P, Jara D (2009) Influence of accommodation on off-axis refractive errors in myopic eyes. J Vis 9:1–13.

Yamaguchi T, Ohnuma K, Konomi K, Satake Y, Shimazaki J, Negishi K (2013) Peripheral optical quality and myopia progression in children. Graefes Arch Clin Exp Ophthalmol 19770614.

Zemax R (2013) Zemax 13. Optical Design Program. Surface Types. 345–346.

Physics > Medical Physics

Two-dimensional relative peripheral refractive error induced by Fractal Contact Lenses for myopia control

Manuel Rodriguez-Vallejo, Karina Naydenova, Juan A. Monsoriu, Vicente Ferrando, Walter D. Furlan

(Submitted on 21 Sep 2016)

Purpose: To assess the peripheral refraction induced by Fractal Contact Lenses (FCLs) in myopic eyes by means of a two-dimensional Relative Peripheral Refractive Error (RPRE) map.
Methods: FCLs prototypes were specially manufactured and characterized. This study involved twenty-six myopic subjects ranging from -0.50 D to -7.00 D. The two-dimensional RPRE was measured with an open-field autorefractor by means of tracking targets distributed in a square grid from -30 degrees (deg) nasal to 30 deg temporal and 15 deg superior to -15 deg inferior. Corneal topographies were taken in order to assess correlations between corneal asphericity, lens decentration and RPRE represented in vector components M, J0 and J45.
Results: The mean power of the FCLs therapeutic zones was 1.32 +/- 0.28 D. Significant correlations were found between the corneal asphericity and vector components of the RPRE in the nacked eyes. FCLs were decentered a mean of 0.7 +/- 0.19 mm to the temporal cornea. M decreased asymmetrically between nasal and temporal retina after fitting the FCLs with a significant increment of the myopic shift besides 10 deg ($p<0.05$) and the induced myopic shift at 25 deg and 30 deg decreased with FCLs decentration to temporal cornea. The peak of maximum myopic shift at the peripheral retina (M= -1.3 D) was located at 20 deg. Two-dimensional maps showed uniform significant differences in extreme positions of the visual field in comparison with the horizontal RPRE for M and J0, but not for J45.
Conclusions: FCLs measured in myopic eyes showed a similar performance than the reported in previous ray-tracing studies with a small bias explained by the manufacturing process and the lens decentration. Two-dimensional maps are preferable for assessing J45 changes due to the lens.

Comments: 12 pages, 3 figures, 1 table
Subjects: **Medical Physics (physics.med-ph)**
Cite as: **arXiv:1609.06987 [physics.med-ph]**
(or **arXiv:1609.06987v1 [physics.med-ph]** for this version)

Submission history

From: Manuel Rodriguez-Vallejo [view email]
[v1] Wed, 21 Sep 2016 18:17:47 GMT (457kb)

2.2. Two-dimensional relative peripheral refractive error induced by Fractal Contact Lenses for myopia control.

Manuel Rodriguez-Vallejo[1*], Karina Naydenova[3], Juan A. Monsoriu[2], Vicen-te Ferrando[3] and Walter D. Furlan[3]

[1]*Qvision, Unidad de Oftalmología, Vithas Hospital Virgen del Mar, 04120, Almería*

[2]*Centro de Tecnologías Físicas, Universitat Politècnica de València, 46022 Valencia, Spain*

[3] *Departamento de Óptica, Universitat de València, 46100 Burjassot, Spain*
[*]*Corresponding author: manuelrodriguezid@qvision.es*

2.2.1. Abstract

Purpose: To assess the peripheral refraction induced by Fractal Contact Lenses (FCLs) in myopic eyes by means of a two-dimensional Relative Peripheral Refractive Error (RPRE) map.

Methods: FCLs prototypes were specially manufactured and characterized. This study involved twenty-six myopic subjects ranging from -0.50 D to -7.00 D. The two-dimensional RPRE was measured with an open-field autorefractor by means of tracking targets distributed in a square grid from -30º nasal to 30º temporal and 15º superior to -15º inferior. Corneal topographies were taken in order to assess correlations between corneal asphericity, lens decentration and RPRE represented in vector components M, J_0 and J_{45}.

Results: The mean power of the FCLs therapeutic zones was 1.32 ± 0.28 D. Significant correlations were found between the corneal asphericity and vector components of the RPRE in the nacked eyes. FCLs were decentered a mean of 0.7 ± 0.19 mm to the temporal cornea. M decreased asymmetrically between nasal and temporal retina after fitting the FCLs with a significant

increment of the myopic shift besides 10º ($p<0.05$) and the induced myopic shift at 25º and 30º decreased with FCLs decentration to temporal cornea. The peak of maximum myopic shift at the peripheral retina (M= -1.3 D) was located at 20º. Two-dimensional maps showed uniform significant differences in extreme positions of the visual field in comparison with the horizontal RPRE for M and J_0, but not for J_{45}.

Conclusions: FCLs measured in myopic eyes showed a similar performance than the reported in previous ray-tracing studies with a small bias explained by the manufacturing process and the lens decentration. Two-dimensional maps are preferable for assessing J_{45} changes due to the lens.

Keywords: myopia progression, contact lenses, fractal, peripheral refractive error, two-dimensional maps.

2.2.2. Introduction

During the last years myopia control therapies have spawned a large interest among researchers and vision care professionals (Wolffsohn et al. 2016). Several methods have been proposed to slow myopia progression, among them, non-pharmacological treatments like orthokeratology and peripheral defocus modifying contact lenses (CLs) achieved very good outcomes (Huang et al. 2016), especially in patients with eso fixation disparity at near (Turnbull et al. 2016). The effect of such CLs is attributed to the induction of a myopic Relative Peripheral Refractive Error (RPRE) (Rodríguez-Vallejo et al. 2014a; González-Méijome et al. 2016; Queirós et al. 2016; Walline 2016). Different designs of multifocal CLs were proposed to this aim (González-Méijome et al. 2016), and consequently, the amount and extension of the induced RPRE vary among lenses (Queirós et al. 2016).

In a previous paper (Rodríguez-Vallejo et al. 2014a) we have proposed, and numerically validated, a new design of CLs for myopia control, named Fractal Contact Lenses (FCLs). However, the promising performance obtained with FCLs in model eyes has still not been validated in real eyes. Therefore, the main aim of this study is to assess the peripheral refraction induced by FCLs in myopic real eyes. To do that, RPRE was measured in a 2D matrix of discrete points of the retina; and this data set was represented as 2D pow-

er contour plot for the three components of the dioptric power vectors (M, J_0 and J_{45}). We show that this new representation of the RPRE, employed in this work for the first time in the literature, offers a more complete view of the lens performance than the usually used only along the horizontal field.

2.2.3. Methods

2.2.3.1 Contact Lenses

FCLs prototypes were specially manufactured for this study. All lenses were made of Hioxifilcon A (Benz G5X p-GMA/HEMA)(Benz 2016), which has 1.401 of refractive index (hydrated and at 35º), using a precision lathe (Optoform 40, Sterling Ultra Precision, Largo, USA). A stock of 15 FCLs with treatment powers of +2.00 D was fabricated according to the design previously described (Rodríguez-Vallejo et al. 2014a). The FCLs prototypes had a diameter of 14.50 mm, and central powers ranging from -0.50 D to -7.00 D in -0.50 D steps with two different base curves: 8.4 mm and 8.6 mm. Power profiles of the stock lenses were measured with the Nimo TR1504 (LAMBDA-X, Nivelles, Belgium)(Joannes et al. 2010) contact lens power mapper (version 4.2.6.0 r477). A custom function in MATLAB (R2013a; Mathworks, Inc., Natwick, MA) was developed in order to detect the power transition between therapeutic and compensation zones. Then, the true therapeutic powers for each lens were redefined as the difference of the mean power along the therapeutic zones and the mean power along the compensation zones.

2.2.3.2 Subjects and Procedures

Twenty-six subjects (mean age 23.77 ± 3.62 years) were recruited from students at the University of Valencia, Spain (18 females and 8 males). All underwent a complete eye exam including objective and subjective refraction and slit-lamp exploration. Inclusion criteria were myopic eyes ranging from -0.50 D to -7 D (mean -2.62 ± 1.59 D) and astigmatism equal or under

-0.75 D with no ocular diseases, strabismus or amblyopia. Only right eyes were considered. The research adhered to the tenets of the Declaration of Helsinki, with the research approved by the University of Valencia and informed consent obtained from all participants.

Before fitting the FCLs, corneal topographies were taken for the naked eye with the Keratron Scout (Optikon 2000 SpA, Rome, Italy) until to obtain at least three of them with a reproducibility inside ±0.25D. Elevation data were exported in binary format (.XLB and .ZLB extension files) and a custom software was programmed in MATLAB in order to compute corneal asphericities, fitting elevation data to a conic function (Calossi 2007), at nasal and temporal sides from the normal vertex along the horizontal 0-180º, considering an extension of 4 mm from the vertex.

Subjects were fitted with the FCL that best matched one of the two possible base curves and the back vertex powers closer to the spectacle refraction. The behaviour of the lenses, movement and centration, were evaluated by the examiner twenty minutes after fitting. Then corneal topographies were taken again but with the patient wearing the best fitted FCL. The distance from the centre of the first therapeutic zone and the pupil entrance centre was measured with the caliper tool of the Keratron Scout software to obtain the FCL decentration.

2.2.3.3 Peripheral Refractive Error

Central and peripheral refraction were measured with an open-field autorefractor (Grand-Seiko WAM-5500, Grand-Seiko Co., Ltd., Hiroshima, Japan) in non-cyclopegic conditions. The environmental light was 150 lux, since at this condition the pupil diameter was higher enough to measure the peripheral refractive error. Tracking targets were distributed in a square grid from -30º (nasal retinal area) to 30º (temporal retinal area) and 15º superior to -15º inferior, as shown in Fig. 1. Fixation targets were 1 inch high contrast squares located on a wall at 2 meters from the eye. Measurements were taken with the eye rotation technique (Queirós et al. 2016).

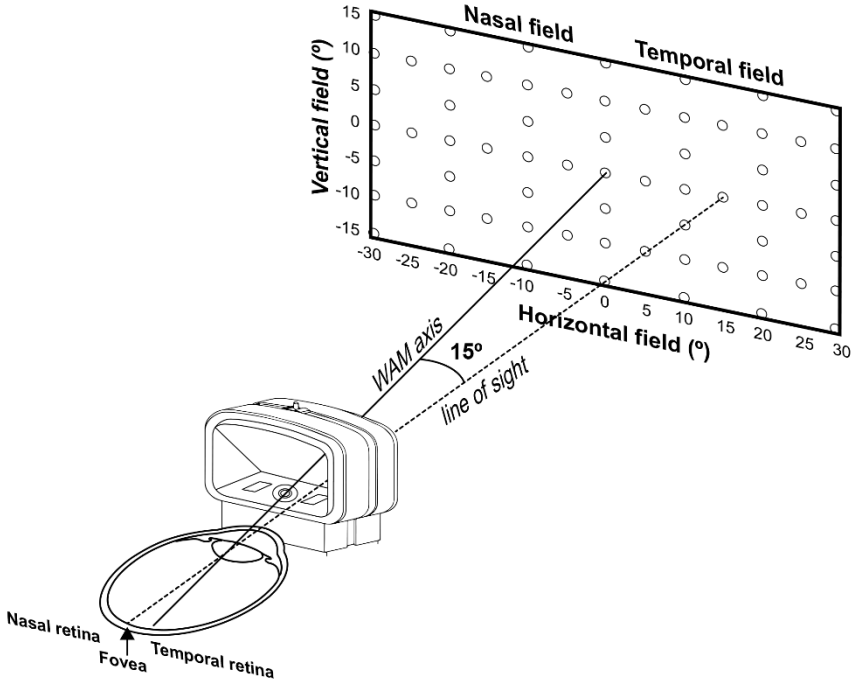

Figure 1. Schematic representation of the measurement process with WAM-5500. With the right eye rotated 15 degrees looking at the temporal field target, the system is measuring the refractive error at the temporal retinal area. The circles over the wall represent the discrete points measured with the eye rotation.

A MATLAB code was developed to obtain repeatable measures of sphere, cylinder and axis at each point of the field and to compute the mean values of vector components according to Fourier analysis (M, J_0 and J_{45}) (Thibos et al. 1997). The peripheral refractive error was measured without FCLs (baseline state) and wearing FCLs. Recorded data was used to compute, the tangential ($F_T = M + J_0$) and sagittal ($F_S = M - J_0$) power errors along the horizontal meridian (Queirós et al. 2016); and two dimensional RPRE contour maps for M , J_0 and J_{45}. These maps were calculated using custom software (Mathematica version 10; Wolfram Research, Inc., Oxfordshire, UK). A cubic interpolation was employed to represent contour lines of equal powers in steps of 0.12 D.

2.2.3.4 Statistical Analysis

Normal distributions were confirmed with the Shapiro-Wilk test. Paired t-tests were used to analyze the differences between the RPRE vector components with the FCLs and the nacked eye. Pearson correlation analyses were performed to determine the relationship between variables. Power analysis was performed using G Power version 3.1.9.2 (available at http://www.gpower.hhu.de/). The sample size in this study offered 88% statistical power at a 5% level to detect a difference in RPRE of 0.25 D with and without FCLs when the expected standard deviation (SD) of the mean difference was 0.44 D (obtained from previous measures). The data were managed using SPSS software version 20 (SPSS Inc., Chicago, IL, USA), and $p<0.05$ was considered to indicate significance.

2.2.4. Results

2.2.4.1 Contact Lenses: Power Profiles and Fitting

The power profiles measured with NIMO resulted in a mean power of 1.32 ± 0.28 D at the therapeutic zones. Theoretical compensation power of the FCL prototypes was negatively correlated with the experimental therapeutic power ($r = -0.786$, $p = 0.007$).

Topological data revealed that contact lenses were decentered towards temporal cornea, ranging from 0.39 mm to 1.05 mm (mean 0.7 ± 0.19 mm) whereas mean vertical displacement was 0.00 ± 0.49 mm [ranging from 0.64 mm down to 1.38 mm up]. Considering the lens decentration in polar coordinates, the lenses were decentered a mean of 0.83 ± 0.27 mm at 185 ± 32 degrees. The mean value of the pupil entrance diameter was 3.67 ± 0.53 mm measured with the Keratron in the nacked eye.

2.2.4.2 Horizontal Relative Peripheral Refractive Error

Mean corneal asphericity from the corneal vertex to the 4 mm of semi-chord at temporal cornea was -0.07 ± 0.09 and -0.24 ± 0.18 for the same extension at nasal cornea in the nacked eyes. Significant correlations were found between the corneal asphericity and vector components of the RPRE (Table 1) and no correlations were found between the amount of lens decentering and the asphericity of the cornea along temporal and nasal sides.

Table 1. Significant correlations between Relative Peripheral Refractive Error (RPRE) vector components and asphericity at the Temporal or Nasal semi-chord of the cornea from the normal vertex to 4 mm of radial position. Correlations for retinal areas evaluated and not represented in the table were not significant.

Retinal Area (°)	RPRE (D) Mean ± SD	Corneal side	Pearson r
M			
-25 (NR)	-0.22±0.47	Temporal	-0.452, p=0.040
-15 (NR)	-0.21±0.40	Temporal	-0.526, p=0.014
-10 (NR)	-0.27±0.29	Temporal	-0.436, p=0.048
J0			
+25 (TR)	-0.82±0.29	Nasal	-0.572, p=0.007
+20 (TR)	-0.56±0.22	Nasal	-0.562, p=0.008
+10 (TR)	-0.1±0.2	Nasal	-0.505, p=0.019
J45			
+30 (TR)	0.11±0.25	Nasal	-0.581, p=0.006
+20 (TR)	0.05±0.15	Nasal	-0.465, p=0.033
+10 (TR)	-0.01±0.09	Nasal	-0.478, p=0.028
+5 (TR)	0.01±0.09	Nasal	-0.467, p=0.033

NR=Nasal retina; TR= Temporal retina.

Fig. 2A shows the spherical equivalent (M) along the horizontal retinal area at the baseline state and wearing the FCLs. An increase of the myopic shift was found with the FCLs at the temporal retina from 10º to 30º ($p<0.05$). The F_T myopic shift was increased after the FCLs fitting as it is shown is Fig. 2B with a peak located at 20º of the temporal retina, in the same way that the M component (Fig. 2A). F_S was also increased myopically even

though less markedly than F_T but highly enough to move the sagittal foci to the front of the retina with the FCL (Fig. 2C).

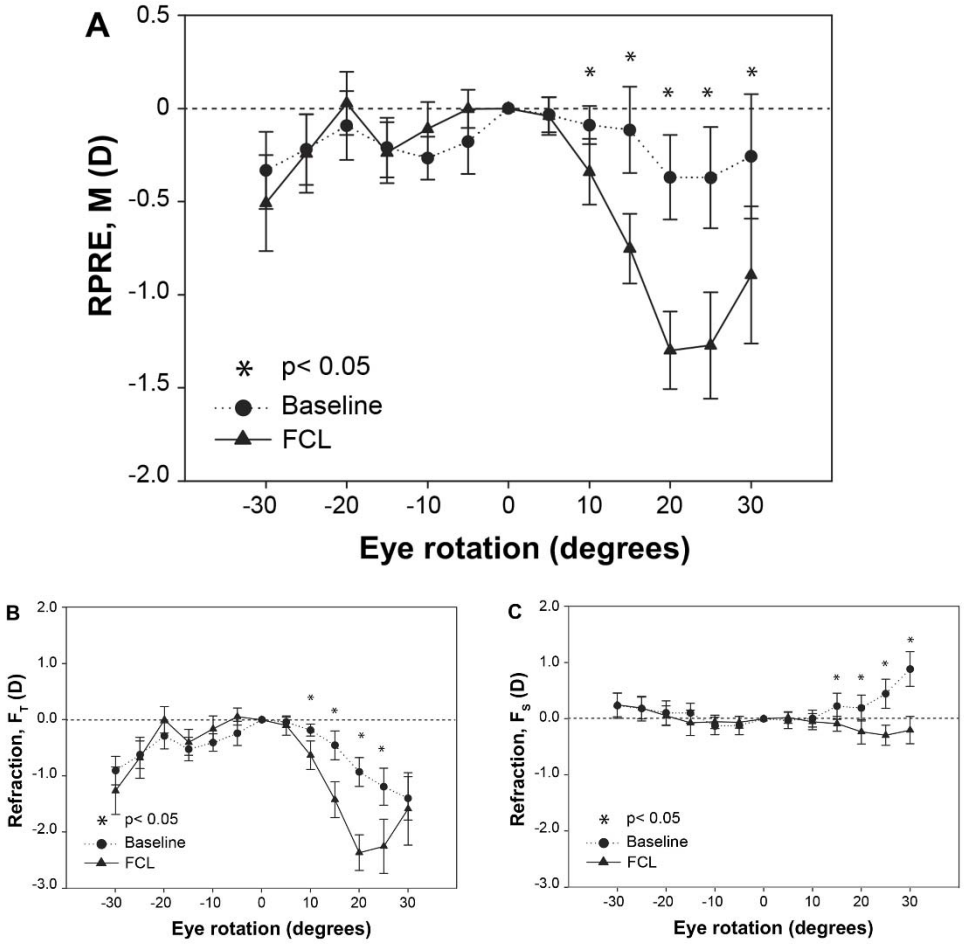

Figure 2. (A) Refractive spherical equivalent in the nacked eye (Baseline) and with Fractal Contact Lenses (FCL). (B) Tangential and (C) Sagittal powers along the horizontal retina in the baseline state and with FCLs. Positive values of eye rotation correspond to the temporal retina and negative values to nasal retina. An asterisk over each eccentricity was represented to describe significant differences between baseline and with FCLs (p<0.05).

2.2.4.3 Two-Dimensional Relative Peripheral Refractive Error

Baseline mean values of the RPRE for M, J_0 and J_{45} are represented in Figs. 3A, 3D and 3G, respectively. Figs. 3B, 3E and 3H show the mean values for the same eyes wearing FCLs. The measured points are represented by means of circles over the difference maps (Figs. 3C, 3F and 3I). Crosses were drawn inside the circles for those positions where significant differences ($p<0.05$) between eyes with and without the FCLs were found.

Fig. 3C shows that for the spherical equivalent, the mean myopic shift induced by FCLs increases with the eccentricity and becomes significant ($p < 0.05$) at 10º in the temporal field. A clear oblique astigmatism was presented at extreme positions of the visual field in both situations (see Fig. 3G and Fig. 3H) with opposite signs for J_{45} between temporal/nasal and inferior/superior. However, as can be seen in Fig. 3I, the oblique astigmatism induced by the FCLs was almost negligible along the horizontal and vertical central coordinates but significant in extreme positions.

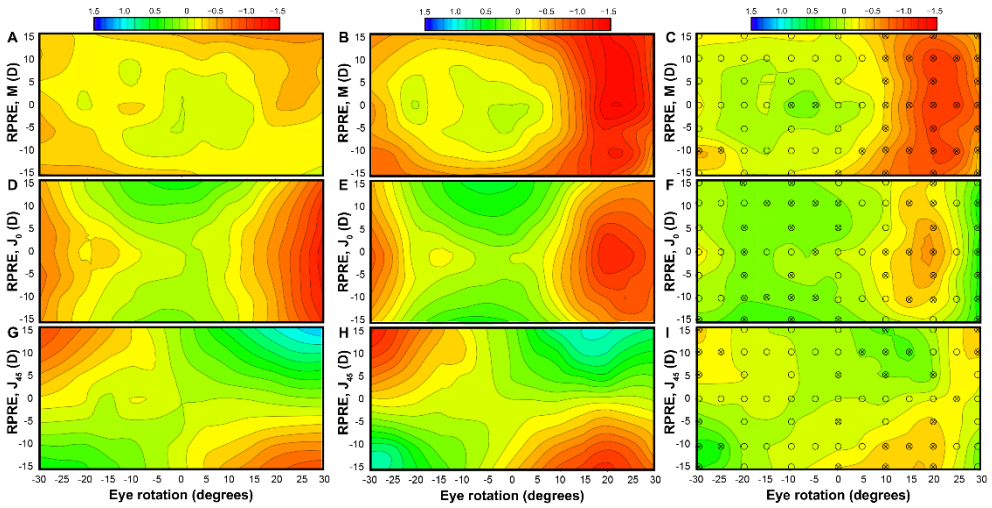

Figure 3. Relative peripheral refractive error (RPRE) vector components M, J0 and J45 in the baseline state (A, D and G) and with FCLs (B, E and H). Differences for the three components between FCLs and baseline state are represented in C, F and I. Circles in the difference maps were used to describe the eye rotation for which direct measures were taken whereas crosses were used to indicate the rotations with significant differences (P<0.05). Color maps were obtained with cubic interpolations across the most nearest measured points.

We found that myopic shift (M) induced by the FCLs at 25º and 30º along the temporal field decreased with the lens decentration through the temporal side of the cornea (r=0.46, p=0.022) and (r=0.47, p=0.018) respectively. These correlations were more marked when the displacement vector (considering x and y) was considered instead of the unique displacement along the horizontal, r = 0.50 (p = 0.013) at 25º and r = 0.54 (p = 0.006) at 30º.

2.2.5. Discussion

Studies conducted on animals have established bases of the optical compensations to slow down myopia progression on humans. However, the mechanisms by which the visual system responds to the optical cues in the emmetropization process are still not clear. Experimental studies in animals found that refractive error in the peripheral retina can regulate the eye growth (Smith et al. 2005), and derived from these studies, relative peripheral hyperopia was suggested as a possible factor that could cause the progression of myopia (Smith 2012). Thus the goal in the current treatments, such as ortokeratology or multifocal contact lenses is to create a relative peripheral myopia to slowing down myopia progression (Huang et al. 2016). In this context, it is important to take into account that recent studies (Atchison et al. 2015; Hartwig et al. 2016), involving children and young adults, demonstrated that a relative peripheral hyperopia along the horizontal visual field does not predict development nor progression of myopia in these populations. One of the possible explanations of these apparently contradictory results could be the lack of information in clinical studies about the behaviour of RPRE for the M, J_0 and J_{45} on regions of the retina beyond the horizontal meridian. Related to this, findings obtained from animal studies suggest that the analysis of M component might not be enough to describe the emmetropization process (Queirós et al. 2016). Kee et. al found that emmetropization in infant monkeys can also vary with the imposition of cylindrical lenses by means of directing the process towards one of the two focal planes with independence of the astigmatism orientation (Kee et al. 2004). This is in a partial agreement with Chu et al. who also reported an eye expansion according to the amount of the cylinder in chicks, but in this case with dependence of the cylinder orientation (Chu and Kee 2015). Furthermore, the optical responses during the emmetropization process might vary

depending on the stimulated retinal areas (Charman 2011) because of the neural anisotropy between central and peripheral retina (Zheleznyak et al. 2016). Therefore, to obtain information about RPRE for the three components M, J_0 and J_{45} of the eye refraction seems to be of essential importance in understanding basic phenomena with important clinical consequences. In this sense, the main advantage of our approach from previous studies is that we have analysed the effect in the central and paracentral retina obtaining 2D information about the astigmatism at other positions besides the horizontal direction.

2.2.5.1 Contact Lenses

Some important issues should be taken into account in order to interpret our results and correlate them with the theoretical optical performance of the FCLs design (Rodríguez-Vallejo et al. 2014a). First, the mean power at the treatment zones (+1.32 D) was lower than the theoretical power of +2.00 D. A negative correlation was also obtained between the compensation power of the prototypes and the power at the therapeutic zones, which means that high power minus lenses had less power in the therapeutic zones than lower power FCLs. This suggests that the manufacturing process should be optimized because the lenses would have less therapeutic power in myopes who have higher peripheral relative hyperopia (Atchison 2006). The FCLs fitted to the subjects also presented a mean decentration of 0.83 mm. The theoretical performance of the FCL was computed in a previous work (Rodríguez-Vallejo et al. 2014a) for a mean decentration of 0.7 mm obtaining a peak myopic shift of around -2 D at 30º. Our results in this study have shown a peak around -1.3 D (the same value of the mean treatment power of the prototypes) at 20º-25º (Fig. 2A). Thus, in comparison to the ray tracing analysis (Rodríguez-Vallejo et al. 2014a), the displacement of the peak can be explained by the decentration of the lens whereas the undercorrection the periphery, is justified by the lower experimental power at the treatment zones of the prototypes.

2.2.5.2 Horizontal Relative Peripheral Refractive Error

For the nacked eye we found that corneal asphericity along temporal and nasal semichords in the horizontal meridian was negatively correlated with the M; but only for temporal cornea and nasal retina whereas for J_{45} and J_0 the negative correlations where found between nasal cornea and temporal retina (Table 1). This is in agreement with theoretical models, which assert that: as more positive is the asphericity (Q), more myopic is the peripheral refraction induced for M and J_0 (Atchison 2006; He 2014). Therefore, corneal asphericity has a correlation with RPRE and this fact should be considered by clinicians, who usually cannot measure the RPRE, because as less prolate (more positive Q) is the corneal semi-meridian as more myopic is the RPRE and more prolate corneas might be expected to progress into more myopia (Horner et al. 2000). We also found a trend for the J_{45} to become more positive with increasing the eccentricity in the temporal retinal area and more negative in the nasal area, whereas J_0 become more negative in both sides of the retina. These results agree the previous reported in other studies that measure peripheral refraction in myopes (Atchison et al. 2006; Davies and Mallen 2009; Radhakrishnan et al. 2013).

At the baseline state, the sample showed a relative peripheral myopia lower than -0.50D for M, which agrees the previous reported studies considering that in our study the mean value of the central refraction was -2.62 D (Atchison 2006). Sagittal power was hyperopic along the temporal retina (Fig. 2C), but become myopic with the FCLs. This is an advantage of FCLs for myopia control over the ortokeratology because in ortokeratology, especially in low myopes, it cannot be guaranteed that the sagittal power became myopic (González-Méijome et al. 2015), whereas with FCLs the power at treatment zones can be modified to achieve higher values of RPRE (Queirós et al. 2016).

2.2.5.3 Two-dimensional Relative Peripheral Refractive Error

The two dimensional representation of the RPRE offered us further information about what happens in a wide area of the retina, especially considering the lens decentration. The mean M showed a significant increase of the

myopic shift in the temporal retina that was almost uniform along the explored vertical field (Fig. 3C) which means that only representing the horizontal section such as in Fig. 2A would be enough to know the change in RPRE for M with this kind of FCLs. Furthermore, although the effect of the FCLs on the spherical equivalent M is almost uniform around the centre it was not symmetric from nasal to temporal retina, which is explained by the lens decentration to the temporal cornea. Note that the same asymmetry was obtained for J_0 and J_{45}. However, the changes in the J_0 (Fig. 3F) and J_{45} (Fig. 3I) along the vertical were not uniform as happened with M, that suggests an advantage of the two-dimensional representation for increasing the understanding about the changes in the astigmatism components due to the lens. Particularly, we found that the sign of the J_{45} component changed in extreme positions of the superior and inferior retina (Fig. 3G), which could be explained by a modification in the orientation of the main focal points due to the astigmatism originated by the oblique incidence of the light over the optical structures. This finding is also in agreement with other authors (Ehsaei et al. 2011) and it has been demonstrated by ray tracing models (Rojo et al. 2015). The components J_0 and J_{45} were more myopic with the FCLs (Figs. 3F and 3I), and the peaks of maximum induction power were located near to the same area of the peak of M (Fig. 3C).

2.2.5.4 Conclusions

Despite peripheral defocus modifying CLs proved their effectiveness in slowing down myopia progression (Huang et al. 2016), the optical theories for which these lenses are founded remain controversial (Radhakrishnan et al. 2013; Atchison et al. 2015; Hartwig et al. 2016). New studies on animals with dual focus lenses are increasing the knowledge about the optical signals that modulate the eye growing. For instance, it was recently found that in the presence of more than one foci, the refractive development was dominated by the more anterior image plane (Arumugam et al. 2014) and also, that the refractive development is dominated by the relative myopic defocus even though the therapeutic area is reduced to one-fifth the total area (Arumugam et al. 2016). Furthermore, the peripheral retinal area might respond in a different way to optical defocus than the central retina due to the neural anisotropy in the paracentral retina (Zheleznyak et al. 2016). While

appear new findings about optical signals that modulate eye growing in research literature, the complete representation of the changes produced by peripheral defocus modifying CLs can help to understand the nature of the optical signals produced by these lenses.

In summary, a new two-dimensional representation of the RPRE was proposed. This representation was employed for validating the performance of the FCLs (Rodríguez-Vallejo et al. 2014a). Very good agreement between the theoretical prediction and the experimental results was obtained. In fact, differences are explained considering both the imperfections in the manufacturing process of the prototypes, and the lens decentration.

2.2.6. Acknowledgements

This study was supported by the Ministerio de Economía y Competitividad and FEDER (Grant DPI2015-71256-R), and by the Generalitat Valenciana (Grant PROMETEOII-2014-072), Spain.

2.2.7. Conflict of interest

The author(s) have made the following

disclosure(s): Karina Naydenova: None.

Vicente Ferrando: None.

M. Rodríguez-Vallejo, J. A. Monsoriu and W. D. Furlan inventors (P) ES Patent P201330862, relating to contact lens design: assigned to Universidad Politécnica de Valencia and Universitat de Valéncia.

2.2.8. References

Arumugam B, Hung LF, To CH, Holden B, Smith EL (2014) The effects of simultaneous dual focus lenses on refractive development in infant monkeys. Invest Ophthalmol Vis Sci 55:7423–7432.

Arumugam B, Hung LF, To CH, Sankaridurg P, Smith EL (2016) The effects of the relative strength of simultaneous competing defocus signals on emmetropization in infant rhesus monkeys. Invest Ophthalmol Vis Sci 57:3949.

Atchison DA (2006) Optical models for human myopic eyes. Vis Res 46:2236–50.

Atchison DA, Li SM, Li H, Li SY, Liu LR, Kang MT, Meng B, Sun YY, Zhan SY, Mitchell P, Wang N (2015) Relative peripheral hyperopia does not predict development and progression of myopia in children. Invest Ophthalmol Vis Sci 56:6162–6170.

Atchison DA, Pritchard N, Schmid KL (2006) Peripheral refraction along the horizontal and vertical visual fields in myopia. Vis Res 46:1450–8.

Benz (2016) G5X p-GMA/HEMA (Hioxifilcon A). http://benzrd.com/benz_g5x.php. Accessed 27 Mar 2016.

Calossi A (2007) Corneal asphericity and spherical aberration. J Refract Surg 23:505–514.

Charman WN (2011) Keeping the world in focus: how might this be achieved? Optom Vis Sci 88:373–376.

Chu CH, Kee CS (2015) Effects of optically imposed astigmatism on early eye growth in chicks. PLoS One 10:e0117729.

Davies LN, Mallen EA (2009) Influence of accommodation and refractive status on the peripheral refractive profile. Br J Ophthalmol 93:1186–90.

Ehsaei A, Mallen EA, Chisholm CM, Pacey IE (2011) Cross-sectional sample of peripheral refraction in four meridians in myopes and emmetropes. Invest Ophthalmol Vis Sci 52:7574–7585.

González-Méijome JM, Faria-Ribeiro MA, Lopes-Ferreira DP, Fernandes P, Carracedo G, Queiros A (2015) Changes in peripheral refractive profile after orthokeratology for different degrees of myopia. Curr Eye Res 41:199–207.

González-Méijome JM, Peixoto-de-Matos SC, Faria-Ribeiro M, Lopes-Ferreira DP, Jorge J, Legerton J, Queiros A (2016) Strategies to

regulate myopia progression with contact lenses: a review. Eye Contact Lens 42:24–34.

Hartwig A, Charman WN, Radhakrishnan H (2016) Baseline peripheral refractive error and changes in axial refraction during one year in a young adult population. J Optom 9:32–39.

He JC (2014) Theoretical model of the contributions of corneal asphericity and anterior chamber depth to peripheral wavefront aberrations. Ophthalmic Physiol Opt 34:321–330.

Horner DG, Soni PS, Vyas N, Himebaugh NL (2000) Longitudinal changes in corneal asphericity in myopia. Optom Vis Sci 77:198–203.

Huang J, Wen D, Wang Q, McAlinden C, Flitcroft I, Chen H, Saw SM, Chen H, Bao F, Zhao Y, Hu L, Li X, Gao R, Lu W, Du Y, Jinag Z, Yu A, Lian H, Jiang Q, Yu Y, Qu J (2016) Efficacy comparison of 16 interventions for myopia control in children. Ophthalmology 123:697–708.

Joannes L, Hough T, Hutsebaut X, Dubois X, Ligot R, Saoul B, Van Donink P, De Coninck K (2010) The reproducibility of a new power mapping instrument based on the phase shifting schlieren method for the measurement of spherical and toric contact lenses. Cont Lens Anterior Eye 33:3–8.

Kee CS, Hung LF, Qiao-Grider Y, Roorda A, Smith EL (2004) Effects of optically imposed astigmatism on emmetropization in infant monkeys. Invest Ophthalmol Vis Sci 45:1647–1659.

Queirós A, Lopes-Ferreira D, González-Méijome JM (2016) Astigmatic peripheral defocus with different contact lenses: review and meta-analysis. Curr Eye Res Feb 2:1–11.

Radhakrishnan H, Allen PM, Calver RI, Theagarayan B, Price H, Rae S, Sailoganathan A, O'Leary DJ (2013) Peripheral refractive changes associated with myopia progression. Investig Ophthalmol Vis Sci 54:1573–1581.

Rodríguez-Vallejo M, Benlloch J, Pons A, Monsoriu JA, Furlan WD (2014a) The effect of Fractal Contact Lenses on peripheral refraction in myopic model eyes. Curr Eye Res 39:1151–60.

Rojo P, Royo S, Caum J, Ramírez J, Madariaga I (2015) Generalized ray tracing method for the calculation of the peripheral refraction induced by an ophthalmic lens. Opt Eng 54:25106–25113.

Smith EL (2012) The Charles F. Prentice award lecture 2010: A case for peripheral optical treatment strategies for myopia. Optom Vis Sci 88:1029–1044.

Smith EL, Kee CS, Ramamirtham R, Qiao-Grider Y, Hung LF (2005) Peripheral vision can influence eye growth and refractive development in infant monkeys. Invest Ophthalmol Vis Sci 46:3965–3972.

Thibos LN, Wheeler W, Horner D (1997) Power vectors: an application of Fourier analysis to the description and statistical analysis of refractive error. Optom Vis Sci 74:367–75.

Turnbull PR, Munro OJ, Phillips JR (2016) Contact lens methods for clinical myopia control. Optom Vis Sci 93:1–7.

Walline JJ (2016) Myopia control: A review. Eye Contact Lens 42:3–8.

Wolffsohn JS, Calossi A, Cho P, Gifford K, Jones L, Li M, Lipener C, Logan NS, Malet F, Matos S, Meijome JMG, Nichols JJ, Orr JB, Santodomingo-Rubido J, Schaefer T, Thite N, van der Worp E, Zvirgzdina M (2016) Global trends in myopia management attitudes and strategies in clinical practice. Cont Lens Anterior Eye 39:106–116.

Zheleznyak L, Barbot A, Ghosh A, Yoon G (2016) Optical and neural resolution in peripheral vision. J Vis 16:1–11.

Optometry and Vision Science
AMERICAN ACADEMY of OPTOMETRY
Wolters Kluwer Subscribe
Enter Keywords All Issues Search Advanced Search
Home Current Issue Previous Issues Published Ahead-of-Print Collections For Authors Journal Info

Optometry & Vision Science:
Post Author Corrections: August 24, 2016
doi: 10.1097/OPX.0000000000000972
ORIGINAL ARTICLE: PDF Only

Inter-Display Reproducibility of Contrast Sensitivity Measurement with iPad.

Rodríguez-Vallejo, Manuel; Monsoriu, Juan A.; Furlan, Walter D.

PAP

Abstract

Purpose: To evaluate the reliability of measuring CS with uncalibrated iPads.

Methods: Six random iPads with retina display were calibrated with a colorimeter and the correlation between Luminance (L) and pixel level (y) was computed according to an exponential function. The mean and confidence interval (+/-2SD) obtained from the six iPads were calculated and the bit-stealing technique was applied for expanding y from 256 to 2540 possible values. The L of the optotype was computed for the selected contrast values (logC) represented in log units, using 0.1 log and 0.05 log steps. At each particular y, the contrast was considered reliable when the mean L plus 2SD was less than half the difference of luminance between two consecutive levels of contrast. Differences between the iPads for the Experimental logC were evaluated with the Friedman test.

Results: Luminance properties vary between devices, which were reflected in the computed Experimental logC ($p < 0.0005$). The contrast was found to be reliable for 0.1 log steps in the range from 0 to -2.2 log. On the other hand, for steps of 0.05 log, the contrast was only reliable for values ranging from 0 to -1.7 log.

Discussion: Both luminance and contrast steps differed between iPads with the same retina display, making it necessary to calibrate each display to achieve accurate luminance and contrast steps of 0.05 log units or less. However, for screening purposes utilizing contrast steps of 0.1 log unit or greater for a validated psychophysical test, calibration is not required to achieve accurate results across the displays described herein.

2.3. Inter-display Reproducibility of Contrast Sensitivity Measurement with iPad

Manuel Rodriguez-Vallejo[1*], Juan A. Monsoriu[2] and Walter D. Furlan[3]

[1]*Qvision, Unidad de Oftalmología, Vithas Hospital Virgen del Mar, 04120, Almería*

[2]*Centro de Tecnologías Físicas, Universitat Politècnica de València, 46022 Valencia, Spain*

[3] *Departamento de Óptica, Universitat de València, 46100 Burjassot, Spain*
[*]*Corresponding author: manuelrodriguezid@qvision.es*

2.3.1. Abstract

Purpose: To evaluate the reliability of measuring contrast sensitivity with uncalibrated iPads.

Methods: Six random iPads with Retina display were calibrated with a colorimeter and the correlation between luminance and pixel level was computed according to an exponential function. The mean and confidence interval (±2SD) obtained from the six iPads were calculated and the bit-stealing technique was applied for expanding the pixel levels from 256 to 2540 possible values. The luminance of the optotype was computed for the selected contrast values (logC) represented in log units, using 0.1 log and 0.05 log steps. At each particular pixel level, the contrast was considered reliable when the mean luminance plus 2SD was less than half the difference of luminance between two consecutive levels of contrast. Differences between the iPads for the Experimental logC were evaluated with the Friedman test.

Results: Luminance properties vary between devices, which was reflected in the computed Experimental logC ($p<0.0005$). The contrast was found to be reliable for 0.1 log steps in the range from 0 log to -2.2 log. On the other

hand, for steps of 0.05 log, the contrast was only reliable for values ranging from 0 log to -1.7 log.

Discussion: Both luminance and contrast steps differed between iPads with the same retina display making it necessary to calibrate each display to achieve accurate luminance and contrast steps of 0.05 log units or less. However, for screening purposes utilizing contrast steps of 0.1 log unit or greater for a validated psychophysical test, calibration is not required to achieve accurate results across the displays described herein.

Keywords: contrast sensitivity, iPad, reliability, calibration

2.3.2. Introduction

Computer-based contrast sensitivity (CS) testing requires accurate calibration of the display. Contrast is computed as the difference between the stimulus and the background luminance (usually in cd/m2) relative to the background for optotypes or to the mean level of luminance for sinusoidal gratings. CS is the reciprocal of this value; hence the lower the contrast, the higher the CS (To et al. 2013). The main reason to use an iPad for testing CS instead of another Android tablet is due to it is expected less variation between units. First, because all iPad Retina Displays come from the same manufacturer (LG displays) and second, because iPad 3rd generation have not apparently changed their retina displays (LP097QX1) in the following models: 4th generation, Air, and Air 2. Authors who have previously characterized the iPads used in their studies have raised the assumption that uniformity in screen luminance properties might be assumed even though it has not been demonstrated yet (Rodríguez-Vallejo et al. 2015). The main aim of this study is to evaluate the need of calibrating the luminance response of an iPad before using APPs devoted to the measurement of CS. This paper is, to the best of our knowledge, the first study that analyzes the CS values that can be reliably measured with an iPad without a previous calibration of its luminance response.

2.3.3. Methods

2.3.3.1 Devices and Calibration

Six iPads with retina display, models A1458 (3 units), A1430 (2 units) and A1416 (1 unit) were measured with a Syper4Elite colorimeter after setting *auto-lock* as *never*, fixing the luminance at 50% and waiting 15 minutes to ensure the stabilization of the screen luminance (Aslam et al. 2013). Each iPad was in use for an unknown number of hours except a new one which was measured after receiving its first complete charge, this new iPad was re-calibrated one month after the first calibration in order to assess the variability attributable to the colorimeter. The characterization of the screens was conducted with an APP which allowed to manipulate the pixel level (*y)* from 0 to 255 for each RGB isolated channel. The luminance (*L)* was then measured for 52 evenly spaced values of *y* per channel. The mean *L* and the standard deviation (SD) obtained from the measurement of the six iPads was computed for each L level for the three RGB channels. The nonlinearity of the mean *L* value was estimated by fitting the scatterplot of the measurements to an exponential function as follows (To et al. 2013):

$$L_R(y) = \left(\frac{y}{y_{max}}\right)^{\gamma} \quad (1)$$

Where *y* is the digital level on the display, y_{max} is the maximum value (y_{max} =255), $L_R(y) \in [0,1]$ is the corresponding relative luminance, and γ is the gamma value. With the data obtained from calibration, the relative *R*:*G*:*B* luminances were calculated by dividing $L(y)$ for each *RGB* channel by the sum of the three and approximating the result to the first decimal. These relative luminances were required for selecting the best matrix (δ_R, δ_G, δ_B) in order to apply the bit-stealing (Tyler 1997) technique and for later computing the Look up Table (LuT) as it has been previously described by To et al. (To et al. 2009).

The L corresponding to each contrast level commonly used for testing CS with optotypes were calculated considering the Weber's law:

$$C = \frac{L_b - L_f}{L_b} \quad (2)$$

where L_b is the background luminance and L_f the luminance of the optotype or foreground. L_f was then computed for the logarithm of the contrast (logC) ranging from logC=0 to logC = -2.2 considering that L_b is 1 after normalization:

$$L_f = 1 - 10^{logC} \quad (3)$$

2.3.3.2 Statistical Analysis

Fig. 1 shows the criteria we adopted to assess the reliability of presenting a contrast in a non-calibrated display. It was computed among the selected *logC* values ranging from *logC*=0 to *logC*=-2.2 in steps of -0.1 (23 levels) and -0.05 (45 levels). The horizontal dashed lines represent the luminances (L_i) corresponding to three consecutive *logC* steps along the mean luminance curve (L_m) obtained from all the iPads. Therefore, the uniformity between devices for presenting a stimulus of certain contrast was considered as reliable when $[(L_i - L_{i-1}) / 2]$, *a* in the Fig. 1, was higher than 2 standard deviations (*SD*) from the mean, *b* in the Fig. 1.In this case, if we present a contrast with the same *y* value in different devices, the luminance offered by the device for this *y* will be closer to the required luminance for a *logC* value than to the luminance required for the next consecutive *logC* value. MATLAB software (R2013a; MathWorks, Natick, MA) was used for processing data. The fitting to the exponential functions for obtaining the gammas was completed with the Curve Fitting Toolbox.

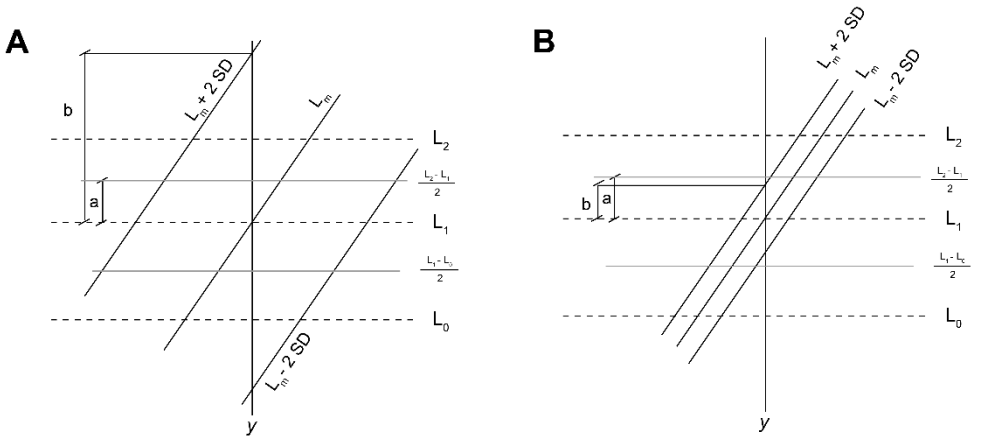

Figure 1. (A) Two standard deviation from the mean (b) was greater than half the difference of luminance between two consecutive logC steps (a), not reliable. (B) Two standard deviation from the mean (b) was less than half the difference of luminance between two consecutive logC steps (a), reliable.

The *y* corresponding to the selected *Theoretical* contrast values from *logC*= -0.05 to *logC*= -2.2 in -0.05 steps and -0.1 steps were calculated for the *LuT* table obtained from the mean gamma of the six iPads. The equivalent contrasts for these *y* in each iPad were computed; resulting in the *Experimental logC* values. Therefore, the *Theoretical logC* are the contrasts that we want to reliably reproduce and the *Experimental logC* are the true contrasts that each iPad displays for these *Theoretical* contrasts. Hence, as higher difference between the *Theoretical* and *Experimental logC*, as poorer is the reliability for contrast displaying in each non-calibrated iPad. The Kolmogorov-Smirnov test resulted in non-normal distributions of the *Experimental logC*. Therefore, a Friedman test was run with SPSS version 20 (SPSS Inc., Chicago, IL, USA) to determine if there were differences in the *Experimental logC* between the six iPads.

2.3.4. Results

Table 1 shows L_{max} and gamma values for *R*, *G*, *B* for each display as well as mean ± 2*SD*. Fig. 2A represents the mean values of L (solid lines) and +/- 2 SD from the mean (dashed lines) for the six devices (solid line). The relative *R: G: B* luminance, approximated to the first decimal, was constant, 0.2: 0.7: 0.1, for digital levels over y=50. This means that $L(y)$ for *R* channel is two times higher than for the *B* channel whereas for *G* channel is seven times higher than for *B* channel. This relative luminance ensured that the bit-stealing technique could be obtained by adding nine levels more of luminance between each one of the 8-bit gray levels according to the next matrix:

$$(\delta_R, \delta_G, \delta_B) \in \{ (0,0,1), (1,0,0), (1,0,1), (1,0,2), (2,0,1), (2,0,2), (0,1,0), (0,1,1), (1,1,0)\}$$

Table 1. Gamma (γ) and maximum luminance (Lmax) for the RGB channels of each iPad. γw values were computed by the combination of measured R, G and B values. Mean values and standard deviations (SD) are presented at the bottom of the Table.

Id	Model	γ_R (L_{max})	γ_G (L_{max})	γ_B (L_{max})	γ_W (L_{max})
1 (1st)	A1458	2.195 (27.35)	2.158 (91.61)	2.024 (9.15)	2.156 (128.11)
(2nd)*		2.197 (27.64)	2.157 (92.07)	2.027 (9.27)	2.156 (128.98)
2	A1416	2.219 (25.98)	2.248 (84.26)	2.096 (9.01)	2.230 (119.25)
3	A1458	2.373 (25.17)	2.351 (79.18)	2.204 (8.24)	2.345 (112.59)
4	A1430	2.074 (24.86)	2.052 (81.45)	1.955 (8.21)	2.049 (114.52)
5	A1430	2.035 (24.95)	2.029 (82.21)	1.921 (8.47)	2.022 (115.63)
6	A1458	2.139 (22.53)	2.124 (79.24)	2.031 (7.07)	2.121 (108.84)
+2 SD		2.101 (28.03)	2.051 (91.45)	1.986 (9.71)	2.056 (129.20)
Mean		2.168 (25.14)	2.154 (82.99)	2.034 (8.36)	2.148 (116.48)
-2 SD		2.253 (22.25)	2.291 (74.53)	2.103 (7.00)	2.270 (103.77)

L_{max} =Value in cd/m^2 for y=255 at each channel.

* A second measure was taken one month after the first for checking variability due to Spyder4Elite. This 2nd measure has not been considered for computing mean and standard deviation (SD).

Fig. 2B represents the result obtained after applying the bit-stealing technique to the mean of the six devices (a total of 2540 pixel grey levels). The L_{bg} was set as y_{max}= 254 at the three *RGB* channels and the bit-stealing curve was normalized to L_{bg}= 1 by computing the relative luminance $L_R(y)$ described in equation 1.

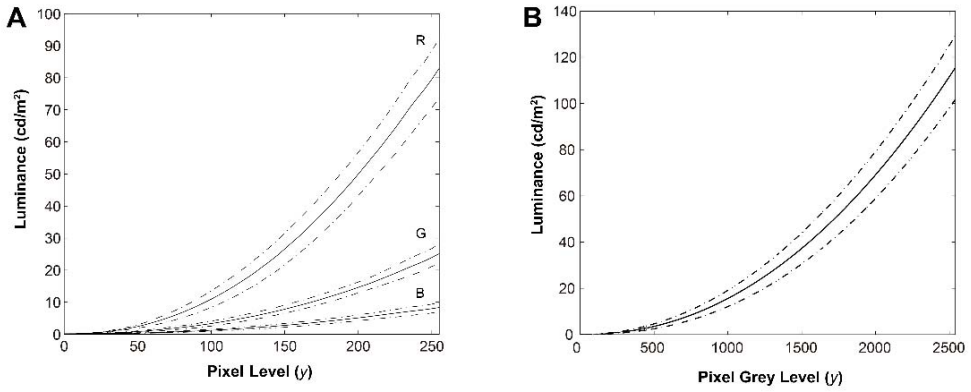

Figure 2. Correlation between luminance and pixel level. (A) Mean (solid lines) and two standard deviations (dashed lines) of the six iPads for each RGB channel. (B) Mean and two standard deviations after bit stealing application considering ymax = 254 (a total of 2540 pixel grey levels).

The difference between the Theoretical logC and the Experimental logC for all the iPads against the Theoretical logC values is shown in Fig. 3. The Experimental logC was statistically significantly different between the iPads for the -0.1 steps $\chi^2(6) = 126.189$, $p < .0005$ and for the -0.05 steps $\chi^2(6) = 257.485$, $p < .0005$. We found that for the iPad 1 the Experimental logC obtained one month apart were exactly the same for all levels except for –1.5 logC (with a variation of 0.01 logC), whereas the variation was considerably greater with the other iPads, especially for lower contrasts (see Fig. 3). In fact, the iPad 1 was the closest to the *Theoretical logC* and a deviation from the *Theoretical logC* up to 0.05 log units was obtained for finest values of contrast for iPads 3 and 5.

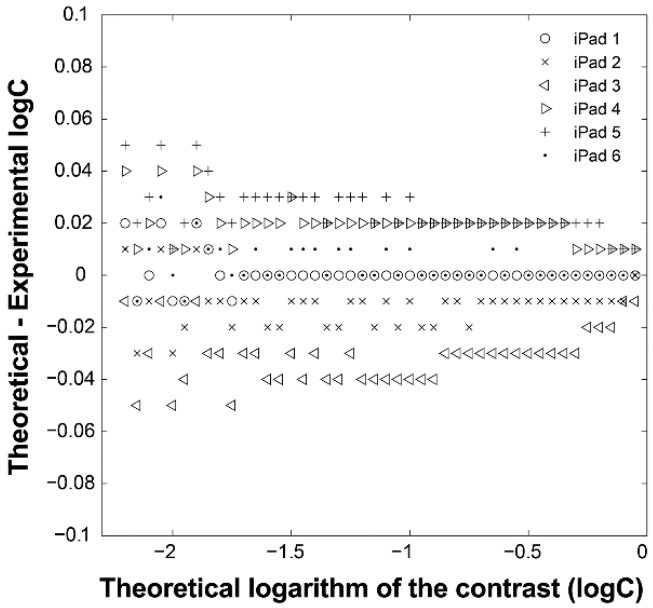

Figure 3. Difference between Theoretical logC and Experimental logC against the selected contrast values obtained for comparison of the six iPads.

In all, as was previously mentioned, the contrast variability among devices was considered as reliable when $[(L_i - L_{i-1}) / 2] > 2SD$ (see Fig. 1). Bearing in mind this condition, Fig. 4A shows that this condition (a>b, in Fig. 1) was satisfied for contrasts from *logC*=0 to *logC*=-2.2 in 0.1 log steps. However as can be seen in Fig. 4B for contrasts lower than *logC* = -1.7 it is not adequate to use even 0.05 log steps because the *L* steps required for these finest contrasts are very small with regard the *L* variability of the screens.

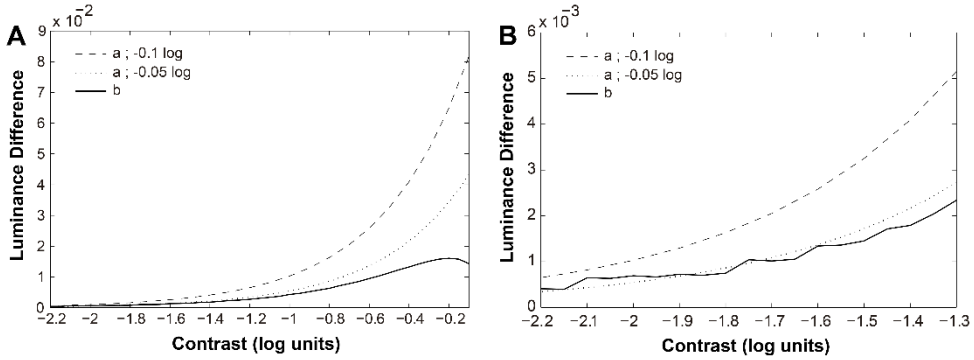

Figure 4. Represents the reliability of using an iPad considering a test developed for the gammas obtained from the mean of the six iPads. The a and b variables were explained in Figure 1 and (A) represents the contrasts from -0.0 to -2.2 and (B) from –1.3 to -2.2 for a clearer view.

2.3.5. Discussion

The proliferation of APPs for testing vision alerted the research community since many of them are not correctly designed and do not follow the current international standards for testing vision (Perera et al. 2015; Rodríguez-Vallejo 2015). Moreover, although the gamma function for a given iPad retina was considered in several papers (Aslam et al. 2013; Tahir et al. 2014; De Fez et al. 2016), the variability among the same iPad displays has not been previously reported. For this reason, in this paper we have studied the variability among different iPads which share the same model of retina display. We demonstrated that there exists statistical significant differences between the luminances of iPads. This evidence, presumed previously by Lin, confirms that for a precise measure of the CS a previous calibration is necessary (Lin et al. 2015). Despite of this, in this work we show that for screening purposes, on which contrast patches vary in log unit steps, the variability among different units of the same iPad is small enough to avoid the previous calibration of each particular device. Particularly for iPad retina displays working at 50% of screen luminance, the calibration should be required only for contrasts decreasing in -0.05 log units if the contrast of the optotype is less than –1.7 log units. On the other hand, if the optotype contrast decrease in -0.1 log units the results would be reliable for any iPad

without a previous calibration. Our results suggest that for normal users who perceive very finest levels of CS (finer than -1.7 log units), the test should be designed in -0.1 log steps for being reliable. However in low vision patients, who normally just perceive contrasts greater than -1.7 log units, the number of contrasts can be expanded by means of designing the test in -0.05 log steps. For instance, Kollbaum et al. reported that the mean of CS (-*logC*) in low vision patients measured with iPad retina was 1.43 ± 0.42 log units, which means that a test designed in -0.05 steps might be used for screenings with this population without having to worry about previous calibration (Kollbaum et al. 2014).

One negative factor regarding our methodology is that we have conducted the study by means of computing $L_R(y)$. This means that even though a reliable contrast value can be extrapolated between the same devices, the luminance may differ between iPads because at the same y_{max} the L could be different and thus better CS could be achieved with higher background luminances (Bühren et al. 2006). Furthermore, we found that the new iPad had the highest screen luminance which suggests that it is likely that, for a given screen, L decreases with the time of use.

We are aware that our calibration data may differ from previous reports (Aslam et al. 2013; Tahir et al. 2014; De Fez et al. 2016), not just for using different instruments for calibration, a spectroradiometer instead of a colorimeter, but also for performing the calibration at different luminance of the screen. We decided to select the 50% of brigtness instead of the 100% to reduce the glare of the screen as it has been previously reported (Kollbaum et al. 2014). On the other hand, the Spyder4Elite Colorimeter has been previously used in vision research (Bogfjellmo et al. 2014; Gu et al. 2014). Furthermore, a colorimeter is considerably cheaper than a photospectroradiometer, making it accesible for users who desire to calibrate their own tablets for personalizing the calibration data of any APP which supports this option. However, it is important to note that luminance of the screen can be underestimated with the Spyder4Elite. This is the reason why our mean brightness was 116.48 cd/m2 versus the 150 cd/m2 reported in oher studies (Kollbaum et al. 2014). Therefore, increasing screen luminance to a percentage slightly upper 50% would be acceptable for mainly for screening elderly/low vision patients who often need high luminance displays for optimal performance. Our results are only applicable

for iPad retina displays and for measuring achromatic CS. For other purposes, such as the design of tests based in chromatic thresholds or in any color discrimination task, the previous calibration should be complemented with a chromatic characterization of the device (De Fez et al. 2016).

In conclusion, differences in *L* properties between iPads suggest that a previous calibration is always recommended before conducting precise CS measurements, however we have demonstrated that for screening purposes reliable measures of CS can be obtained without a previous calibration by using an APP which expands the range of *y* by bit-stealing and that uses a gamma correction of $\gamma_R = 2.168$, $\gamma_G = 2.154$, and $\gamma_B = 2.034$.

2.3.6. Acknowledgements

This study was supported by the Ministerio de Economía y Competitividad and FEDER (Grant DPI2015-71256-R), and by the Generalitat Valenciana (Grant PROMETEOII-2014-072), Spain.

2.3.7. Conflict of interest

MR-V has designed and programmed apps that are currently distributed by the Apple Store with his own developer account. The other authors report no conflicts of interest and have no proprietary interest in any of the materials mentioned in this article.

2.3.8. References

Aslam TM, Murray IJ, Lai MY, Linton E, Tahir HJ, Parry NR (2013) An assessment of a modern touch-screen tablet computer with reference to core physical characteristics necessary for clinical vision testing. J R Soc Interface 10:20130239.

Bogfjellmo L-G, Bex PJ, Falkenberg HK (2014) The development of global motion discrimination in school aged children. J Vis 14:19.

Bühren J, Terzi E, Bach M, Wesemann W, Kohnen T (2006) Measuring

contrast sensitivity under different lighting conditions: comparison of three tests. Optom Vis Sci 83:290–8.

De Fez D, Luque MJ, García-Domene MC, Camps V, Piñero D (2016) Colorimetric characterization of mobile devices. Optom Vis Sci 93:1–9.

Gu X-J, Hu M, Li B, Hu X-T (2014) The role of contrast adaptation in saccadic suppression in humans. PLoS One 9:e86542.

Kollbaum PS, Jansen ME, Kollbaum EJ, Bullimore MA (2014) Validation of an iPad Test of Letter Contrast Sensitivity. Optom Vis Sci 91:291–6.

Lin TP, Rigby H, Adler JS, Hentz JG, Balcer LJ, Galetta SL, Devick S, Cronin R, Adler CH (2015) Abnormal visual contrast acuity in parkinson's disease. J Park Dis 5:125–130.

Perera C, Chakrabarti R, Islam FMA, Crowston J (2015) The Eye Phone Study: reliability and accuracy of assessing Snellen visual acuity using smartphone technology. Eye 29:888–894.

Rodríguez-Vallejo M (2015) Comment on: "The Eye Phone Study: reliability and accuracy of assessing Snellen visual acuity using smartphone technology." Eye 29:1627.

Rodríguez-Vallejo M, Remón L, Monsoriu JA, Furlan WD (2015) Designing a new test for contrast sensitivity function measurement with iPad. J Optom 8:101–108.

Tahir HJ, Murray IJ, Parry NR, Aslam TM (2014) Optimisation and assessment of three modern touch screen tablet computers for clinical vision testing. PLoS One 9:e95074.

To L, Woods RL, Goldstein RB, Peli E (2013) Psychophysical contrast calibration. Vision Res 90:15–24.

To L, Woods RL, Peli E (2009) 17.3: Visual calibration of displays for accurate contrast reproduction. SID Symp Dig Tech Pap 40:216–219.

Tyler CW (1997) Colour bit-stealing to enhance the luminance resolution of digital displays on a single pixel basis. Spat Vis 10:369–377.

Journal of Optometry
Peer-reviewed Journal of the Spanish General Council of Optometry

J Optom 2015;8:101-8 - Vol. 8 Num.2 DOI: 10.1016/j.optom.2014.06.003

ORIGINAL ARTICLE

Designing a new test for contrast sensitivity function measurement with iPad

Diseño de una nueva prueba para medir la función de sensibilidad al contraste con iPad

Manuel Rodríguez-Vallejo [a,b], Laura Remón [a], Juan A. Monsoriu [a], Walter D. Furlan [b]

[a] Centro de Tecnologías Físicas, Universitat Politècnica de València, 46022 Valencia, Spain

[b] Departamento de Óptica, Universitat de València, 46100 Burjassot, Spain

Received 19 February 2014, Accepted 06 May 2014

Abstract

Purpose

To introduce a new application (*ClinicCSF*) to measure Contrast Sensitivity Function (CSF) with tablet devices, and to compare it against the *Functional Acuity Contrast Test (FACT)*.

Methods

A total of 42 subjects were arranged in two groups of 21 individuals. Different versions of the *ClinicCSF (.v1 and .v2)* were used to measure the CSF of each group with the same iPad and the results were compared with those measured with the *FACT*. The agreements between *ClinicCSF* and *FACT* for spatial frequencies of 3, 6, 12 and 18 cycles per degree (cpd) were represented by Bland–Altman plots.

Results

Statistically significant differences in CSF of both groups were found due to the change of the *ClinicCSF* version ($p < 0.05$) while no differences were manifested with the use of the same *FACT* test. The best agreement with the *FACT* was found with the *ClinicCSF.v2* with no significant differences in all the evaluated spatial frequencies. However, the 95% confidence intervals for mean differences between *ClinicCSF* and *FACT* were lower for the version which incorporated a staircase psychophysical method (*ClinicCSF.v1*), mainly for spatial frequencies of 6, 12 and 18 cpd.

Conclusions

The new *ClinicCSF* application for iPad retina showed no significant differences with *FACT* test when the same contrast sensitivity steps were used. In addition, it is shown that the accurateness of a vision screening could be improved with the use of an appropriate psychophysical method.

2.4. Designing a new test for contrast sensitivity measurement with iPad.

Manuel Rodriguez-Vallejo[1*], Laura Remón[1], Juan A. Monsoriu[1] and Walter D. Furlan[2]

[1] *Centro de Tecnologías Físicas, Universitat Politècnica de València, 46022 Valencia, Spain*

[2] *Departamento de Óptica, Universitat de València, 46100 Burjassot, Spain*
[*] *Corresponding author: marodva1@upvnet.upv.es*

2.4.1. Abstract

Purpose: To introduce a new application (*ClinicCSF*) to measure Contrast Sensitivity Function (CSF) with tablet devices, and to compare it against the *Functional Acuity Contrast Test (FACT)*.

Methods: A total of 42 subjects were arranged in two groups of 21 individuals. Different versions of the *ClinicCSF(.v1 and .v2)* were used to measure the CSF of each group with the same iPad and the obtained results were compared with those measured with the *FACT*. The agreements between *ClinicCSF* and *FACT* for spatial frequencies of 3, 6, 12 and 18 cycles per degree(cpd) were represented by Bland-Altman plots.

Results: Statistical significant differences in CSF of both groups were found due to the change of the *ClinicCSF* design ($p<0.05$) while no differences were manifested with the use of the same *FACT* test. The best agreement with the *FACT* was found with the *ClinicCSF.v2* with no significant differences in all the evaluated spatial frequencies. However, the 95% confidence intervals for mean differences between *ClinicCSF* and *FACT* were lower for the version which incorporated a staircase psychophysical method (*ClinicCSF.v1*), mainly for spatial frequencies of 6, 12 and 18 cycles per degree.

Conclusion: The new *ClinicCSF* application for iPad retina showed no significant differences with *FACT* test when the same contrast sensitivity steps were used. In addition, it is shown that the accurateness of a vision screening could be improved with the use of an appropriate psychophysical method.

Key Words: contrast sensitivity function, visual performance, tablet devices, iPad, FACT

2.4.2. Introduction

The Contrast Sensitivity Function (CSF) has been generally accepted as a better predictor of visual performance than high contrast Visual Acuity (VA). In fact, VA is usually considered as a measure of the clarity of vision, and it basically depends on the finest detail that an eye can resolve. On the other hand, the CSF is a more complete metric since it is a measure of the threshold contrast needed to see spatially varying stimuli (Norton et al. 2002). Indeed, the CSF is nowadays considered a routine clinical tool in optical quality assessment of the eye (Kim et al. 2007; Zhao and Zhu 2011) and in eye disease detection (e.g., cataracts (Chylack et al. 1993), optic nerve pathologies (Beck et al. 1984; Rucker et al. 2006), retinitis pigmentosa (Lindberg et al. 1981; Alexander et al. 2004), glaucoma (Hitchings et al. 1981; Ansari et al. 2002), etc.).

When CSF testing was initially introduced in clinical practice and clinical research, tests usually consisted of computer-generated visual images. However, those devices were typically costly, they needed a calibration and normative data were not readily available. Consequently, chart-based methods for assessing CSF were developed in the early 1980s (Owsley 2003).

In clinical practice, Contrast Sensitivity (CS) is generally measured by means of optotypesof different contrast, such as Pelli-Robson chart (Pelli et al. 1988) or by means of sinusoidal gratings of different spatial frequency (Franco et al. 2010). The main difference between them is that an optotype contains a wide range of spatial frequencies whose relative weights depend on the letter and its size, while a sinusoidal grating evaluates the response of the visual system to a single spatial frequency (Alexander and McAnany 2010).

Today, the most popular commercial tests for measuring CSF by means of sinusoidal gratings are: Functional Acuity Contrast Test (FACT)(Ginsburg 1996), and the Vector Vision CSV-1000 (VectorVision, Greenville, OH)(VectorVision 2014a). These tests commonly use 9 patches for each spatial frequency but they differ in: the specific spatial frequencies evaluated, in the step contrast sizes and ranges, and in the psychophysical method to achieve the threshold.

Since tablets appeared, new applications (APPs) have been proposed in the ophthalmology and optometry practice (Dorr et al. 2013; Kollbaum et al. 2014). The great advantages of these devices are that they offer the possibility to standardize vision screenings, and since there are many common models which share characteristics such as screen chromaticity and resolution, the chromatic properties of such devices might be assumed to be nearly the same. The aim of this study is to introduce a new APP, called *ClinicCSF* (Rodríguez-Vallejo 2014b), to measure CSF with tablet devices and to compare it with other commercial device: the *Optec Visual Function Analyzer (Stereooptical, Chicago)*(StereoOptical Co. Inc. 2014), that contains the *FACT*.

2.4.3. Methods

2.4.3.1 Subjects and Instruments

Forty-two subjects divided in two groups participated in this study. Subjects from the Group 1 (mean age, 33 ± 12 years) were examined by a trained optometrist with the *ClinicCSF.v1* in an optometry center. Subjects from the Group 2, members of the staff and students from the University of Valencia (mean age, 37 ± 11 years), were measured by with the *ClinicCSF.v2* by a different practitioner. The iPad retina display (2048-by-1536-pixel resolution at 264 ppi) and the *FACT* used in both screenings were the same. Monocular VA was measured in both groups with the ETDRS procedure included in the Optec, previously to monocular measurement with *ClinicCSF* and *FACT*. Exclusion criteria were strabismus and any cause of monocular reduced visual acuity with habitual correction (worse than 0.3 logMAR). Informed consent

was obtained for each subject and the research was conducted in accordance with the principles laid down in the Declaration of Helsinki.

2.4.3.2 APP description

ClinicsCSF is an APP developed by pure mobile ActionScript 3.0 code that can be compiled for iPad or Android devices. The APP loads 9 patches of sinusoidal gratings for spatial frequencies of 3,6,12 and 18 cpd created with MATLAB software (The MathWorks, Natick, MA) and the COLORLAB (Malo and Luque 2014) library. This library was used to calibrate the iPad screen by computing the function that links the digital values with the XYZ-CIE tristimulus values and to compute the sinusoidal gratings as follows: First, for each RGB channel of the iPad (primary colors) and for an equal combination of the three (grey scale), ten equally spaced colors were generated and measured with a Spyder4Elite colorimeter obtaining the calibration function. Second, the calibration data were loaded and the digital values of the gratings were computed from the tristimulus values with the COLORLAB library. Finally, the true color patches were exported to JPG format to be compiled into the *ClinicCSF* APP. To minimize edge effects, stimuli were generated with blurred edges by means of a half-Gaussian ramp that fades the stimuli with an achromatic (Chauhan et al. 2014) background of 86 cd/m^2 mean luminance (CIE xy coordinates: 0.33, 0.33).

The APP was designed to be presented at a distance of 2 meters for which a stimulus of 4 cm subtended 1 degree (Fig. 1). Two different versions, called "*ClinicCSF.v1" and"ClinicCSF.v2*" were developed. In both versions, the stimuli were presented randomly indifferent orientations: vertical, tilted 15˚ to the right or tilted 15º to the left.

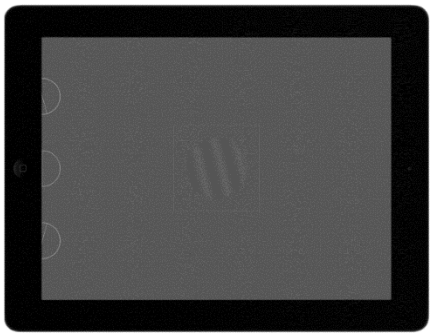

Figure 1. Appearance of the ClinicCSF App during the testing process. A single sinusoidal grating is displayed with a blurred circular edge that smooth the grating into an achromatic background.

The main differences between *ClinicCSF.v1* and *.v2* were the psychophysical method used to achieve the CSF threshold and the step sizes between each one of the CS levels. The *ClinicCSF.v1* was programmed with the same contrast sensitivity values that the *CSV1000* and the *ClinicCSF.v2* with the *FACT* values in order to allow a better comparison with previously reported results (Fig. 2).

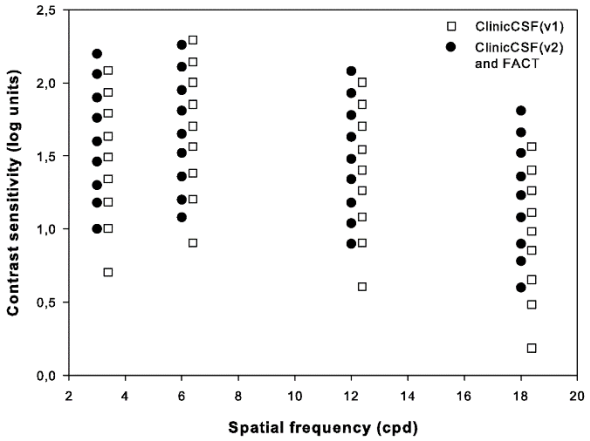

Figure 2. CS values in log units for each one of the patches in both versions of the ClinicCSF. The contrast sensitivity step sizes for the ClinicCSF.v2 and the FACT were the same (black dots).

With the *ClinicCSF.v1,* a simple-up down staircase (Leek 2001) psychophysical method was used starting in the fifth patch level for each spatial frequency. In this method, CS goes one level up (e.g. from level 5 to 6) after each right answer until the observer fails. Then, CS goes down until the observer gets right again. The CS threshold was determined by averaging the sensitivities at the *turnaround points* (i.e. the CS at the levels where direction changed) in the adaptive track for a total of five reversals.

The psychophysical method adopted for *ClinicCSF.v2* consisted of three steps: (1) starting at the first level, it goes one level up after each right answer until the observer fails; (2) the same procedure than previous step but starting two levels below the level on which the answer was wrong in step 1; (3) the exam ends after two successive wrong responses as the *FACT* procedure being the CS threshold the corresponding to the latest correct answer.

2.4.3.3 Experimental Procedures

The same procedure was followed for both groups of subjects who wore their habitual correction. Subjects from Group 1 and Group 2 were evaluated with the *ClinicCSF.v1* and *.v2* respectively, and with the *FACT*. The ambient lighting conditions were around 15 lux during all measurements with *ClinicCSF* and *FACT* in both groups. Pupil size and accommodation were not controlled artificially because this study attempted to gain an understanding of the nature of CSF in the natural state of the eyes. The *FACT* offers four possible configurations in the measurement of the CSF, so the "day condition without glare" was chosen in this experiment. Both, the *ClinicCSF* and the *FACT* were performed in the same session. The time involved in the CSF measurement with each test was approximately two minutes.

2.4.3.4 Statistical Analysis

Both eyes were considered in the statistical analysis due to the low correlation that was obtained between their CS values using the kappa statistic ($k<0.20$)

(Murdoch et al. 1998). Differences in age, VA, and CS between groups were evaluated using the Mann-Whitney test, and comparison between tests in the same group was computed with Wilcoxon test. This analysis was based on a non-normal distribution of the data. On the other hand, as the difference of scores between tests were normally distributed, Bland–Altman procedure (Bunce 2009) was used to assess the agreement between each one of the *ClinicCSF* versions and the *FACT*. The data were managed using SPSS software version 20 (SPSS Inc, Chicago, Illinois, USA), and $P<0.05$ was considered to indicate significance.

2.4.4. Results

No statistical differences were found in age between both groups of subjects (p=0.064) and median monocular visual acuities were 0 logMAR (range, -0.2 to 0.3) in the Group 1 and 0 logMAR (range, -0.2 to 0.2) in the Group 2 (p=0.570).

Median CS and range scores obtained at each spatial frequency are summarized for both groups in Table 1 and graphically represented by means of box plot whiskers in Fig. 3. The CSF median values were generally higher for the *ClinicCSF.v1* than for the *FACT* test in Group 1 (Fig. 3A); the differences were statistically significant (p<0.001) for all frequencies except for 3 cpd. However, the *ClinicCSF.v2* gave similar scores than the *FACT* for all the evaluated spatial frequencies in subjects from Group 2 (p>0.05) (Fig. 3B).

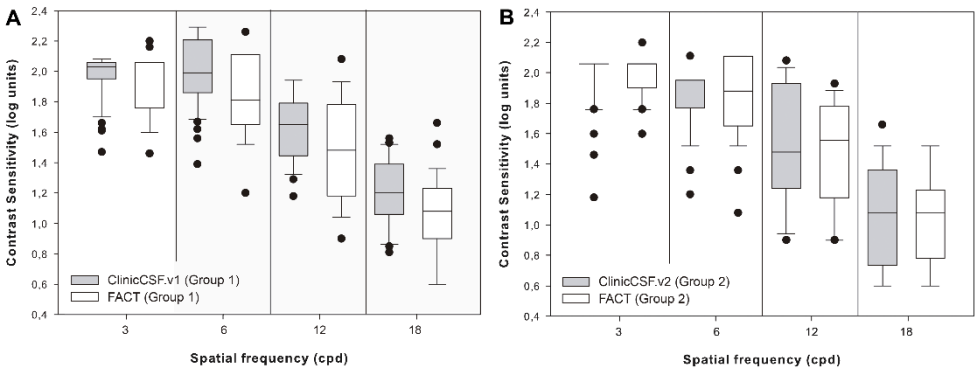

Figure 3. Box plot diagrams showing median contrast sensitivity values. (A) ClinicCSF.v1 and Functional Acuity Contrast Test (FACT) measured in Group 1 of subjects (B) ClinicCSF.v2 and FACT measured in Group 2 of subjects.

Table 1. Comparisons of medians (ranges) between ClinicCSF.v1 vs FACT from Group 1 and ClinicCSF.v2 and FACT from Group 2.

	Subjects Group 1			Subjects Group 2		
SF (cpd)	ClinicCSF.v1 Median (range)	FACT Median (range)	W test	ClinicCSF.v2 Median (range)	FACT Median (range)	W test
3	2.03 (1.47-2.08)	2.06 (1.46-2.20)	p=0.193	2.06 (1.18-2.06)	2.06 (1.60-2.20)	p=0.108
6	1.99 (1.39-2.29)	1.81 (1.20-2.26)	p<0.001	1.95 (1.20-2.11)	1.88 (1.08-2.11)	p=0.636
12	1.65 (1.18-1.94)	1.48 (0.90-2.08)	p<0.001	1.48 (0.90-2.08)	1.55 (0.90-1.93)	p=0.207
18	1.20 (0.81-1.56)	1.08 (0.60-1.66)	p<0.001	1.08 (0.60-1.66)	1.08 (0.60-1.52)	p=0.959

W test= Wilcoxon test; SF = Spatial Frequency

As can be seen in Table 2, both groups gave similar contrast sensitivities when the same *FACT* test was used to perform the exam (*p>0.05*). Even though both groups reported similar CSs with the *FACT* test (Fig. 4A), there existed

significant differences between groups when they were measured with different versions of the *ClinicCSF* for spatial frequencies of 6 and 18 cpd ($p<0.05$) (Fig. 4B).

Table 2. Comparisons of medians (ranges) between groups using the same FACT test and two different versions of the ClinicCSF application.

SF (cpd)	FACT			ClinicCSF		
	Group 1 Median (range)	Group 2 Median (range)	M-W	Group 1 (v1) Median (range)	Group 2 (v2) Median (range)	M-W
3	2.06 (1.46-2.20)	2.06 (1.60-2.20)	p=0.789	2.03 (1.47-2.08)	2.06 (1.18-2.06)	p=0.051
6	1.81 (1.20-2.26)	1.88 (1.08-2.11)	p=0.930	1.99 (1.39-2.29)	1.95 (1.20-2.11)	p=0.009
12	1.48 (0.90-2.08)	1.55 (0.90-1.93)	p=0.881	1.65 (1.18-1.94)	1.48 (0.90-2.08)	p=0.090
18	1.08 (0.60-1.66)	1.08 (0.60-1.52)	p=0.614	1.20 (0.81-1.56)	1.08 (0.60-1.66)	p=0.021

M-W= Mann-Whitney test; ; SF = Spatial Frequency

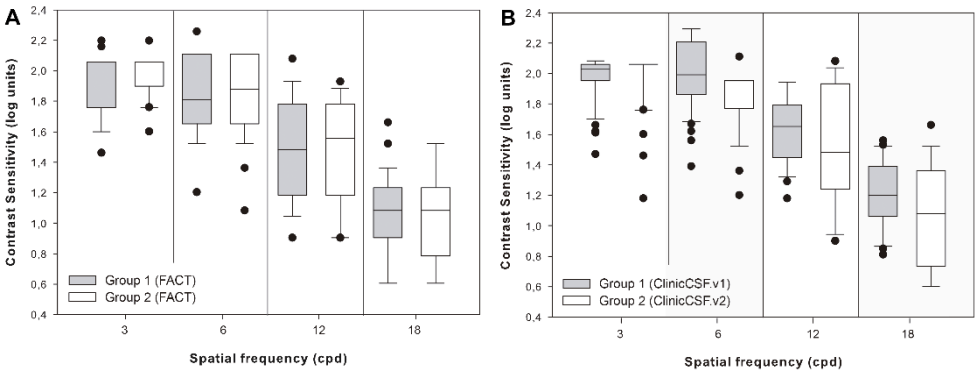

Figure 4 Box plot diagrams showing median contrast sensitivity values. (A) Group 1 and Group 2 of subjects measured with the Functional Acuity Contrast Test (FACT). (B) Group 1 and Group 2 of subjects measured with the ClinicCSF.v1 and ClinicCSF.v2, respectively.

In Fig.5, Bland-Altman plots are represented by means of the difference between the two methods [*ClinicCSF.v1 – FACT*] against the mean [(*ClinicCSF.v1+FACT*)/2]. The same representation was also done for the *ClinicCSF.v2* and the *FACT* in the Fig.6 by a direct comparison of each one of the spatial frequencies. It can be seen that the *ClinicCSF.v1* overestimated the CS with respect to the *FACT*, and this overestimation was not found with the *ClinicCSF.v2* (continuous lines in Figs.5 and 6). It should also be noted that although we found less differences between the *ClinicCSF.v2* vs. *FACT* than between the *ClinicCSF.v1* vs. *FACT*, narrower agreement limits were obtained with the staircase psychophysical method of the *ClinicCSF.v1*; mainly for spatial frequencies of 6, 12, and 18 cpd (dashed lines in Figs. 5 and 6).

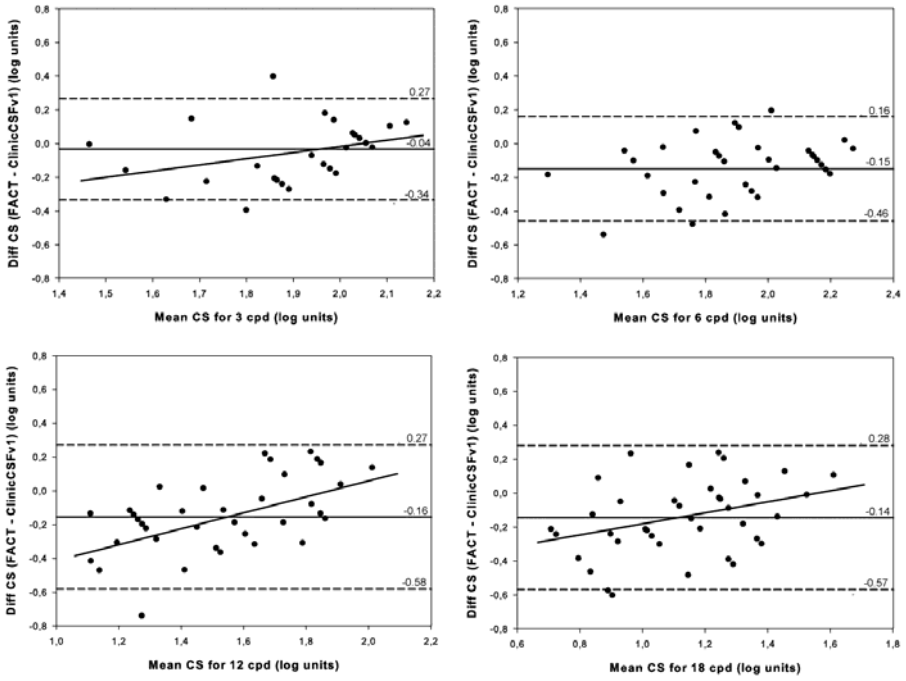

Figure 5. Bland---Altman plots. CS difference between methods versus mean of CS scores measured with FACT and ClinicCSF.v1 for spatial frequencies of 3 cpd (top-left), 6 cpd (top-right), 12 cpd (bottom-left), and 18 cpd (bottom-right). The solid lines represent the mean difference b tween the two instruments and the dashed lines correspond to the 95% confidence interval (mean ± 1.96SD). A linear fit was done

for statistically significant correlations ($p < 0.05$) and the Pearson coefficients (r) are reported for 3 cpd ($r = 0.37$), 12 cpd ($r = 0.56$), and 18 cpd ($r = 0.34$).

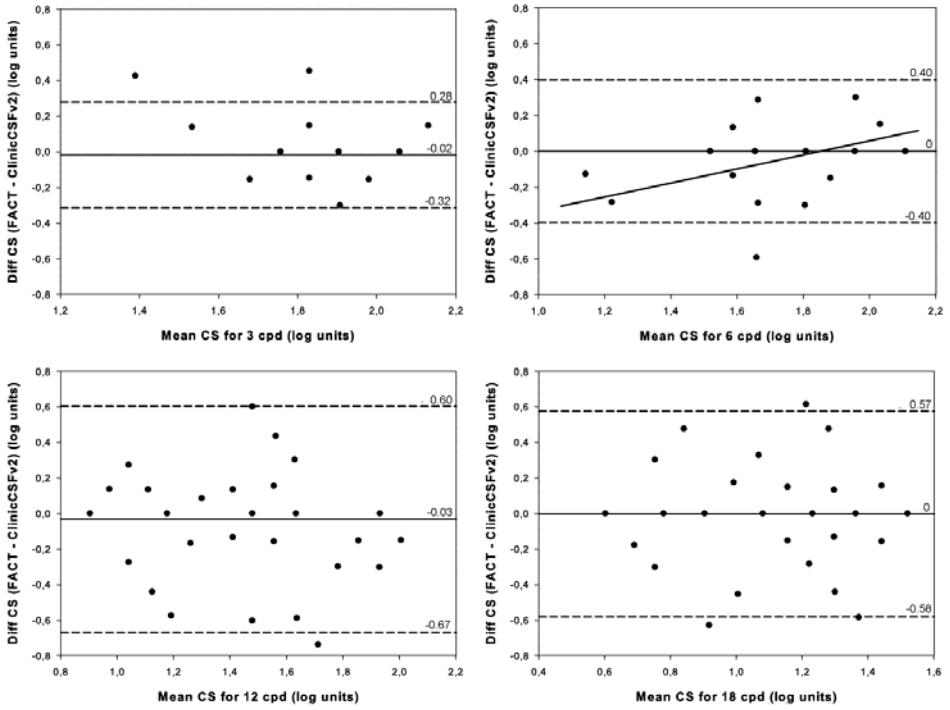

Figure 6. Bland---Altman plots. CS difference between methods versus mean of CS scores measured with FACT and ClinicCSF.v2 for spatial frequencies of 3 cpd (top-left), 6 cpd (top-right), 12 cpd (bottom-left), and 18 cpd (bottom-right). The solid lines represent the mean difference between the two instruments and the dashed lines correspond to the 95% confidence interval (mean ± 1.96SD). A linear fit was done for statistically significant correlations ($p < 0.05$) and the Pearson coefficients (r) are reported for 6 cpd ($r = 0.44$).

Correlations between differences versus mean scores obtained with tests were analyzed by the Pearson coefficient (r) and represented in the Bland-Altman plots by linear least squares fitting in case of being statistically significant ($p<0.05$). Therefore as can be seen in Fig. 3 for the comparison between *ClinicCSF.v1* and *FACT*, the regression line show positive correlations with the increment of mean CS for 3, 12 and 18 cpd (r = 0.37, 0.56 and 0.34, respectively). On the other hand, the correlation was significant only for 6 cpd (r = 0.44) in the comparison between *ClinicCSF.v2* and *FACT*.

2.4.5. Discussion

The aim of this study was to present a new iPad APP to measure CSF. Two versions *(ClinicCSF.v1 and .v2)* have been proposed and tested in comparison with other commercial test *(FACT).* Although two different groups of subjects were used in the evaluation of each one of the *ClinicCSF* versions, no statistical differences in visual acuity and age were found between both groups. Special attention was paid on age of participants considering that CSF could be influenced by this variable (Ross et al. 1985). In fact, some commercially available tests, such as the *CSV1000*, have different normative ranks depending on age of the subjects (VectorVision 2014b).

We found significant differences between *ClinicCSF.v1* and *FACT* for all spatial frequencies except for 3 cpd (Table I). This lack of agreement can be attributed firstly to the fact that each test measures different CS levels (Fig. 2) and secondly to the different psychophysical method employed in each version. Other comparative studies also found discrepancies due to the similar reasons. Franco et al. (Franco et al. 2010) compared the *VCTS-6500* and the *CSV-1000* and found mean differences of 0.30, 0.20, 0.08 and 0.18 for spatial frequencies of 3, 6, 12 and 18 cpd respectively, being the differences statistically significant for all spatial frequencies. Such differences are even higher than those obtained in the present study except for 12 cpd (Fig. 5). As expected, the differences between the *ClinicCSF.v2*and the *FACT* were very much lower due to both tests have the same CS levels and use the same thresholding technique, unlike the *ClinicCSF.v1*and *FACT* (Fig.6).

Other researchers have sounded a note of caution with regard to the comparison of the same test with different configurations. For instance, *FACT* differs from the previous *Vistech* version in several characteristics: using smaller step sizes, a 3 alternative forced choice, “blurred” grating patch edges with the gratings smoothed, and a larger patch size to increase number of cycles at low spatial frequencies. Pesudovs et al. (Pesudovs et al. 2004) attributed dissimilar results between *Vistech* and *FACT* to the fact that this new version uses smaller step sizes with the same number of steps, and thus ranges of measurement are also smaller. As a consequence, they reported a ceiling effect in post-LASIK patients and a floor effect in cataract patients. Furthermore, Hitchcock et al. showed that not only step sizes could have influence on the CS since they found that although contrast levels were the same, results could

be different depending on the way tests were presented (Hitchcock et al. 2004).

Positive correlations between mean differences and the average of CS were found with the *ClinicCSF.v1* for three spatial frequencies (Fig.5). These correlations represent that the CS with *ClinicCSF.v1* was higher than *FACT* mainly in subjects with poorer CS. Significance of this correlation disappeared with the *ClinicCSF.v2* and curiously the only significant correlation between *ClinicCSF.v2* and *FACT* was discovered at 6cpd (Fig.6), spatial frequency that was not significant with *ClinicCSF.v1*. We consider these correlations might mainly be due tostep sizes with the same number of steps as was mentioned before when we discussed the conclusions of Pesudovs et al. (Pesudovs et al. 2004). This would appear to indicate that ceeling and floor effects might also appear for the comparison between *ClinicCSF.v1* and *FACT* in cataract and refractive surgery patients.

We also found that mean differences confidence intervals were highly influenced by the psychophysical method used to achieve the CS threshold. Confidence intervals of the Bland-Altman plots for differences between *ClinicCSF.v1* and *FACT* were narrowed by using a staircase method (Fig. 5). This fact underlines the importance of including a psychophysical method in iPad based screening tests instead of using it simply as an illuminated screen (Zhang et al. 2013; Black et al. 2013).

The biggest differences in the CSFs between groups were found when we changed some properties of the test design (Table II). This demonstrates just how important is to use the same test in the comparison between groups of subjects. Consequently, clinical results in studies which implement different CS tests might also differ due to the configuration of tests used. In fact, the discrepancies in the comparison of several CS tests have been widely studied, mainly in order to obtain normative data for contrast sensitivity functions (Long and Penn 1987).

One limitation of this study is that two different groups of subjects were used to compare each one of the *ClinicCSF* versions with the *FACT*. The reason is that *ClinicCSF.v1* was first designed and evaluated clinically with one group of subjects. Lately *ClinicCSF.v2* was developed as an improved version of *ClinicCSF.v1* and it was no possible to measure the same group of subjects.

A better statistical analysis of variance could have been done if we had measured the CSF with the three tests in the same group of subjects. Other limitation of our current proposal is related to the maximum brightness configuration of the iPad that might produce a glare effect in some patients, and a possible post-image after each answer. This issue should be considered in future versions of the app.

Our work led us to conclude that *ClinicCSF* APP, designed for a given tablet device, can give similar results than *FACT* in CSF measurement in a normal population. Further experiments using the *ClinicCSF* APP in different versions of the same device are required in order to extrapolate our results. The findings might not be generalized to all the iPad Retina screens because it has not yet been proven the uniformity of colorimetric and photometric properties among all iPads. We think that our new test could be useful to popularize the CSF measurement in centers that do not usually perform it, due to the high cost of current commercial equipment. Further experimental investigations are also needed to estimate normative ranges and ROC curves.

2.4.6. Ackowledgments

We acknowledge financial support from Ministerio de Economía y Competitividad (Grant FIS2011-23175), GeneralitatValenciana (grant PROMETEO2009-077), and Universitat Politècnica de València (INNOVA SP20120569).

2.4.7. Conflict of interest

Rodríguez-Vallejo, M. has designed and programmed the ClinicCSF APP which he currently distributes by the Apple Store with his own developer account. The other authors report no conflicts of interest and have no proprietary interest in any of the materials mentioned in this article.

2.4.8. References

Alexander KR, Barnes C, Fishman GA, Pokorny J, Smith VC (2004) Contrast sensitivity deficits in inferred magnocellular and parvocellular pathways in retinitis pigmentosa. Invest Ophthalmol Vis Sci 45:4510–4519.

Alexander KR, McAnany JJ (2010) Determinants of contrast sensitivity for the Tumbling E and Landolt C. Optom Vis Sci 87:28–36.

Ansari E, Morgan J, Snowden R (2002) Psychophysical characterisation of early functional loss in glaucoma and ocular hypertension. Br J Ophthalmol 86:1131–1135.

Beck RW, Ruchman MC, Savino PJ, Schatz NJ (1984) Contrast sensitivity measurements in acute and resolved optic neuritis. Br J Ophthalmol 68:756–9.

Black JM, Jacobs RJ, Phillips G, Chen L, Tan E, Tran A, Thompson B (2013) An assessment of the iPad as a testing platform for distance visual acuity in adults. BMJ Open 3:e002730.

Bunce C (2009) Correlation, agreement, and Bland-Altman analysis: statistical analysis of method comparison studies. Am J Ophthalmol 148:4–6.

Chauhan T, Perales E, Xiao K, Hird E, Karatzas D, Wuerger S (2014) The achromatic locus: Effect of navigation direction in color space. J Vis 14:25,1-11.

Chylack LT, Padhye N, Khu PM, Wehner C, Wolfe J, McCarthy D, Rosner B, Friend J (1993) Loss of contrast sensitivity in diabetic patients with LOCS II classified cataracts. Br J Ophthalmol 77:7–11.

Dorr M, Lesmes LA, Lu ZL, Bex PJ (2013) Rapid and reliable assessment of the contrast sensitivity function on an iPad. Inves Opthal Vis Sci 54:7266–7273.

Franco S, Silva AC, Carvalho AS, Macedo AS, Lira M (2010) Comparison of the VCTS-6500 and the CSV-1000 tests for visual contrast sensitivity testing. Neurotoxicology 31:758–61.

Ginsburg AP (1996) Next generation contrast sensitivity testing. In: Fuctional

assessment of low vision. St Louis: Mosby Year Book Inc, pp 77–88

Hitchcock EM, Dick RB, Krieg EF (2004) Visual contrast sensitivity testing: a comparison of two F.A.C.T. test types. Neurotoxicol Teratol 26:271–7.

Hitchings RA, Powell DJ, Arden GB, Carter RM (1981) Contrast sensitivity gratings in glaucoma family screening. Br J Ophthalmol 65:515–7.

Kim CY, Chung SH, Kim T, Cho YJ, Yoon G, Seo KY (2007) Comparison of higher-order aberration and contrast sensitivity in monofocal and multifocal intraocular lenses. Yonsei Med J 48:627–633.

Kollbaum PS, Jansen ME, Kollbaum EJ, Bullimore MA (2014) Validation of an iPad Test of Letter Contrast Sensitivity.

Leek MR (2001) Adaptive procedures in psychophysical research. Percept Psychophys 63:1279–92.

Lindberg C, Fishman G, Anderson R, Vasquez V (1981) Contrast sensitivity in retinitis pigmentosa. Br J Ophthalmol 65:855–858.

Long GM, Penn DL (1987) Normative contrast sensitivity functions: the problem of comparison. Am J Optom Physiol Opt 64:131–5.

Malo J, Luque MJ (2014) COLORLAB: A color processing tool-box for Matlab. http://www.uv.es/vista/. Accessed 5 May 2014.

Murdoch IE, Morris SS, Cousens SN (1998) People and eyes: statistical approaches in ophthalmology. Br J Ophthalmol 82:971–3.

Norton T, Corliss D, Bailey J (2002) The psychophysical measurement of visual function. MA: Butterworth-Heinemann, Burlington.

Owsley C (2003) Contrast sensitivity. Ophthalmol Clin North Am 16:171–178.

Pelli DG, Robson JG, Wilkins AJ (1988) The design of a new letter chart for measuring contrast sensitivity. Clin Vis Sci 2:187–199.

Pesudovs K, Hazel C, Doran R, Eliot D (2004) The usefulness of Vistech and FACT contrast sensitivity charts for cataract and refractive surgery outcomes research. Br J Ophthalmol 88:11–16.

Rodríguez-Vallejo M (2014b) ClinicCSF. Contrast sensitivity test for tablets.

http://www.test-eye.com. Accessed 5 May 2014.

Ross J, Clarke D, Bron A (1985) Effect of age on contrast sensitivity function: uniocular and binocular findings. Br J Ophthalmol 69:51–56.

Rucker JC, Sheliga BM, FitzGibbon EJ, Miles FA, Phil D, Leigh RJ (2006) Contrast sensitivity, first-order motion and initial ocular following in demyelinating optic neuropathy. J Neurol 253:1203–1209.

StereoOptical Co. Inc. (2014) Optec functional vision analyzer. http://www.stereooptical.com/. Accessed 5 May 2014.

VectorVision (2014a) CSV-1000. http://www.vectorvision.com. Accessed 5 May 2014.

VectorVision (2014b) Contrast Sensitivity Values for the CSV-1000E in Log Units. http://www.vectorvision.com/. Accessed 5 May 2014.

Zhang Z-T, Zhang S-C, Huang X-G, Liang L-Y (2013) A pilot trial of the iPad tablet computer as a portable device for visual acuity testing. J Telemed Telecare 19:55–9.

Zhao LQ, Zhu H (2011) Contrast sensitivity after zyoptix tissue saving LASIK and standard LASIK for myopia with 6-month followup. J Ophthalmol 2011:839371.

Displays

Volume 44, September 2016, Pages 15–20

Visual acuity and contrast sensitivity screening with a new iPad application ☆

Manuel Rodríguez-Vallejo[a, b], Clara Llorens-Quintana[a], Walter D. Furlan[a], Juan A. Monsoriu[b]. ♟ ✉

Show more

doi:10.1016/j.displa.2016.06.001

Highlights

- We present a new iPad App for a fast assessment of Visual Acuity and Contrast Sensitivity.
- The iPad test shows a good agreement with conventional tests.
- The new App is proposed as a convenient and faster alternative to commercial screening devices.

Abstract

We present a new iPad application (app) for a fast assessment of Visual Acuity (VA) and Contrast Sensitivity (CS) whose reliability and agreement was evaluated versus a commercial screening device (Optec 6500). The measurement of VA was programmed in the app in accordance with the Amblyopia Treatment Study protocol. The CS was measured with sinusoidal gratings of four different spatial frequencies: 3, 6, 12 and 18 cpd at the same contrast values of the Functional Acuity Contrast Test (FACT) included in the Optec 6500. Forty-five healthy subjects with monocular corrected visual acuities better than 0.2 logMAR participated in the agreement study. Bland-Altman analyses were performed to assess the agreement and Deming regressions to calculate Mean Differences (MDs) and Limits of Agreement (LoAs). Coefficients of reliability were 0.15 logMAR for our method and 0.17 logMAR for the ETDRS testing protocol. For testing the CS, our test showed no statistically significant differences compared with the FACT at any spatial frequency ($p > 0.05$). The MDs were lower than 0.05 log units for all spatial frequencies.

Keywords

Visual acuity; Contrast sensitivity; Screening; iPad

☆ This paper was recommended for publication by Richard H.Y. So.

♟ Corresponding author.

2.5. Visual acuity and contrast sensitivity screening with a new iPad application.

Manuel Rodriguez-Vallejo[1,2*], Clara Llorens-Quintana[2], Walter D. Furlan[2] and Juan A. Monsoriu[1]

[1] *Centro de Tecnologías Físicas, Universitat Politècnica de València, 46022 Valencia, Spain*

[2] *Departamento de Óptica, Universitat de València, 46100 Burjassot, Spain*
[*] *Corresponding author: marodva1@upvnet.upv.es*

2.5.1. Abstract

We present a new iPad application (APP) for a fast assessment of Visual Acuity (VA) and Contrast Sensitivity (CS) whose reliability and agreement was evaluated versus a commercial screening device (Optec 6500). The measurement of VA was programmed in the APP in accordance with the Amblyopia Treatment Study protocol. The CS was measured with sinusoidal gratings of four different spatial frequencies: 3, 6, 12 and 18 cpd at the same contrast values of the Functional Acuity Contrast Test (FACT) included in the Optec 6500. Forty-five healthy subjects with monocular corrected visual acuities better than 0.2 logMAR participated in the agreement study. Bland-Altman analyses were performed to assess the agreement and Deming regressions to calculate Mean Differences (MDs) and Limits of Agreement (LoAs). Coefficients of reliability were 0.15 logMAR for our method and 0.17 logMAR for the ETDRS testing protocol. For testing the CS, our test showed no statistically significant differences compared with the FACT at any spatial frequency ($p > 0.05$). The MDs were lower than 0.05 log units for all spatial frequencies.

2.5.2. Introduction

Vision screening programs are intended to identify eye problems which occur in children or adults and refer them for further evaluation. Although there is a battery of screening methods designed to detect specific eye disorders, some screening techniques can be considered ‘‘multi-purpose,” minimizing the need for several individual tests (Ciner et al. 1998). For instance, visual acuity (VA) is considered an essential part of any eye examination (American Academy of Ophthalmology 2010) and it is used in the screening of refractive errors (Tong et al. 2002) and amblyopia (Kemper et al. 1999). On the other hand, the Contrast Sensitivity Function (CSF) is considered an additional test for specialized clinical evaluation, and has been generally accepted as a better predictor of visual performance than high contrast VA (Sokol et al. 1985; Elliott and Situ 1998; Lahav et al. 2011).

Several tests and methods have been proposed for the assessment of VA and CSF. Nowadays, the Early Treatment of Diabetic Retinopathy Study (ETDRS) testing protocol is generally accepted as the gold standard of VA measurement in adults (Ferris and Bailey 1996; Stewart et al. 2006; Shah et al. 2012). With regard to contrast sensitivity (CS), although the Pelli-Robson chart is considered the gold standard to compare optotype’s based CS tests (Pelli et al. 1988), currently there is not a commercial gold standard test to measure CS by sinusoidal gratings. Despite this fact, some clinical tests have been developed and they represent a good solution in vision screening programs; the most used are the Functional Acuity Contrast Test (FACT) (Ginsburg 1996; Hitchcock et al. 2004) and the Vector Vision CSV-1000 (Pomerance and Evans 1994; Franco et al. 2010). Clinical CS tests commonly use 9 patches of sinusoidal gratings with different contrast levels. They could differ in the step sizes, ranges, or the psychophysical method to achieve the threshold (Pesudovs et al. 2004). The Optec 6500_ is a commercial screening device that complies with the ANSI standard (American National Standard 1992) and includes the ETDRS and FACT tests to evaluate VA and CS respectively.

Ever since computer tablets appeared, new applications (APPs) have been proposed in the field of visual science (Black et al. 2013; Dorr et al. 2013;

Leising et al. 2013; Kollbaum et al. 2014). The great advantage of using these portable devices is the potential standardization of measurements. This is because many models of tablets have screens with similar characteristics such as chromaticity and resolution. Therefore, it can be hypothesized that if a developer takes into account the technical data of the tablets in the design of an APP, any operator who uses the same display in any part of the world will measure the visual function under the same conditions. However, to provide accurate presentation of test stimuli, individual device calibration may be necessary to ensure that any variances between devices, even of the same manufacturer and model, are taken into account. In this respect, in a recent paper Tahir et al. suggested practical means to optimise quality of display for vision testing including screen calibration (Tahir et al. 2014).

The assessment of the VA and CS with an iPad has recently been proposed under different approaches: Black et al. (Black et al. 2013) implemented a platform for testing distance VA. To evaluate CS, Kollbaum et al. developed an elementary test consisting of two letters on each page of an iBook, having 0.1 log units of difference between pages (Kollbaum et al. 2014). This test was compared with the Pelli-Robson and Freiburg VA tests and gave significantly lower values with the first one and good agreement with the second one. On the other hand Dorr et al. implemented the quick CSF method proposed Lesmes et al., to evaluate the response to sinusoidal gratings of 16 spatial frequencies log-spaced from 0.42 to 13.7 cycles per degree (cpd) (Lesmes et al. 2010; Dorr et al. 2013). This test was validated with measurements obtained from four normally sighted subjects on specialized laboratory equipment. However, in spite of its name, this method is still rather time-consuming for screening purposes (up to 5 min) (Dorr et al. 2013). The aim of this study is to introduce a new iPad APP designed for a fast screening of VA and CS, which represents an alternative to other expensive and large-format screening instruments. The obtained VA and CS records and test-retest reliabilities are compared with those achieved with the Optec6500.

2.5.3. Methods

The proposed APP was developed with ActionScript 3.0 programming language for mobile devices and then compiled for IOS with Adobe Flash Builder (Adobe Systems, Inc.). The tablet used to perform this research was a third generation iPad with a retina display (2048-by-1536-pixel resolution at 264 pixels per inch). The suitability of this device for visual psychophysics purposes has been previously reported (Aslam et al. 2013; Dorr et al. 2013). A Spyder4Elite colorimeter was used to measure the chromaticity of the iPad screen at maximum brightness. Data obtained from the colorimeter were used to create the CS stimuli. The room lighting during measurements was controlled with the luminance meter LX1330B Luxmeter. The APP consists of two primary components, intended to be useful for a fast screening of VA and CS.

2.5.3.1 Fast Screening of Visual Acuity (FSVA)

In assessing VA with the proposed APP, each subject has to recognize which of the four letters (HOTV) with 50% crowding bars appear isolated in the centre of the screen (Fig 1, left). On each visual acuity level, a black optotype is presented over a white background with luminance of 342 cd/m^2. An automated psychophysical method (described by the Amblyopia Treatment Study (ATS) testing protocol (Holmes et al. 2001)) was included in the APP to reach the VA threshold, thereby the operator task consist only in touching the corresponding button according to the answer given by the observer. An empty button was placed next to the HOTV buttons to be pressed when the observer could not recognize the letter. Even though the ATS protocol consists of a binocular pre-test followed by a monocular screening, the first one was omitted to shorten the task and directly it starts with monocular screening at 0.8 logMAR. The reinforcement phase described in the ATS protocol was also omitted and the APP automatically passed from phase 1 to phase 2. In our experiments the presentation distance for the test was 3 m. Each VA measurement was completed in approximately one minute.

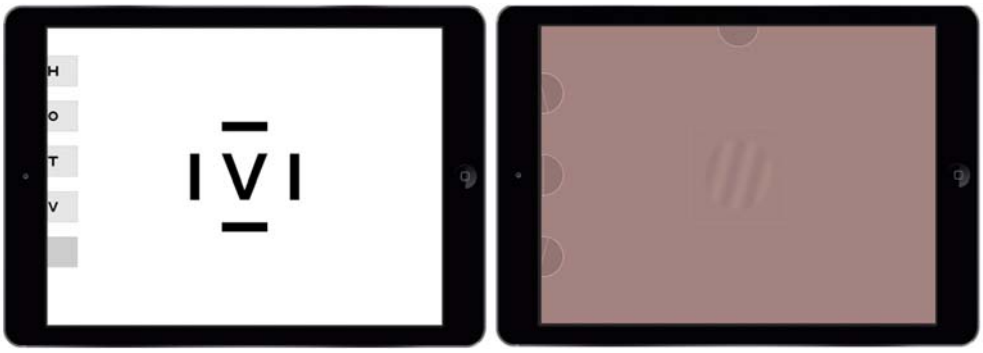

Figure 1. iPad APP patterns. Crowded optotype in the FSVA (left) and sinusoidal grating in the FSCS (right). FSVA: Fast Screening of Visual Acuity, FSCS: Fast Screening Contrast Sensitivity.

2.5.3.2 Fast Screening Contrast Sensitivity (FSCS)

For a rapid assessment of the CS we propose the use of sinusoidal gratings of four different spatial frequencies: 3, 6, 12 and 18 cpd. The contrast of the gratings was determined by the luminance difference of the white and dark bars, as described by Pelli in Ref. (Peli 1990). The sinusoidal gratings appear in a vertical orientation or tilted ±15º from the vertical and are presented in circular patches with blurred edges that fade the gratings into an achromatic background of mean luminance (85 cd/m2). The angle subtended by the patchs from the presentation distance was 1º. A total of 9 patches of different contrasts were generated for each spatial frequency and each orientation. Stimuli were programmed with MATLAB software (The MathWorks, Natick, MA) and the library COLORLAB (Malo and Luque 2014). The CS values for each frequency and the psychophysical procedure were programmed using the same parameters of the FACT (Ginsburg 1996; Hitchcock et al. 2004; Bühren et al. 2006) in order to obtain comparable results (see Table 1). The measurements of the CS thresholds for four spatial frequencies were completed in a mean of two minutes and a half per eye.

Table 1. Contrast sensitivity values (in log units) for the patches of the four spatial frequencies in FSCS APP. These values are the same values comprised in the FACT. FSCS: Fast Screening Contrast Sensitivity, FACT: Functional Acuity Contrast Test, cpd: cycles per degree.

	Spatial frequency (cpd)			
Patch	3	6	12	18
9	2.20	2.26	2.08	1.81
8	2.06	2.11	1.93	1.66
7	1.90	1.95	1.78	1.52
6	1.76	1.81	1.63	1.36
5	1.60	1.65	1.48	1.23
4	1.46	1.52	1.34	1.08
3	1.30	1.36	1.18	0.90
2	1.18	1.20	1.04	0.78
1	1.00	1.08	0.90	0.60

2.5.3.3 Subjects and Procedures

Forty-five subjects, comprised of 21 males (mean age: 36 ± 11 years) and 24 females (mean age: 33 ± 10 years), were recruited from university staff and students at the University of Valencia, Spain. Exclusion criteria included strabismus or any cause of monocular reduced visual acuity worse than 0.2 logMAR with habitual correction (measured with ETDRS). Informed consent was obtained from each subject just before starting the procedures. The research was conducted in accordance with the principles laid down in the Declaration of Helsinki. Approval from the human research ethics committee of the Universitat de València (Spain) was obtained before the study began.

All trials were performed in the same room illumination (15 Lux). The same procedure was carried out in all sessions by the same operator and with the patient wearing the habitual correction. VA and CS were measured with the iPad test and, after a short break, with the *Optec6500* using the *day testing* option (85cd/m^2 target illumination). Twenty-five subjects from the total were cited for two more sessions, spaced a week apart, in order to evaluate the reliability of both devices.

2.5.3.4 *Statistical Analysis*

Although both of the subjects' eyes were measured during testing procedures, only one was included in the agreement and reliability analyses after a random selection (McAlinden et al. 2011). VA and CS variables were not normally distributed; therefore non-parametric tests were employed. Statistical significances of VA and CS inter-eyes and inter-test differences were assessed with the Wilcoxon signed-rank test. On the other hand, differences between tests followed an approximately normal distribution, therefore the Bland-Altman analysis (Bland and Altman 1999) was performed to evaluate the agreement between iPad APPs and Optec6500 tests and to assess test-retest reliabilities. The *MethComp (version 1.25)* package was used with the *R* statistics software *(version 3.1, R Development Core Team, 2014)* in order to complete the statistical analyses described below.

2.5.3.5 *Agreement*

Differences between measurements for each test were plotted against the average and the 95% limits of agreement (LoAs) were computed depending on whether the average difference and the variability of differences were constant throughout the range of measurement (Bland and Altman 1999). We checked the hypotheses of constant differences and constant standard deviations by means of a Deming regression (function *DA.reg*) (Carstensen 2010). If the corresponding *p* values for both hypotheses were significant ($p<0.05$), conversion equations were employed on the plot, and mean differences (MDs) or LoAs were represented considering linear correlations (function *BA.plot,* parameters *dif.type = "lin"*, *sd.type = "lin"*).

2.5.3.6 *Reproducibility*

A Friedman 2-way analysis of variance by ranks with multiple comparisons was used to evaluate differences in medians among the three days (Armstrong et al. 2011). The residual standard deviation (σ_m) with each test

was computed with the data from the subjects who completed a total of 3 sessions (replicates). LoAs were estimated again considering models of exchangeable or linked replicates. A random permutation (function *perm.repl*) was done comparing the resulted LoAs with the original data by a Bland-Altman plot in order to apply the exchangeable or linked models proposed by Cartensen et al (Carstensen et al. 2008). Since the random permutation of replicates had little effect in the LoAs, they were computed as exchangeable. LoAs of test differences were compared with the reproducibility coefficients (r) of each test defined as $1.96\times\sqrt{2}\times\sigma_m$ (exchangeable replicates) in order to know if test agreement might be related with test reliability (*RepCoef* in function *BA.est*).

2.5.4. Results

2.5.4.1 Visual Acuity

No statistically significant differences were found in the comparison between right and left eyes with both tests, although as it can be seen in Fig. 2, the difference between eyes was higher with ETDRS (p=0.09) than with FSVA (p=0.85) at around 0.1 logMAR. In the comparison between tests (Fig. 3), VA scores obtained with FSVA had better results than those obtained with ETDRS with a MD of 0.06 logMAR (p<0.001). This difference would be approximately three letters on a logMAR chart with five letters per line. The null hypotheses of constant MDs and constant SDs were accepted (p>0.05) which suggest that EDTRS results could easily be predicted with the FSVA along the range of visual acuities measured (-0.2 to 0.2) by simply subtracting MD from FSVA results.

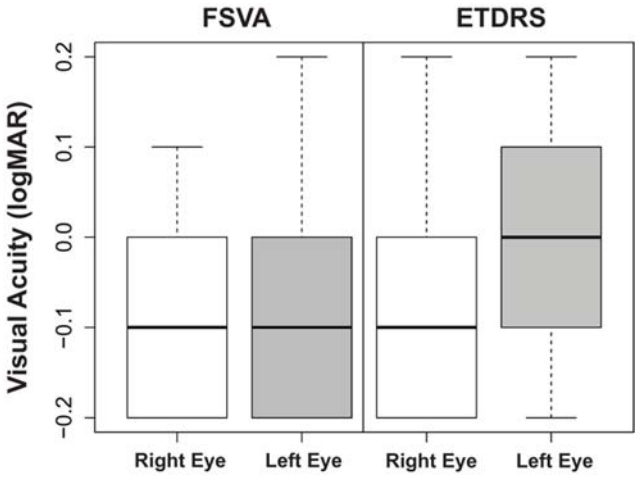

Figure 2. Box plot diagrams showing visual acuities from right and left eyes measured with both visual acuity tests. FSVA: Fast Screening of Visual Acuity, ETDRS: Early Treatment of Diabetic Retinopathy Study, logMAR: logarithm of the minimum angle of resolution.

Friedman test showed significant median differences between days χ^2 (2, n=25) =12.15, p=0.002 with ETDRS. The median was 0 logMAR for the first day and -0.1 logMAR for the other two days. On the other hand, medians with FSVA were -0.1 logMAR in the three days with no statistically significant differences among days χ^2 (2, n=25) =2.61, p=0.27. The number and percentage of subjects that reported differences within 0.1 logMAR in the three days were 24 (96%) with FSVA and 21 (84%) with ETDRS. The permutation indicated that replicates should be treated as exchangeable, therefore a recalculation of LoAs was performed under this condition obtaining a value of ±0.2 logMAR, similar to that reported in the agreement study (Fig. 3). Coefficients of reliability (r) were 0.15 logMAR for FSVA and 0.17 logMAR for ETDRS.

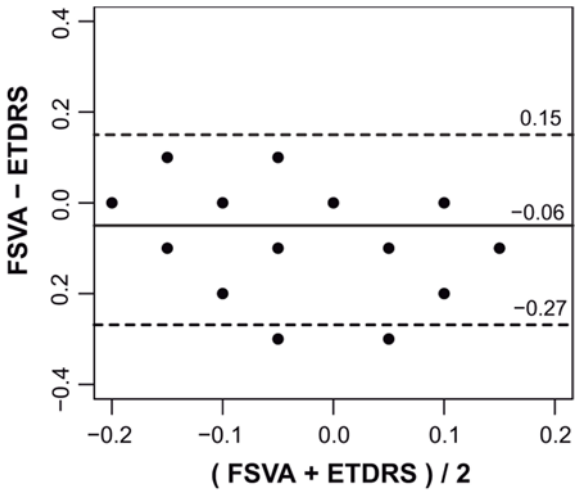

Figure 3. Bland–Altman plot showing the mean difference against the average of FSVA and ETDRS (solid line), limits of agreement are also represented by dashed lines. FSVA: Fast Screening of Visual Acuity, ETDRS: Early Treatment of Diabetic Retinopathy Study.

2.5.4.1 Contrast Sensitivity

The analyses of median differences between right and left eyes were not significant for all spatial frequencies and with both tests ($p>0.05$). There was a ceiling effect for spatial frequencies of 3 and 6 cpd which was manifested by a negative skewed distribution in the box plot diagrams (see Fig. 4). Even though the differences between the distributions of FSCS and FACT increase with the increment of the spatial frequency, no statistically significant differences were found at any spatial frequency ($p>0.05$).

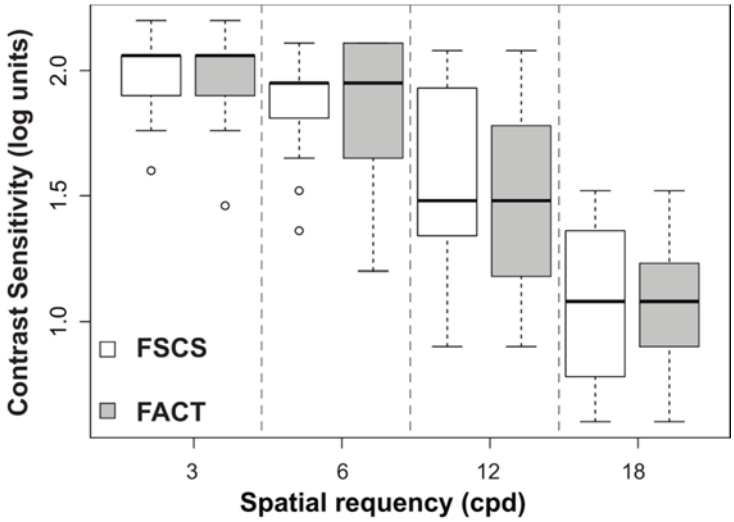

Figure 4. Box plot diagrams showing the contrast sensitivities obtained with FSCS and FACT for spatial frequencies of 3, 6, 12 and 18 cpd. The boxes indicate the first and third quartiles, the dark horizontal lines represent the median, and the extreme horizontal lines are the minimum and maximum. Other points represent outliers. FSCS: Fast Screening Contrast Sensitivity, FACT: Functional Acuity Contrast Test, cpd: cycles per degree.

MDs were below 0.05 log units for all spatial frequencies and LoAs were increased with the spatial frequency (see Fig. 5). Deming regression showed that although there were constant MDs for all the spatial frequencies ($p > 0.05$), constant SDs could not be assumed for 3, 6 and 18 cpd ($p < 0.05$). Therefore LoAs for non-constant SDs were also represented on Bland-Altman plots with the corresponding equations to compute the LoAs along the average of test measurements (a).

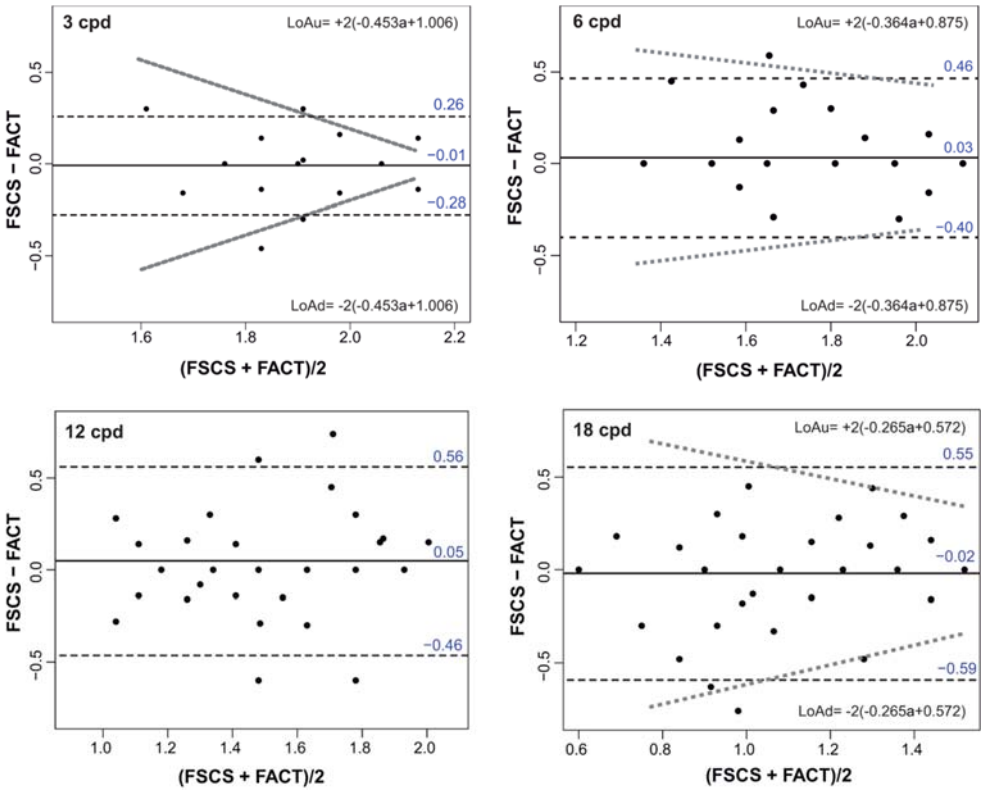

Figure 5. Bland–Altman plots showing the mean difference against the average of FSCS and FACT. Mean differences were nearly zero for all spatial frequencies even though the limits of agreement (dashed lines) were increased with the spatial frequency and with the decrease in average of contrast sensitivity for 3, 6 and 18 cpd. The variable a in the LoAs equations corresponds to the contrast sensitivity average from both tests. FSCS: Fast Screening Contrast Sensitivity, FACT: Functional Acuity Contrast Test, cpd: cycles per degree.

Table 2 shows that even though no statistical significant differences were found in the Friedman analysis of variance of the three days, a low reproducibility was obtained with both tests, but this was slightly better with the FACT. Considering step sizes between patches around 0.15 log units, reproducibility coefficients (*r*) from Table 2 correspond to a maximum difference of 2, 3, 4 and 4 patches for 3, 6, 12 and 18 cpd, respectively, with FSCS. Reproducibility slightly improved to 2 patches for 3, 6, and 12 cpd while a maximum difference of 3 patches was obtained for 18 cpd with FACT. The *r* was very close to the LoAs; therefore, the lack of agreement between FSCS and FACT can be attributed to the low reliability of both tests.

Table 2. Mean differences and limits of agreement (FSCS-FACT) calculated by exchangeable replicates in 25 subjects who completed the tests in three different days. Coefficients of reproducibility and a non-parametric analysis of variance are also represented. FSCS: Fast Screening Contrast Sensitivity, FACT: Functional Acuity Contrast Test, MD: Mean Differences, LoAs: Limits of Agreement, cpd: cycles per degree.

	MD	LoAs	Reproducibility (r)		Friedman χ^2 (2, n =25)	
			FSCS	FACT	FSCS	FACT
3cpd	-0.01	0.30	0.31	0.19	0.92 (p=0.63)	0.95 (p=0.62)
6cpd	-0.01	0.43	0.36	0.31	0.85 (p=0.65)	1.40 (p=0.50)
12cpd	0	0.55	0.50	0.31	0.24 (p=0.89)	1.71 (p=0.43)
18cpd	-0.03	0.56	0.53	0.42	2.47 (p=0.29)	0.29 (p=0.88)

2.5.5. Discussion

2.5.5.1 Visual Acuity

We found statistically significant differences between the records of VA obtained with FSVA and ETDRS, resulting in a better VA of 0.06 logMAR with our test. This result is coincident with the outcomes reported by Rice et al. (Rice et al. 2004) who found an MD of 0.06 logMAR between ATS and ETDRS. Leone et al (Leone et al. 2014) also found a better VA with the ATS procedure than with HOTV and ETDRS charts even though the latter ones incorporated a staircase method that improves the VA results. Therefore, the apparent lack of agreement between tests in our study can be attributed to the differences in the VA protocols rather than to the use of different instruments. It is also important to note that even though non-statistically significant differences were found between eyes with both tests, lower differences were manifested with FSVA. In regards to test reliabilities, we obtained a better coefficient of reproducibility with FSVA than with ETDRS. 96% of subjects reported differences within 0.1 logMAR with the FSVA, this percentage is consistent with the 93% previously reported with ATS protocol (Holmes et al. 2001). It is important to note that, even though we applied little modifications to the ATS in order to reduce time of testing (such as skipping the reinforcement phase), reliability has not been reduced.

Unlike a previous work carried out with another VA test for iPad (Black et al. 2013), we did not have glare problems. Given that our study was conducted preventing reflections over the screen, there is a possibility that dissimilar results would have arisen if the VA had been measured in a high light environment with reflections over the screen. One limitation of our methodology might be that the brightness of the screen was set on the maximum level (342cd/m^2), which is over the recommended background luminance (Consilium Ophthalmologicum Universale 1984). We decided to perform the study in this way to ensure that all evaluations were conducted under the same lighting conditions. Future work will concentrate on developing a system to measure environmental illumination and automatically set up the background luminance in accordance to the measured value.

2.5.5.1 Contrast Sensitivity

Dorr M. et al. have recently demonstrated that the CSF assessment on a mobile device may be indistinguishable from that obtained with specialized laboratory equipment (Dorr et al. 2013). Although they implemented the quick CSF method that reduces the testing time to no more than 5 minutes, this method could still be very time-consuming for screening procedures (Lesmes et al. 2010). Thus our proposal is a valuable alternative since it can be completed in half the time. The FSCS results demonstrated a good agreement with FACT with no statistically significant differences between tests at any spatial frequency. Specifically, the MDs were lower than 0.05 log units for all spatial frequencies. In a previous work, Franco et al. compared the agreement between VCTS-6500 and CSV-1000 (Franco et al. 2010). They found statistically significant differences with MDs of 0.3, 0.08, 0.2 and 0.18 log units for 3, 6, 12 and 18 cpd respectively. These differences can be attributed to the fact that these tests employ different step sizes between CS levels.

In our case, we found a lower agreement between tests at high spatial frequencies, but this fact could be related to test-retest reliabilities of FSCS and FACT. In fact, even though this issue was not mentioned in their discussion, Pesudovs et al. also found similar test-retest reliabilities, being poorer (as in the present study) with the increment of the spatial frequency (Pesudovs et al. 2004). The dependency of reliability with the CS level was also reported by Kollbaum et al. although they used optotypes which contain a wide range of spatial frequencies instead of sinusoidal gratings (Kollbaum et al. 2014). Therefore, it is possible that the FSCS and FACT reliabilities also vary in subjects who present any ocular disease that affects the CSF. FSCS has several advantages in regards to the Kollbaum et. al test, including testing individual spatial frequencies; random presentation of grating orientation, to avoid the learning effect.

2.5.6. Conclusion

In this work we have presented an iPad APP for screening visual performance by measuring VA and CS. We have shown that the FSVA improves the test-retest reliability compared with ETDRS. It is important to note that, even though we applied little modifications to the ATS in order to reduce time of testing (such as skipping the reinforcement phase), the reliability of the method has not been reduced. Therefore, we believe that the reinforcement phase might not be necessary to improve testing reliability in the ATS procedure and thus, We also found lower (non-statistically significant) differences between eyes with FSVA than with the EDTRS, this fact could be an advantage in screenings for amblyopia, providing a lower rate of false positive referral rates (Leone et al. 2014).

Further improvements in FSVA protocol are in progress and include the variation of letter contrast and a user calibration for its use at several test distances. In the first case this will be an interesting feature, for example, in studies of perceptual learning in amblyopia cases (Zhou et al. 2006). In the second case, the FSVA could be used, for instance, as test for the assessment of visual performance with multi-focal intraocular lenses or multifocal contact lenses.

Regarding FSCS, further developments are in progress to find the best contrast sensitivity levels for an iPad and to improve the reliability employing a best suited psychophysical method.

As a final conclusion, we have demonstrated that the APP we proposed is an efficient alternative in screening against more expensive large-format instruments that are difficult to transport and store, such as Optec6500. It can be very useful as a clinical tool for VA and CS screening of school-age children and it is fast, easy to perform and inexpensive. The method allows the procedure's standardization even when more than one examiner performs the test.

2.5.7. Acknowledgements

This work was funded by 'Ministerio de Economía y Competitividad' – 'Spain' (Grants FIS2011-23175 and DPI2015-71256-R) and 'Generalitat Valenciana' – 'Spain' (Grants PROMETEOII/2014/072 and ACOMP/2014/180).

2.5.8. References

American Academy of Ophthalmology (2010) Preferred Practice Pattern Guidelines. Comprehensive Adult Medical Eye Evaluation. American Academy of Ophthalmology, San Francisco CA.

American National Standard (1992) Ophthalmics-Instruments- General-Purpose Clinical Visual Acuity Charts. ANSI Z80.21-1992(R1998).

Armstrong RA, Davies LN, Dunne MCM, Gilmartin B (2011) Statistical guidelines for clinical studies of human vision. Ophthalmic Physiol Opt 31:123–36.

Aslam TM, Murray IJ, Lai MY, Linton E, Tahir HJ, Parry NR (2013) An assessment of a modern touch-screen tablet computer with reference to core physical characteristics necessary for clinical vision testing. J R Soc Interface 10:20130239.

Black JM, Jacobs RJ, Phillips G, Chen L, Tan E, Tran A, Thompson B (2013) An assessment of the iPad as a testing platform for distance visual acuity in adults. BMJ Open 3:e002730–e002730.

Bland JM, Altman DG (1999) Statistical methods in medical research. Stat Methods Med Res 8:135–160.

Bühren J, Terzi E, Bach M, Wesemann W, Kohnen T (2006) Measuring contrast sensitivity under different lighting conditions: comparison of three tests. Optom Vis Sci 83:290–298.

Carstensen B (2010) Comparing methods of measurement: Extending the LoA by regression. Stat Med 29:401–10.

Carstensen B, Simpson J, Gurrin LC (2008) Statistical models for assessing

agreement in method comparison studies with replicate measurements. Int J Biostat 4:Article 16.

Ciner EB, Schmidt PP, Orel-Bixler D, Dobson V, Maguire M, Cyert L, Moore B, Schultz J (1998) Vision screening of preschool children: evaluating the past, looking toward the future. Optom Vis Sci 75:571–84.

Consilium Ophthalmologicum Universale (1984) Visual acuity measurement standard. Visual Functions Committee, International Council of Ophthalmology.

Dorr M, Lesmes LA, Lu ZL, Bex PJ (2013) Rapid and reliable assessment of the contrast sensitivity function on an iPad. Inves Opthal Vis Sci 54:7266–7273.

Elliott DB, Situ P (1998) Visual acuity versus letter contrast sensitivity in early cataract. Vis Res 38:2047–2052.

Ferris FL, Bailey I (1996) Standardizing the measurement of visual acuity for clinical research studies: Guidelines from the Eye Care Technology Forum. Ophthalmology 103:181–182.

Franco S, Silva AC, Carvalho AS, Macedo AS, Lira M (2010) Comparison of the VCTS-6500 and the CSV-1000 tests for visual contrast sensitivity testing. Neurotoxicology 31:758–61.

Ginsburg AP (1996) Next generation contrast sensitivity testing. In: Fuctional assessment of low vision. St Louis: Mosby Year Book Inc, pp 77–88.

Hitchcock EM, Dick RB, Krieg EF (2004) Visual contrast sensitivity testing: a comparison of two F.A.C.T. test types. Neurotoxicol Teratol 26:271–7.

Holmes JM, Beck RW, Repka MX, Leske DA, Kraker RT, Blair RC, Moke PS, Birch EE, Saunders RA, Hertle RW, Quinn GE, Simons KA, Miller JM (2001) The amblyopia treatment study visual acuity testing protocol. Arch Ophthalmol 119:1345–53.

Kemper AR, Margolis PA, Downs SM, Bordley WC (1999) A systematic review of vision screening tests for the detection of amblyopia. Pediatrics 104:1220–1222.

Kollbaum PS, Jansen ME, Kollbaum EJ, Bullimore MA (2014) Validation of an iPad Test of Letter Contrast Sensitivity. Optom Vis Sci 91:291–6.

Lahav K, Levkovitch-Verbin H, Belkin M, Glovinsky Y, Polat U (2011) Reduced mesopic and photopic foveal contrast sensitivity in glaucoma. Arch Ophthalmol 129:16–22.

Leising KJ, Wolf JE, Ruprecht CM (2013) Visual discrimination learning with an iPad-equipped apparatus. Behav Process 93:140–147.

Leone JF, Mitchell P, Kifley A, Rose KA (2014) Normative visual acuity in infants and preschool-aged children in Sydney. Acta Ophthalmol 92: e521-9.

Lesmes LA, Lu ZL, Baek J, Albright TD (2010) Bayesian adaptive estimation of the contrast sensitivity function: the quick CSF method. J Vis 10:1–21.

Malo J, Luque MJ (2014) COLORLAB: A color processing tool-box for Matlab. http://www.uv.es/vista/. Accessed 5 May 2014.

McAlinden C, Khadka J, Pesudovs K (2011) Statistical methods for conducting agreement (comparison of clinical tests) and precision (repeatability or reproducibility) studies in optometry and ophthalmology. Ophthalmic Physiol Opt 31:330–8.

Peli E (1990) Contrast in complex images. J Opt Soc Am A 7:2032–40.

Pelli DG, Robson JG, Wilkins AJ (1988) The design of a new letter chart for measuring contrast sensitivity. Clin Vis Sci 2:187–199.

Pesudovs K, Hazel C, Doran R, Eliot D (2004) The usefulness of Vistech and FACT contrast sensitivity charts for cataract and refractive surgery outcomes research. Br J Ophthalmol 88:11–16.

Pomerance GN, Evans DW (1994) Test-retest reliability of the CSV-1000 contrast test and its relationship to glaucoma therapy. Invest Ophthalmol Vis Sci 35:3357–3361.

Rice ML, Leske D a, Holmes JM (2004) Comparison of the amblyopia treatment study HOTV and electronic-early treatment of diabetic retinopathy study visual acuity protocols in children aged 5 to 12 years. Am J Ophthalmol 137:278–82.

Shah N, Laidlaw DA, Rashid S, Hysi P (2012) Validation of printed and computerised crowded Kay picture logMAR tests against gold standard ETDRS acuity test chart measurements in adult and amblyopic paediatric subjects. Eye 26:593–600.

Sokol S, Moskowitz A, Skarf B, Evans R, Molitch M, Senior B (1985) Contrast sensitivity in diabetics with and without background retinopathy. Arch Ophthalmol 103:51–54.

Stewart CE, Hussey A, Davies N, Moseley MJ (2006) Comparison of logMAR ETDRS chart and a new computerised staircased procedure for assessment of the visual acuity of children. Ophthal Physiol Opt 26:597–601.

Tahir HJ, Murray IJ, Parry NR a, Aslam TM (2014) Optimisation and assessment of three modern touch screen tablet computers for clinical vision testing. PLoS One 9:e95074.

Tong L, Saw SM, Tan D, Chia KS, Chan WY, Carkeet A, Chua WH, Hong CY (2002) Sensitivity and specificity of visual acuity screening for refractive errors in school children. Optom Vis Sci 79:650–657.

Zhou Y, Huang C, Xu P, Tao L, Qiu Z, Li X, Lu Z-L (2006) Perceptual learning improves contrast sensitivity and visual acuity in adults with anisometropic amblyopia. Vis Res 46:739–50.

Fast and reliable stereopsis measurement at multiple distances with iPad

Manuel Rodriguez-Vallejo, Clara Llorens-Quintana, Diego Montagud, Walter D. Furlan, Juan A. Monsoriu

(Submitted on 21 Sep 2016)

Purpose: To present a new fast and reliable application for iPad (ST) for screening stereopsis at multiple distances.
Methods: A new iPad application (app) based on a random dot stereogram was designed for screening stereopsis at multiple distances. Sixty-five subjects with no ocular diseases and wearing their habitual correction were tested at two different distances: 3 m and at 0.4 m. Results were compared with other commercial tests: TNO (at near) and Howard Dolman (at distance) Subjects were cited one week later in order to repeat the same procedures for assessing reproducibility of the tests.
Results: Stereopsis at near was better with ST (40 arcsec) than with TNO (60 arcsec), but not significantly ($p = 0.36$). The agreement was good ($k = 0.604$) and the reproducibility was better with ST ($k = 0.801$) than with TNO ($k = 0.715$), in fact median difference between days was significant only with TNO ($p = 0.02$). On the other hand, poor agreement was obtained between HD and ST at far distance ($k=0.04$), obtaining significant differences in medians ($p = 0.001$) and poorer reliability with HD ($k = 0.374$) than with ST ($k = 0.502$).
Conclusions: Screening stereopsis at near with a new iPad app demonstrated to be a fast and realiable. Results were in a good agreement with conventional tests as TNO, but it could not be compared at far vision with HD due to the limited resolution of the iPad.

Comments: 14 pages, 3 figures, 4 tables
Subjects: **Computer Vision and Pattern Recognition (cs.CV)**
Cite as: **arXiv:1609.06669 [cs.CV]**
(or **arXiv:1609.06669v1 [cs.CV]** for this version)

2.6. Fast and reliable stereopsis measurement at multiple distances with iPad

Manuel Rodriguez-Vallejo[1*], Clara Llorens-Quintana[3], Diego Montagud[3], Walter D. Furlan[3] and Juan A. Monsoriu[2]

[1] *Qvision, Unidad de Oftalmología Vithas Hospital Virgen del Mar, 04120, Almería*

[2] *Centro de Tecnologías Físicas, Universitat Politècnica de València, 46022 Valencia, Spain*

[3] *Departamento de Óptica, Universitat de València, 46100 Burjassot, Spain*
[*] *Corresponding author: manuelrodriguezid@qvision.es*

2.6.1. Abstract

Purpose: To present a new fast and reliable application for iPad (ST) for screening stereopsis at multiple distances.

Methods: A new iPad application (app) based on a random dot stereogram was designed for screening stereopsis at multiple distances. Sixty-five subjects with no ocular diseases and wearing their habitual correction were tested at two different distances: 3 m and at 0.4 m. Results were compared with other commercial tests: TNO (at near) and Howard Dolman (at distance) Subjects were cited one week later in order to repeat the same procedures for assessing reproducibility of the tests.

Results: Stereopsis at near was better with ST (40 arcsec) than with TNO (60 arcsec), but not significantly ($p = 0.36$). The agreement was good ($k = 0.604$) and the reproducibility was better with ST ($k = 0.801$) than with TNO ($k = 0.715$), in fact median difference between days was significant only with TNO ($p = 0.02$). On the other hand, poor agreement was obtained between HD and ST at far distance ($k=0.04$), obtaining significant differ-

ences in medians (p = 0.001) and poorer reliability with HD (k = 0.374) than with ST (k = 0.502).

Conclusions: Screening stereopsis at near with a new iPad app demonstrated to be a fast and realiable. Results were in a good agreement with conventional tests as TNO, but it could not be compared at far vision with HD due to the limited resolution of the iPad.

Key Words: screening, stereopsis, stereoacuity, iPad, Howard Dolman, TNO

2.6.2. Introduction

Stereopsis is a measure of the visual perception of three-dimensional space. It is based on the binocular retinal disparity and it is included in vision examination of adults and children (American Optometric Association 1994a; American Optometric Association 1994b). The smallest binocular disparity that can be detected is known as stereoacuity or stereothreshold and is recorded in seconds of arc (arcsec) (Westheimer 2013). The Howard–Dolman (HD) two-rod apparatus is considered the gold standard to measure stereoacuity; however, this device has important drawbacks to be used in clinical practice: it is time-consuming, it should be performed at distance to avoid monocular clues, and requires that the subject makes a complex motor task with repeated measurements (Saladin 2005). Three types of tests are preferred in clinical practice depending on the type of stereopsis in which they are based: local stereopsis with contours or bars, global stereopsis with random dots, and a combination of both known as real stereopsis (Fricke et al. 1997). Even though all these tests are appropriated for vision screening in clinical practice, results may differ between them since they have not been designed to measure continuous stereoacuity as HD (Simons 1981). On the other hand, they are mainly used to detect, by discrete step sizes, whether there is any abnormality that affects binocular vision.

The most popular stereopsis tests are conducted at near. However, in the last decade distance stereotesting has been also suggested as a good screening procedure, highly sensitive to small refractive error changes, heterophorias and strabismus (Wang et al. 2010), and Snellen visual acuities under 20/25

(Rutstein and Corliss 2000). Even though distance stereopsis can provide additional information not detectable by near tests, the fact is that there are a lot of clinicians who have not incorporated this testing in their routines, perhaps because there are few tests designed to measure distance stereopsis, which are also very expensive.

New vision tests have been developed with the emerge of portable screens such as IPad or Android Tablets and smartphones (Zhang ZT, Zhang SC, Huang XG 2013; Perera et al. 2015). Several of the advantages of computerized tests have been implemented in these portable devices: randomized letters, automated scoring, wide range of optotypes, bright screen calibration, normal population databases, remote connection, etc. (Rodríguez-Vallejo et al. 2015). Other applications to measure stereopsis for portable devices such as iPod have been proposed but for only using at one distance, in long time (3 minutes), and not compared with conventional stereotests (Hess et al. 2016). Thus, the introduction of versatile, fast and portable stereopsis tests which can be used at different distances is of primary importance. This is the main goal of this work, a new iPad application for stereopsis measurement is presented and its reliability is assessed against the results obtained with the HD and TNO tests.

2.6.3. Materials (or Subjects) and Methods

In this section we first introduce the principles in which the new test was inspired. Thus, we begin with a brief review of the Howard Dolman and TNO test in order to put our analysis in a proper framework.

2.6.3.1 Howard Dolman

HD principle is schematized in Fig. 1A. Two vertical rods are seen in front of an empty field, one of them (O) is fixed and the other one (O') is movable back and forth along a lane. The rods are seen by the observer at 3 meters and the task is to align the movable rod, with a string attached to it, until the observer perceives that both rods are at the same distance. The stereo-

acuity (γ in radians is obtained in a continuous scale from the measurement of the relative distance between the two rods along the line of sight (Δz):

$$\gamma = \frac{a\Delta z}{z^2} \tag{1}$$

where z is the distance from the observer to the fixed rod and *a* is the inter-pupillary distance (see Fig. 1A) (Westheimer 2013).

The HD (Bernell Corporation)(Bernell 2014) used in this study has a continuous scale up to 73 arcsec, but measurements above 66 arcsec were considered outside of the instrument limits (OL), or suspended stereopsis.

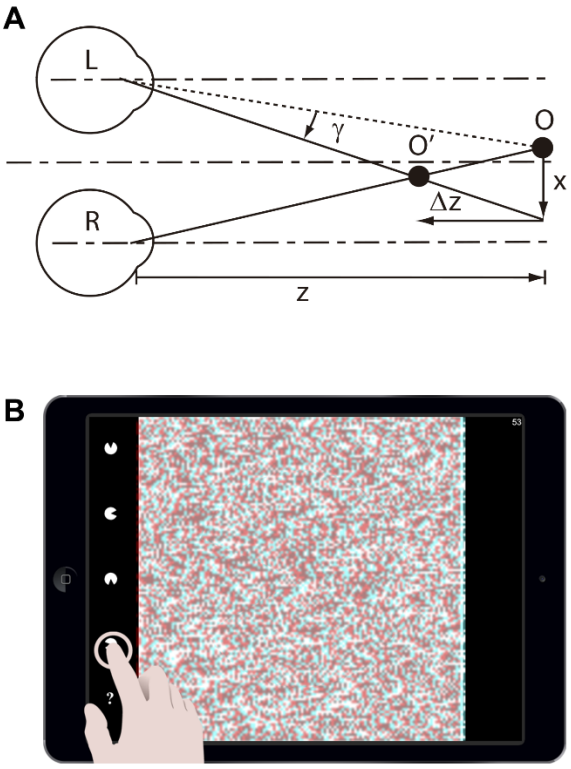

Figure 1. (A) Two objects scheme for computing the stereoacuity. (B) Screen capture of the app during the measurement process.

2.6.3.2 TNO

The TNO is a random dot test to measure global stereopsis at near (40 cm) with anaglyph eyeglasses (van Doorn et al. 2014). It consists of seven plates: three for screening purposes, a suppression test, and three plates to measure stereoacuity. In this last case, the task is to identify the position of a missing section of a circle that appears at one of four possible orientations. These figures are presented at six different depth levels corresponding to a disparity in the range from 15 to 480 arcsec (see Table 1) (van Doorn et al. 2014).

Table 1. Discrete steps of measurement with ST and TNO at near. A variable conversion from arcsec to an ordinal scale of five levels was performed for computing the Cohen's k with quadratic weights.

Level (Range)	ST (arcsec)	TNO (arcsec)
5 (OL*)	OL*	OL*
4 (278-480)	397	480
	357	
	318	
	278	
3 (159-240)	238	240
	199	
	159	
2 (79-120)	119	120
	79	
1 (15-60)	40	60
		30
		15

* Outside Device Limits (OL). The subject cannot resolve the stimulus with the TNO or ST.

2.6.3.3 iPad-Stereo Test

The iPad Stereotest (ST) we propose was developed with pure ActionScript 3.0 programming language for mobile devices and then compiled for IOS with Adobe Flash Builder (Adobe Systems, Inc.). Two identical arrays of random colored dots (one in red and one in cyan) are displayed in such a way that each array is visible with one of the patient's eyes when it wears anaglyph eyeglasses (red filter on the left eye). Some ordered dots inside a circle with a gap (similar to those in plates V, VI, and VII in the TNO test), are laterally displaced to produce fixed amounts of binocular disparity degree in arcsec (see the values in Tables 1 and 2). The binocular fusion of both patterns simulates a stereoscopic object when the disparity is crossed. As can be seen in Fig. 1A, if the displacement between the corresponding dots images at the reference (iPad) plane, is x; the stereoacuity can be expressed as $\gamma \approx x/z$ provided that in practice $z >> \Delta z$. Considering that, due to screen's pixels density (*SPD;* in pixels per inch (ppi)), the lateral displacement (x) is limited by pixel size, the stereopsis, can be computed (in radians) in terms of the *SPD* as:

$$\gamma = \frac{i}{SPD\ z_0} \tag{2}$$

where i is the number of pixels of displacement corresponding to the distance z_0. In order to evaluate the same level of stereopsis at multiple distances z_j greater than z_0, an integer multiplicative constant must be inserted on the right member of Eq. (2) such that $k = z_j/z_0$. However, the display resolution imposes a limit on the finest value that can be measured. For the iPad *retina* this limit is 40 arcsec for a presentation distance of 0.5 m. The *SPD* value is automatically recovered from the tablet by means of the programming code in order to avoid the need to calibrate the stimulus size with an external rule. On the other hand, the size of the random dots is variable with the presentation distance in a way that each dot subtends an angle of 1.32' at all distances which corresponds to a minimum visual acuity of 0.125 logMAR. The stereoscopic stimulus size is constant and subtends 1.88º at 3 m. Fig. 1B shows a screen capture of the app during the trial.

The stereoacuity scale is divided in ten discrete steps, being the lower value of the scale limited the pixel size and the following values of the scale are obtained by increasing one pixel of disparity between the images. An automated method to achieve the threshold was included in the app. In it, the level of stereopsis goes one level down with each right answer until the subject fails, then stereopsis goes one level up after the patient fails again. Stereo-threshold was considered the last level on which subject's response is correct after the first fail. The time spent for complete the trial is around 30 seconds.

2.6.3.4 Subjects and Procedures

Sixty-five subjects (mean age: 27.7 ± 7.2 years) were requited during a vision screening in the University of Valencia. Informed consent was obtained for each subject and the research was conducted in accordance with the principles laid down in the Declaration of Helsinki. Previous to stereopsis measurements, monocular visual acuity and cover test were evaluated; as well as objective refraction and interpupilar distance with WAM-5500 (Grand Seiko Co., Ltd., Hiroshima, Japan) (Sheppard and Davies 2010). Exclusion criteria were ocular diseases, strabismus, monocular visual acuity under 0.1 logMAR, a difference of 0.1 logMAR between both eyes with best compensation, and a residual spherical equivalent higher than ±0.50D from the objective value measured with the WAM-5500 with the subject wearing the habitual correction in spectacles or contact lenses.

All measurements were undertaken in the same room under artificial lighting conditions: 285 lux (LX1330B luxmeter). The device used to perform this research was an iPad third generation with retina display (2048-by-1536-pixel resolution and 264 ppi) with brightness at 100%; which corresponded to 342 cd/m^2 for white color (Spyder4Elite colorimeter).

Stereopsis was first measured at 3 m with the HD, each value was obtained with a psychophysical method, averaging the absolute values of six measures, three of them obtained starting with the movable rod ahead of the fixed rod (descending) and other three starting with the movable rod behind of the fixed rod (descending) (Ehrenstein and Ehrenstein 1999). Then, stere-

oacuity was measured with ST at the same distance with ten different threshold levels of stereoacuity (see Table 2).

Table 2. Discrete steps of measurement with ST and reorganization of HD measurements from a continuous scale to a range for computing the agreement with the Cohen's k with linear weights.

Level (Range)	ST (arcsec)	HD (arcsec)
11 (OL*)	OL*	OL*
10 (66-63)	66	66-63
9 (56-62)	60	56-62
8 (55-50)	53	55-50
7 (49-44)	46	49-44
6 (43-37)	40	43-37
5 (36-30)	33	36-30
4 (29-24)	26	29-24
3 (23-18)	20	23-18
2 (10-17)	13	10-17
1 (9 – 0)	7	9 - 0

* Outside Device Limits (OL). The subject cannot resolve stimulus with the ST or the movable bar is above 66 arcsec with the HD.

Once distance stereopsis was evaluated, the patient was positioned at 50 cm from the iPad and the near stereoacuity was measured for other ten different threshold levels (see Table 1).

Finally, the procedure was completed by testing each subject with the TNO at 40 cm under warm light of 945 lux. Subjects were cited a week after the first session to repeat all the procedures described above in order to assess the reproducibility of each test.

2.6.3.5 Statistical Analysis

Non-parametric statistics were used because of the non-normal distributions of the variables. Median significant differences between instruments at first day and between days for the same instrument were evaluated with the Wilcoxon Signed Rank test whereas the agreement and reproducibility was computed with the Cohen's k with linear weights for distance stereopsis and quadratic weights for near stereopsis, the reason for linear weights at distance and quadratic at near was because stereoacuity steps are increased in an approximated linear way at distance but not at near. To evaluate the agreement at far, taking into account that HD measures stereopsis in a continuous scale whereas ST uses discrete step sizes, HD data were discretized in a set of values closer to the nearest stereoacuity in ST scale (see Table 2). On the other hand, for measurements of the stereoacuity at near a reorganization of data was performed in order to compare results from TNO and ST, since ST and TNO use different discrete steps. In this case, results were recoded to an ordinal scale from 1 to 5 depending on the stereopsis achieved with TNO and ST (see Table 1). Statistical analyses were performed using the SPSS software (ver. 20; SPSS Inc., Chicago, IL, USA) and MedCalc (ver. 12.7; MedCalc Inc., Belgium). The significance was accepted at the $p<.05$ level.

2.6.4. Results

2.6.4.1 Near Stereopsis

The results for near stereopsis are shown in Fig. 2. Median stereopsis was slightly better for ST (40 arcsec) than for TNO (60 arcsec) even though no statistically significant differences were found in the comparison of medians between both tests ($p = 0.36$). A total of 84.6% of subjects achieved the finest level of 40 arcsec with the ST whereas 63.1% perceived up to 60 arcsec value with TNO. From the latter group, only six subjects perceived the 30 arcsec plate and one subject the 15 arcsec plate. The cumulated percentage of subjects who achieved the second level of stereopsis was closer for both

tests, 83.1% with TNO and 92.3% with ST, and were equal at third level (see Fig 2A).

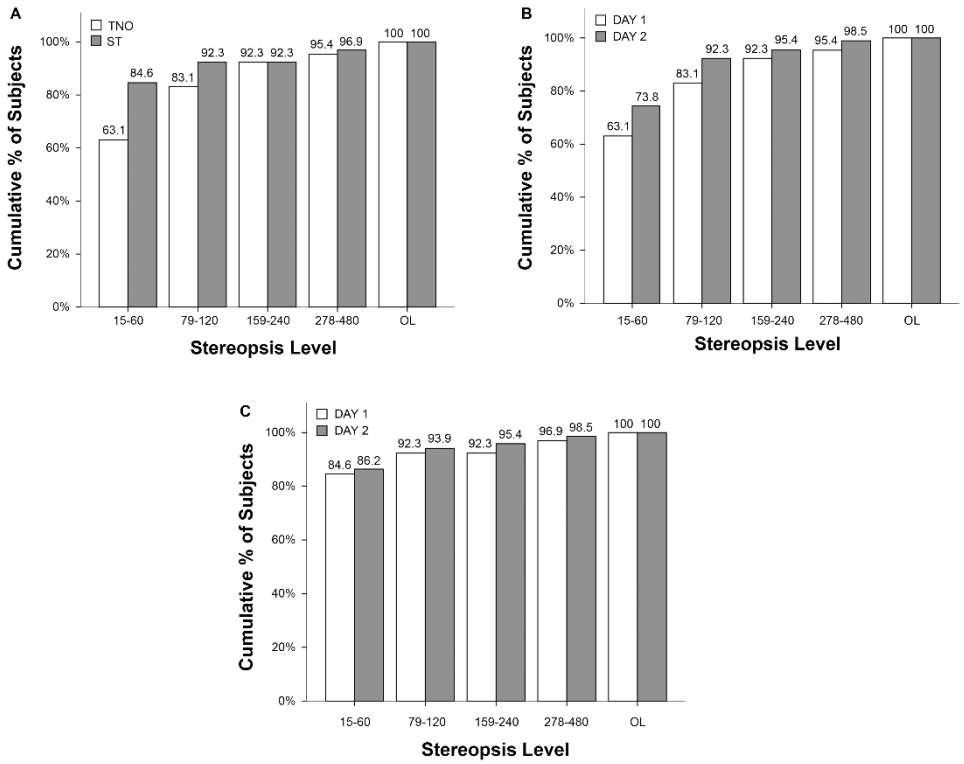

Figure 2. Cumulative percentage of subjects who achieved a value of stereopsis at near inside the range of each level for (A) TNO and ST at first day, (B) TNO at both days, and (C) ST at both days.

The Cohen's k for quadratic weights resulted in substantial agreement k=0.604 95% CI (0.300, 0.908) between both instruments according with Landis & Koch criteria (Landis and Koch 1977). Only one subject failed with ST and TNO at both days whereas two subjects failed the TNO at first day but not the ST. On the contrary way, one subject failed the ST but not the TNO also at first day. All subjects except the one mentioned above passed both near stereopsis tests at the second day (see Table 4).

Statistically significant differences were found for the median of both days with the TNO (p= 0.02) but not with the ST (p= 0.301) (see Table 3). In addition reproducibility was better with ST (k=0.801, IC95% [0.584, -1.000]) than with TNO (k=0.715, IC95% [0.520, -0.909]). This poorer reproducibility of TNO was more remarkable for the first two levels of stereopsis (see Figs. 2B and 2C)

2.6.4.2 Far Stereopsis

The results for far distance stereopsis are shown in Fig.3. A Wilcoxon signed rank test revealed statically significant differences between medians of the measurements obtained with HD and ST (p=0.001). Fig. 3A shows that 82% of subjects achieved stereopsis between 18 and 23 arcsec; however, this percentage of subjects was not reached up to the range of 56-62 arcsec with ST. Therefore, ST underestimates the stereoacuity with regard to the HD as can be seen in medians at Table 3. The Cohen's k with linear weight was run to determine if there was agreement between stereoacuity obtained with HD and ST. Slight agreement was found between both instruments according with Landis & Koch criteria (Landis and Koch 1977): k=0.040 95% CI [-0.063, 0.142].

All patients aligned the bars of the HD inside of instrument limits, however seven subjects failed with ST in both days (see Table 4). With regard reproducibility, no significant differences in median were found between days for both tests (see Table 3) even though better reproducibility was obtained with ST (k= 0.502 95%CI [0.356-0.648]) than with HD (k= 0.374 95%CI [0.185-0.564]). (see Figs. 3B and 3C)

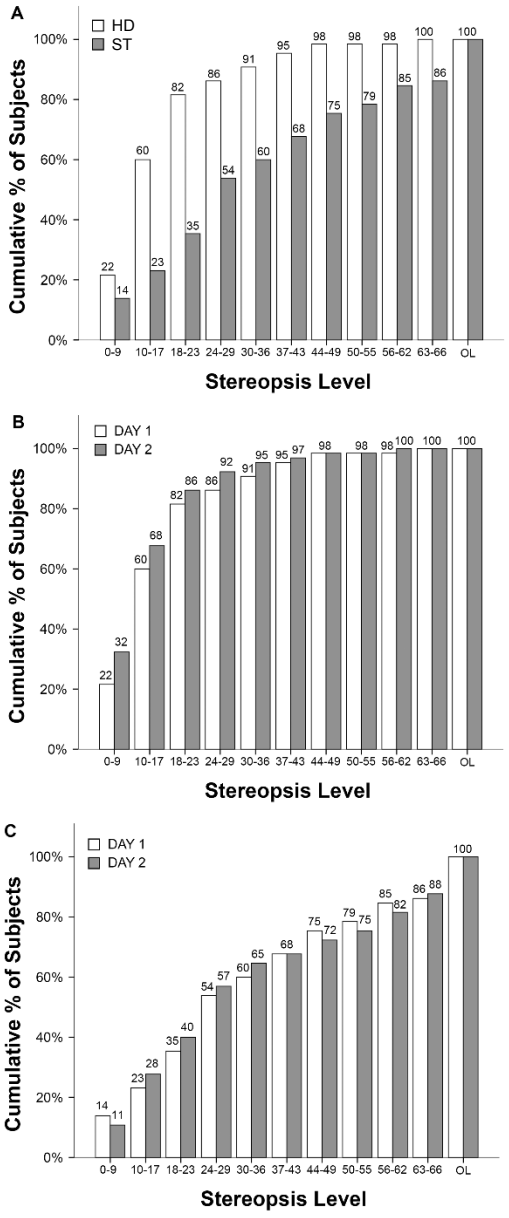

Figure 3. Cumulative percentage of subjects who achieved a value of stereopsis at distance inside the range of each level for (A) HD and ST at first day, (B) HD at both days, and (C) ST at both days.

Table 3. Reproducibility analysis between days with distance and near stereo-tests. Wilcoxon and Cohen's K were computed in order to assess the difference in medians and the concordance, respectively.

		Day	Median (arcsec) [interquartile range]	Wilcoxon	Cohen's k [95% CI]
Distance	HD	1	16 [10 to 22]	z=-1.670, p= .095	0.374 [0.185-0.564]
		2	12 [8 to 20]		
	ST	1	26 [20 to 46]	z=-.992, p= .321	0.502 [0.356 -0.648]
		2	26 [13 to 53]		
Near	TNO	1	60 [60 to 120]	z=-3.112, p= .02	0.715 [0.520-0.909]
		2	60 [60 to 90]		
	ST	1	40 [40 to 40]	z=-1.034 p= .301	0.801 [0.584-1.000]
		2	40 [40 to 40]		

Table 4. Results with each test for subjects who failed or whose stereopsis was outside the device limits (OL) with at least one of the tests.

	Distance				Near			
	HD (arcsec)		ST (arcsec)		TNO (arcsec)		ST (arcsec)	
Subject id	D1	D2	D1	D2	D1	D2	D1	D2
17	7	7	OL	13	120	120	40	40
26	9	4	53	26	OL	480	40	79
27	23	13	OL	OL	60	60	40	40
29	15	11	OL	OL	OL	OL	OL	OL
31	28	8	60	40	240	120	OL	397
32	13	20	40	OL	240	120	397	159
35	34	9	OL	OL	OL	240	357	397
44	2	3	OL	OL	120	60	119	40
48	8	8	OL	OL	60	79	30	40
52	25	10	OL	46	60	60	40	40
62	22	12	OL	OL	60	60	79	40
64	39	43	OL	OL	60	120	40	40

2.6.5. Discussion

The goals of this study were to validate a new stereopsis test for iPad and to assess its reproducibility in comparison with TNO at near and HD at distance. The stereopsis at near is widely used in clinical practice in order to improve paediatric vision screening programs, to provide an overall indication of binocularity, and to monitor binocularity after vision therapy or after monovision (Fricke et al. 1997; Rutstein et al. 2015). On the other hand, the measurement of distance stereopsis is uncommon in clinical practice even though it has been suggested that may be more effective than near stereopsis testing in screening for binocular vision disorders, reduced visual acuity, and uncorrected refractive errors (Rutstein and Corliss 2000). Particularly, distance stereopsis is useful in cases of intermittent exotropia on which patients pass near stereoacuity but fail at distance (Holmes et al. 2009), therefore it has been used for assessing the effect of surgery on binocular restoration in adolescents with this condition (Feng et al. 2015). In our opinion, the reasons why distance stereopsis is not widely used in clinical practice are that there are not many commercial tests to measure distance stereopsis, they are considerably expensive in comparison with near stereotests and two different tests are required to measure stereopsis at near and distance. Therefore, the use of a single and non-expensive test for measuring stereopsis at multiple distances is of major value.

TNO is one of the most popular tests in clinical practice and it has been used to determine how stereoacuity decreases with age (Lee and Koo 2005), in preschool screenings (Friendly 1978), and it has been compared with other tests (Simons 1981). Since ST and TNO do not measure the stereoacuity with the same discrete steps, we applied a transformation of variables by dividing subjects in groups depending on stereoacuity ranges. The agreement between both tests was good which means that ST and TNO can be used interchangeably for screening purposes; moreover, reproducibility of ST was better than TNO. One reason for this difference could be the illumination of the screen: the retro-illuminated screen of the iPad could make easier the fusion of images and the perception of the stereoscopic image than the TNO, even though it was very well illuminated in our experiment. This may be also the reason for the higher cumulative percentage of subjects

for the ST up to the 79-120 arcsec range. The evidence of this study points towards the idea that ST could be more useful during screening programs on which room lighting is under 945 lux, conversely in exteriors under extreme sunlight conditions iPad screen brightness would not be enough to perform the test properly. Moreover, the measurement of stereopsis at very high luminances would not be adequate because stereoacuity may suffer from a decrement of performance in this condition (Westheimer 2013). Particular attention should be paid to avoid reflections from any overhead glare sources when we use the iPad in opposite to the TNO on which overhead light could be required (Black et al. 2013).

One of the strengths of ST is the possibility to measure stereopsis at multiple distances maintaining the same sensitivity of stereoacuity. This makes the app especially useful to measure stereopsis at near, intermediate and distance vision with multifocal contact lenses or after cataract surgery with multifocal refractive intraocular lenses (Rutstein et al. 2015), even though an understimation with diffractive intraocular lenses might be found due to be a wavelength-based stereotest (Varón et al. 2014).

Differences between results at near and distance might be attributable to the variation in the angular size of the stimulus between both distances. This could be of great importance in the evaluation of micro-strabismus in children because it has been demonstrated that stimulus size matters and central areas of suppression may difficult the perception of small stimulus (Pageau et al. 2015). As the angular size of the stimulus decreases when the iPad is moved away from the observer, a patient with central suppression might fail the test at distance but not at near on which the stimulus subtends a high angle. Future versions will include the possibility to vary angular size of the stimulus dynamically to assess the extension of suppression.

The ST has been designed with a minimum distance between random dots corresponding at all distances to a visual acuity of 0.125 logMAR. Therefore, subjects who pass the test at distance should have a monocular visual acuity better than 0.1 logMAR. This would improve the speed of vision screenings by performing the ST test at distance and assuming the absence of visual acuities poorer than 0.1 logMAR without conducting a visual acuity test. Myopic refractive errors could be easily detected with ST at distance even though hyperopia may go undetected because the subject might accommodate like with a visual acuity test (Suryakumar and Allison 2015).

Hess et al., with a similar random dot stereotest, also reported a loss in stereopsis with the reduction in visual acuity (Hess et al. 2016). For this reason for the validation of ST, we decided to include subjects with monocular visual acuity better than 0.1 logMAR in order to ensure that they would perceive properly the ST at distance.

The agreement of ST with HD at distance was low even though the reproducibility was better for ST. Gantz & Bedell assumed that the disagreement between thresholds using local (HD) and global stereotargets (like ST) can be explained by differences in the properties of the targets or by differences in the neural mechanisms that underlie the processing of local and global stereograms (Gantz and Bedell 2011). A person performing well on a global test will perform acceptably well on a local stereopsis test, but the reverse is not true (Saladin 2005). In local stereopsis, this is due in part to the presence of contours that provide assistance to the fusion and that there is not a need for an accurate motor control; conversely in global stereopsis it is required an accurate bifoveal fixation (Fricke et al. 1997). Although we expected to have not very high agreement with HD before the study we decided to use the HD for comparison because it is considered the gold standard for stereopsis measurement (Saladin 2005).

2.6.6. Conclusion

We have validated a new application to measure stereopsis with iPad which has the primary advantage of measuring stereopsis at multiple distances, being more reproducible than other current clinical stereotests such as TNO or HD, and spending less time than other apps (Hess et al. 2016). The main limitation of this new test is that stereoacuity levels depends on pixel size; therefore, the limit for the iPad Retina (264 ppi) at 0.5m is 40 arcsec. In addition, the stereoacuity steps change depending on the tablet on which the ST is presented achieving finest values of stereopsis at near with tablets or phones with highest SPD (i.e., finest stereopsis value would be 32 arcsec at near with iPhone 6 or iPad mini which have 326 ppi). If we want to measure properly stereopsis at distance it is important to note that some conditions such as small refractive errors, anisometropia or visual acuities poorer than 0.1 logMAR should be controlled. The test could be difficult to perceive at

distance in comparison with the same at near because of the smaller background pattern or stimulus size. Future studies are needed with subjects with different ocular anomalies in order to determine the sensitivity and specificity of this new test in some of the applications that we have commented in the discussion.

2.6.7. Acknowledgements

This study was supported by the Ministerio de Economía y Competitividad and FEDER (Grant DPI2015-71256-R), and by the Generalitat Valenciana (Grant PROMETEOII-2014-072), Spain.

2.6.8. Conflict of interest

Rodríguez-Vallejo, M. has designed and programmed the stereopsis app which he currently distributes by the Apple Store with his own developer account. The other authors report no conflicts of interest and have no proprietary interest in any of the materials mentioned in this article.

2.6.9. References

American Optometric Association (1994a) Comprehensive Adult Eye and Vision Examination. In: Optom. Clin. Pract. Guidel.

American Optometric Association (1994b) Pediatric eye and vision examination. In: Optom. Clin. Pract. Guidel.

Bernell A division of vision training products (2014) Howard-Dolman type test. http://www.bernell.com/product/HDTEST/126. Accessed 11 Sep 2014.

Black JM, Jacobs RJ, Phillips G, Chen L, Tan E, Tran A, Thompson B (2013) An assessment of the iPad as a testing platform for distance

visual acuity in adults. BMJ Open 20; 3(6).

Ehrenstein WH, Ehrenstein A (1999) Psychophysical Methods. In: Modern techniques in neuroscience research. Springer, p 1214.

Feng X, Zhang X, Jia Y (2015) Improvement in fusion and stereopsis following surgery for intermittent exotropia. J Pediatr Ophthalmol Strabismus 52:52–57.

Fricke TR, Siderov J, Faa M (1997) Stereopsis, stereotests, and their relation to vision screening and clinical practice. Clin Exp Optom 80:165–172.

Friendly DS (1978) Preschool visual acuity screening tests. Trans Am Ophthalmol Soc 76:383–480.

Gantz L, Bedell HE (2011) Variation of stereothreshold with random-dot stereogram density. Optom Vis Sci 88:1066–71.

Hess RF, Ding R, Clavagnier S, Liu C, Guo C, Viner C, Barrett BT, Radia K, Zhou J (2016) A robust and reliable test to measure stereopsis in the clinic. Invest Ophthalmol Vis Sci 57:798–804.

Holmes JM, Birch EE, Leske DA, Flu VL, Mohney BG (2009) New tests of distance stereoacuity and their role in evaluating intermittent exotropia. Ophthalmology 114:1215–1220.

Landis JR, Koch GG (1977) The measurement of observer agreement for categorical data. Biometrics 33:159–174.

Lee SY, Koo NK (2005) Change of stereoacuity with aging in normal eyes. Korean J Ophthalmol 19:136–9.

Pageau M, de Guise D, Saint-Amour D (2015) Random-dot stereopsis in microstrabismic children: stimulus size matters. Optom Vis Sci 92:208–216.

Perera C, Chakrabarti R, Islam FMA, Crowston J (2015) The Eye Phone Study: reliability and accuracy of assessing Snellen visual acuity using smartphone technology. Eye 29:888–894.

Rodríguez-Vallejo M, Remón L, Monsoriu JA, Furlan WD (2015) Designing a new test for contrast sensitivity function measurement with iPad. J Optom 8:101–8.

Rutstein RP, Corliss DA (2000) Distance stereopsis as a screening device. Optom Vis Sci 77:135–9.

Rutstein RP, Fullard RJ, Wilson JA, Gordon A (2015) Aniseikonia induced by cataract surgery and its effect on binocular vision. Optom Vis Sci 92:201–207.

Saladin JJ (2005) Stereopsis from a performance perspective. Optom Vis Sci 82:186–205.

Sheppard AL, Davies LN (2010) Clinical evaluation of the Grand Seiko Auto Ref/Keratometer WAM-5500. Ophthal Physiol Opt 30:143–51.

Simons K (1981) A comparison of the Frisby, Random-Dot E, TNO, and Randot circles stereotests in screening and office use. Arch Ophthalmol 99:446–52.

Suryakumar R, Allison RS (2015) Accommodation and pupil responses to random-dot stereograms. J Optom 9:40–6.

van Doorn LL, Evans BJ, Edgar DF, Fortuin MF (2014) Manufacturer changes lead to clinically important differences between two editions of the TNO stereotest. Ophthal Physiol Opt 34:243–9.

Varón C, Gil MA, Alba-Bueno F, Cardona G, Vega F, Millán MS, Buil JA (2014) Stereo-Acuity in patients implanted with multifocal intraocular lenses: Is the choice of stereotest relevant? Curr Eye Res 39:711–719.

Wang J, Hatt SR, O'Connor AR, Drover JR, Adams R, Birch EE, Holmes JM (2010) The final version of the distance Randot Stereotest: normative data, reliability, and validity. J AAPOS 14:142–146.

Westheimer G (2013) Clinical evaluation of stereopsis. Vis Res 90:38–42.

Zhang ZT, Zhang SC, Huang XG LL (2013) A pilot trial of the iPad tablet computer as a portable device for visual acuity testing. J Telemed Telecare 19:55–9.

Physics > Medical Physics

Design, characterization and visual performance of a new multizone contact lens

Manuel Rodriguez-Vallejo, Clara Llorens-Quintana, Juan A. Monsoriu, Walter D. Furlan

(Submitted on 21 Sep 2016)

Objectives: To analyze the whole process involved in the production of a new bifocal Multizone Contact Lens (MCL) for presbyopia.
Methods: The optical quality of a new MCL was evaluated by ray tracing software in a model eye with pupil different diameters with the lens centered and decentered. A stock of low addition (+1.5 D) MCL for presbyopia was ordered for manufacturing. Power profiles were measured with a contact lens power mapper, processed with a custom software and compared with the theoretical design. Nine lenses from the stock were fitted to presbyopic subjects and the visual performance was evaluated with new APPs for iPad Retina.
Results: Numerical simulations showed that the trough the focus curve provided by MCL has an extended depth of focus. The optical quality was not dependent on pupil size and only decreased for lens decentered with a pupil diameter of 4.5 mm. The manufactured MCL showed a smoothed power profile with a less-defined zones. The bias between experimental and theoretical zone sizes was uniform along the optical zone unless for the most central area. Eyes fitted with the manufactured MCL showed an improvement in near Visual Acuity (VA) and near stereopsis. Althouh Contrast Sensitivity (CS) at distance decreased, the defocus curve for contrast showed an extended depth of focus correlated to the ray tracing results.
Conclusions: The understanding of vision with MCL requires a process that involves design and characterization for detecting any defect that may have impact in the final visual performance. Keywords: Multifocal contact lenses, design, characterization, visual performance

Comments: 12 pages, 4 figures, 2 Tables
Subjects: **Medical Physics (physics.med-ph)**
Cite as: **arXiv:1609.06712 [physics.med-ph]**
(or **arXiv:1609.06712v1 [physics.med-ph]** for this version)

Submission history

From: Manuel Rodriguez-Vallejo [view email]
[v1] Wed, 21 Sep 2016 17:55:17 GMT (535kb)

2.7. Design, characterization and visual performance of a new multizone contact lens.

Manuel Rodriguez-Vallejo[1*], Clara Llorens-Quintana[3], Juan A. Monsoriu[2] and Walter D. Furlan[3]

[1] *Qvision, Unidad de Oftalmología Vithas Hospital Virgen del Mar, 04120, Almería*

[2] *Centro de Tecnologías Físicas, Universitat Politècnica de València, 46022 Valencia, Spain*

[3] *Departamento de Óptica, Universitat de València, 46100 Burjassot, Spain*
[*] *Corresponding author: manuelrodriguezid@qvision.es*

2.7.1. Abstract

Objectives: To analyze the whole process involved in the production of a new bifocal Multizone Contact Lens (MCL) for presbyopia.

Methods: The optical quality of a new MCL was evaluated by ray tracing software in a model eye with pupil different diameters with the lens centered and decentered. A stock of low addition (+1.5 D) MCL for presbyopia was ordered for manufacturing. Power profiles were measured with a contact lens power mapper, processed with a custom software and compared with the theoretical design. Nine lenses from the stock were fitted to presbyopic subjects and the visual performance was evaluated with new APPs for iPad Retina.

Results: Numerical simulations showed that the trough the focus curve provided by MCL has an extended depth of focus. The optical quality was not dependent on pupil size and only decreased for lens decentered with a pupil diameter of 4.5 mm. The manufactured MCL showed a smoothed power profile with a less-defined zones. The bias between experimental and theo-

retical zone sizes was uniform along the optical zone unless for the most central area. Eyes fitted with the manufactured MCL showed an improvement in near Visual Acuity (VA) and near stereopsis. Althouh Contrast Sensitivity (CS) at distance decreased, the defocus curve for contrast showed an extended depth of focus correlated to the ray tracing results.

Conclusions: The understanding of vision with MCL requires a process that involves design and characterization for detecting any defect that may have impact in the final visual performance.

Keywords: Multifocal contact lenses, design, characterization, visual performance

2.7.2. Introduction

Presbyopia correction with multifocal contact lenses (MCLs) has been for years one of the most important topics in optometry research from the emergence of early designs on the latter half of the 1980s (Toshida et al. 2008). Two solutions: alternating vision, and simultaneous vision, have been widely studied, being the latter the most popular nowadays (Charman 2014). Simultaneous vision is achieved through varying the power along some areas of the lens in such a way that light is distributed in more than one single focus. This concept has evolved from the design proposed by de Carle (de Carle 1989) with multiple variations including diffractive MCLs and refractive MCLs with centre-distance aspheric, centre-near aspheric or multiple zones (Hough 2006). During the last 20 years, some improvements have been proposed in the design, characterization and visual performance assessment with these MCLs (Plakitsf and Charman 1995). Advanced ray tracing software is currently used to design and simulate the optical performance of the MCLs in model eyes (Bradley et al. 2014; Rodríguez-Vallejo et al. 2014a). Manufactured lenses can be precisely characterized by means of new objective instruments (Joannes et al. 2010; Plainis et al. 2013b; Wagner et al. 2014), and the visual performance for a wide range of distances can be assessed by through-focus plots (Plainis et al. 2013b). The whole process involved in the development of a new design of MCL is a linked chain which must accept feedbacks of the partial results obtained in the pro-

cess. In this work, we propose an approach that covers all the steps involved in the development of new MCLs, from the optical design to the final visual performance obtained by the observer, through the manufacturing process and the characterization of the prototypes.

2.7.3. Methods

2.7.3.1 Contact Lenses Modelling

A new design of bifocal MCL for presbyopia treatment has been designed and evaluated. It consists of 6 refractive zones, (3 for distance correction (D) and 3 for near correction (N)). Zone diameters from center to periphery were 1.76 mm (D), 2.48 mm (N), 3.04 mm (D), 4.30 mm (N), 4.64 (D), and 4.96 mm (N). The theoretical optical performance of the MCL was computed by means of the Through Focus Modulation Transfer Function (TF-MTF) for spatial frequencies of 12, 25 and 50 line pairs per mm (lp/mm) over the Atchison model eye (Atchison 2006), setting the refractive error to emmetropia and taking account the Stiles-Crawford apodisation (Bradley et al. 2014). The characteristics of the model eye fitted with a MCL have been described in detail elsewhere (Rodríguez-Vallejo et al. 2014a). In this case, the back vertex power of the correction zones was set to zero in such a way the distance (D) focus was on the retina, while the power of near zones was +1.50 D for producing simultaneously an additional, near (N), focus in front of the retina. The effect on the TF-MTF of decentring the MCL in reference to the pupil center was also computed. Simulations were performed with the ray-tracing software package, Zemax 13 SE (Zemax Development Corporation, Bellevue, WA, USA).

2.7.3.2 Manufacturing and Characterization

MCLs were manufactured with Hioxifilcon A (Benz G5X p-GMA/HEMA) (Benz 2016), which has a 1.401 refractive index (hydrated and at 35º), using a precision lathe (Optoform 40). Two stocks of MCLs from 0.00 D to +2.00 D (in +0.50 D steps) with an addition of +1.50 D were ordered for manufac-

turing (base curves: 8.4 mm or 8.6 mm; diameter: 14.50 mm). The Nimo TR1504 (LAMBDA-X, Nivelles, Belgium)(Joannes et al. 2010) contact lens power mapper was used to characterize the power profiles of the manufactured lenses. Nimo software (version 4.2.6.0 r477) allows to obtain the power of multizone MCLs but only up to five zones defined by the operator. Therefore for computing the D and N powers of our lenses, we exported the power raw data and we developed a custom function in Matlab (version R2013a, The Math-works, Inc.) for detecting D and N zones in the MCLs and for calculating the mean of power along each zone. To do that, changes in the slope of the power profiles higher than 0.25 D were detected by means of computing the first derivative of the radial power function. These changes represent the maxima and minima at D and N zones respectively and the half of power between a minimum and the consecutive maximum (or vice versa) was assumed as the transition between zones. Then the mean experimental power of each zone was computed.

2.7.3.3 Subjects and Visual Performance

Five presbyopic volunteers with a mean age of 49.8 ± 4.3 years (range 45 – 56 years) participated in the study. Subjects were subjected to a complete eye exam including objective and subjective refraction, and slit-lamp exploration. In order to homogenize the sample, inclusion criteria were: hyperopic patients (0.25 D ≤ Rx ≤1.75 D) who need an addition lower than 1.50 D, with no ocular diseases affecting the visual performance, subjective astigmatism under 0.75 D, and normal binocular function (except one subject who was amblyope and only the healthy eye was included in the sample). The addition was defined as the minimum positive power over the distance subjective refraction to comfortably recognize a high contrast optotype of 20/20 at 40 cm. The research adhered to the tenets of the Declaration of Helsinki, with the research approved by Ethics Commission of University of Valencia, and an informed consent was obtained from all participants.
Subjects were fitted with MCLs from an existing stock previously characterized by the Nimo TR1504 as it has been described in the previous section. Therefore, the power of the MCLs fitted to each eye was the closest one to the spectacle refraction in the stock of MCLs. The best base curve from the both possible values, 8.40 mm or 8.60 mm, was selected by the investigator

after evaluating, with a slit lamp, the movement and centration of the soft lens after 15 minutes of wearing. Then, the visual performance measurement was conducted with the selected lens.

The visual performance of subjects fitted with MCLs was assessed by measuring: visual acuity (VA) (Rodríguez-Vallejo et al. 2016b), contrast sensitivity function (CSF) (Rodríguez-Vallejo et al. 2015), stereopsis (ST) (Rodríguez-Vallejo et al. 2014b), and through-focus response (TFR) (Fernández et al. 2016b) with Applications (APPs) developed for iPad Retina. All subjects were tested monocularly (with the exception of the stereopsis test) first, without compensation, and then, wearing the MCLs. The APPs allow to measure VA and ST at 3 m and also at near at 0.40 m and 0.50 m respectively. CSF and TFR were conducted at 2 m of distance, the latter varying the contrast (in log units) with an optotype of 0.3 logMAR (TFR-C) or varying the visual acuity (logMAR) of a high contrast optotype (TFR-VA). The optotype used for the measurement of TFR was the Snellen E. For TFR-C, the optotype size was 0.3 logMAR which corresponds to a spatial frequency of 50 mm^{-1} or equivalently 15 cpd.(ISO-11979-2 2014) (Holladay et al. 1990). The absolute area under the TFR was calculated considering a baseline of 0.3 logMAR (Wolffsohn et al. 2013) for TFR-VA and -0.6 log units of contrast for TFR-C. Finally, patients were asked about their satisfaction in terms of general quality of vision achieved with the MCL fitted to each individual eye through an ordinal scale ranging from 1 to 5 (very dissatisfied, dissatisfied, neutral, satisfied, and very satisfied).

2.7.3.4 Statistical Analysis

Normal distributions were tested with the Shapiro-Wilk test and non-parametric statistical tests were used for $p < 0.05$. A Bland–Altman procedure was used to assess the agreement between theoretical and experimental zone sizes. Paired t-tests were used for computing mean differences between theoretical MCL power fitted to the eye and experimental MCL power measured with the Nimo for near and far distance zones. The mean differences in the visual performance, with and without MCLs, were also assessed with paired t-tests. The mean and standard deviation of TFR were computed and represented with Matlab and the areas under the TFR curves were calculated with the included *trapz* function. The data were managed using SPSS

software version 20 (SPSS Inc., Chicago, IL, USA), and $p<0.05$ was considered to indicate significance.

2.7.4. Results

2.7.4.1 Contact Lenses Modelling

Fig. 1 shows the theoretical TF-MTF for the naked eye and pupil diameters of 3.5 mm (panel A) and 4.5 mm (panel D) compared with the same eye with MCLs centered (panels B and E) and decentered (panels C and F). As can be seen, the theoretical effect of the MCL is to produce an extended depth of focus (DOF) with a concomitant myopic focal shift of the whole focal volume. Particularly for the 25 lp/mm frequency, two peaks can be observed: one at 0 mm (infinite in the object space) and at 0.5 mm in front of the retina which is conjugated with a plane at 67 cm in front of the eye. As expected, the best performance of the MCL was obtained for the lens centered on the pupil.

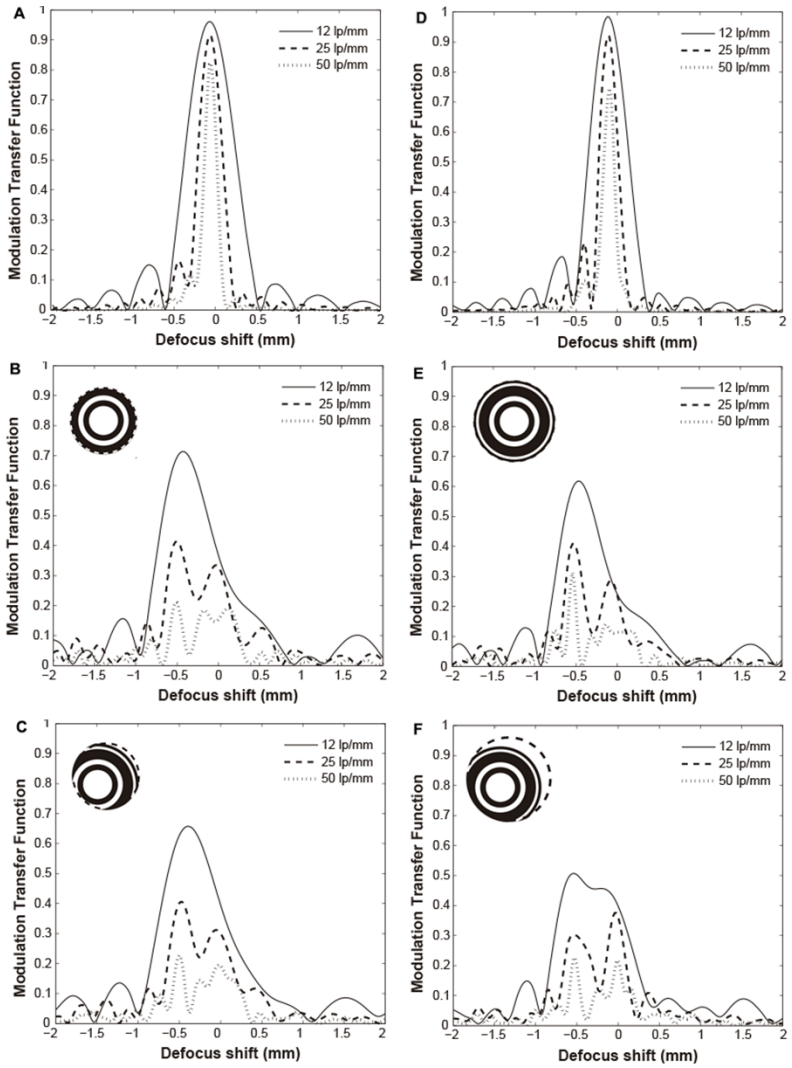

Figure 1. Theoretical, 12 lp/mm, 25 lp/mm and 50 lp/mm, TF-MTF for an emmetropic model eye. Upper row shows results for pupil diameter of 3.5 mm for the model eye: (A) without CL, (B) with MCL, and (C) with MCL decentered. Bottom row describes results for pupil diameter of 4.5 mm for the model eye: (D) without CL, (E) with MCL, and (F) with MCL decentered. MCL Add was +1.50 D and the decentering was 0.5mm downward and 0.5mm sideward. The inset diagram describes the distance zones (white) and the near zones (black) covering the pupil (dotted circle).

2.7.4.2 Manufacturing and Characterization

The assessment of the manufacturing process was performed using a customized algorithm as explained in the Methods. A typical result of the power profile of one of the MCLs is shown in Fig. 2. Vertical lines represent the transition zones detected by the algorithm and the horizontal lines along +1.00 D and +2.50 D represent the theoretical powers for distance and near respectively. The grey areas represent the differences between the theoretical power and the experimental power profile. Similar results were found for the nine MCLs fitted to the subjects in the experiment, we found that, compared with theoretical power, the the mean experimental power of the lenses was +0.12 ± 0.22 D for distance [$t(8) = 1.538, p=0.16$] and -0.57 ± 0.19 D for near [$t(8) = -8.9, p < 0.0005$]. Table 1 shows the experimental powers measured at far and near for each MCLs (MCL fitted) and the corresponding theoretical powers of each fitted lens.

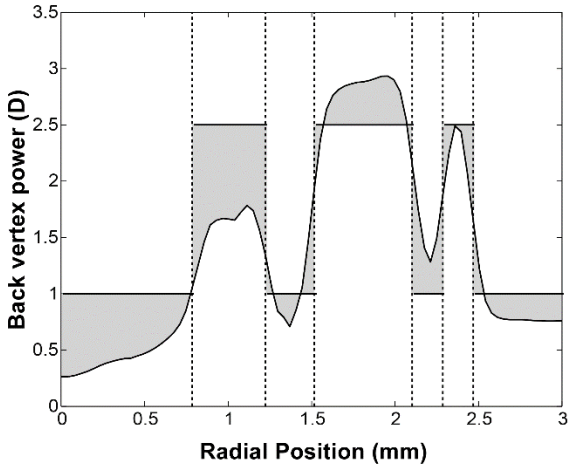

Figure 2. Power profile of one of the MCLs. The vertical lines represent the transition between zones detected by the algorithm, horizontal lines are the theoretical powers ordered for manufacturing, +1.00 D for distance zones and +2.50 D for near zones in this case. Grey areas show the difference between the experimental power and the theoretical power.

Table 1. Spectacle Rx and powers for MCL fitted to each eye in the sample (Experimental power). The theoretical powers of each lens are also included.

Subject Id	Eye	Spectacle Rx Far/Near	Experimental Power Far/Near	Theoretical Power Far/Near
1	RE	+0.25 /+1.25	+0.61 /+0.70	+0.00 /+1.50
	LE	+0.50 /+1.50	+0.54 /+1.39	+0.50 /+2.00
2	RE	+1.00 /+2.00	+0.30 /+1.72	+0.50 /+2.00
	LE	+1.50 /+2.50	+1.55 /+2.39	+1.50 /+3.00
3	RE	+1.00 /+2.00	+1.03 /+2.09	+1.00 /+2.50
	LE	+0.50 /+1.50	+0.54 /+1.39	+0.50 /+2.00
4	RE	+1.00 /+2.00	+1.04 /+2.18	+1.00 /+2.50
	LE	+1.25 /+2.25	+1.74 /+2.22	+1.50 /+3.00
5	RE	+1.75 /+3.50	+2.17 /+2.78	+2.00 /+3.50
mean		+0.97 /+2.06	+1.06 /+1.87	+0.94 /+2.44
±SD		+0.49 /+0.67	+0.64 /+0.63	+0.63 /+0.63

In general, we found that the bias between theoretical (*Pt*) and experimental (*Pe*) powers of MCLs was different depending on the zone. Fig. 3A shows lower *Pe* than *Pt* at zones 1 (D) and 2 (N) and the opposite at zones 5 (D) and 6 (N). A Kruskal-Wallis H test was conducted to determine if there were differences in the power bias between zones. As can be seen in the box plot the distributions of power bias were not similar for all zones, The distributions of power bias were statistically significantly different between zones, $\chi^2(5) = 36.319$, $p < 0.0005$. Pairwise comparisons were performed with a Bonferroni correction for multiple comparisons. This post-hoc analysis revealed statistically significant differences in power bias between central zones (zones 1 and 2) and peripheral zones (zones 5 and 6) ($p < 0.05$). The agreement between theoretical and experimental diameter of the zones is shown in Fig. 3B. Iit can be seen that the first zone of the manufactured lenses is smaller than the theoretical one. On the other hand, from zones 2 to 6 the bias between theoretical and experimental zones is reduced except for the 4th zone for which appear a slight overestimation of the experimental diameter.

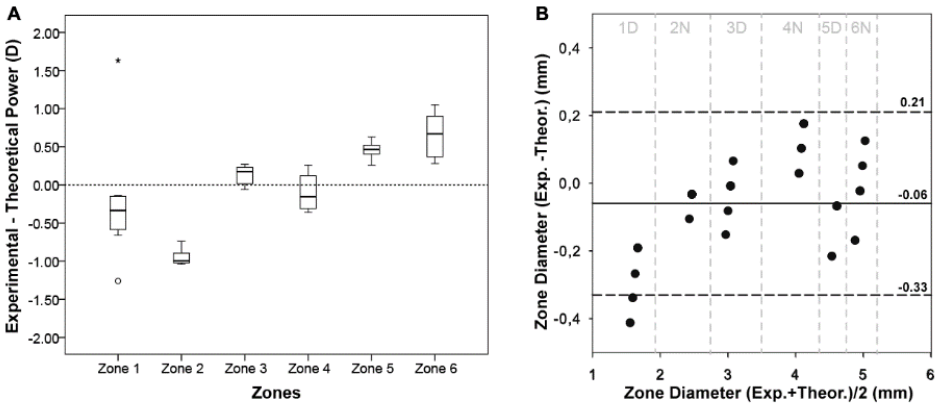

Figure 3. (A) Difference between the experimental and theoretical powers at each zone (B) Bland-Altman plot. Difference between experimental and theoretical and zone diameters versus mean of experimental and theoretical zone diameters.

2.7.4.1 Clinical Visual Performance

Table 2 shows that MCLs improved the visual performance at near versus the no presbyopia compensation. Although with the MCLs the improvements ST and VA at near were significant, distance VA was not significantly increased and CSF decreased at frequencies equal or greater than 6 cpd.

Fig. 4 shows the mean TFR performance of the MCLs for the VA (panel A) and C (panel B). The mean area under the TFR-VA and TFR-C curves, was 1.29 ± 0.32 and 0.94 ± 0.56 respectively. Both TFR curves were positively correlated (r = 0.741, p=0.022) exhibiting an extended DOF with a peak at -1.00 D. Mean VA obtained from TFR were 0.1 ± 0.17 logMAR at 40 cm, -0.08 ± 0.12 logMAR at 67 cm and -0.06 ± 0.1 logMAR at distance. Mean C were -0.62 ± 0.3 log at 40 cm, -0.93 ± 0.23 log at 67 cm, and -0.88 ± 0.19 log at distance.

Table 2. Visual performance before and after fitting MCLs for presbyopia correction.

Visual performance (distance)	Without FCLs mean ± SD	With FCLs mean ± SD	p-value paired t-test
Near VA (0.4 m) in logMAR	0.46 ± 0.17	0.26 ± 0.17	0.001
Far VA (3 m) in logMAR	0.09 ± 0.62	0.03 ± 0.07	0.214
***Near ST (0.5 m) in arcsec**	258 [119, 397]	119 [79, 119]	0.023
***Far ST (3 m) in arcsec**	397 [278, 397]	397 [40, 397]	0.157
CSF (2 m) in log units			
3 cpd	2.03 ± 0.08	1.96 ± 0.16	0.084
6 cpd	2.10 ± 0.20	1.89 ± 0.22	0.044
12 cpd	1.67 ± 0.22	1.51 ± 0.12	0.045
18 cpd	1.32 ± 0.23	1.03 ± 0.14	0.005

* Median [min, max] and Wilcoxon signed rank test used instead of mean ± SD and paired t-test due to a non-normal distribution of the variable.

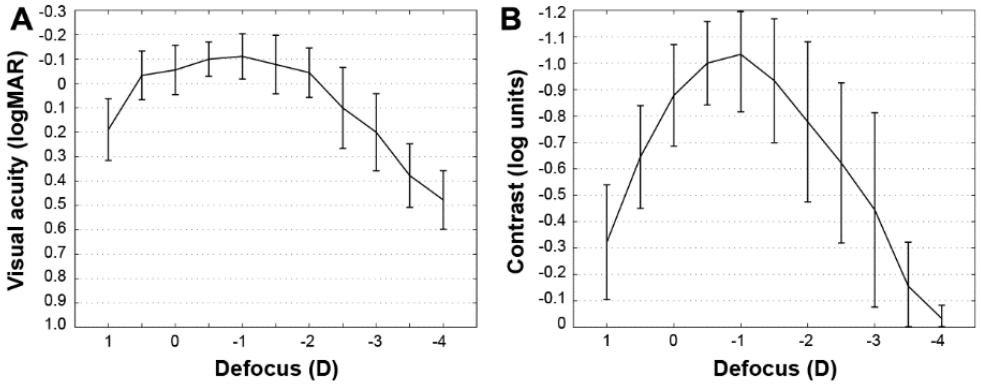

Figure 4. (A) Through-Focus response for visual acuity (TFR-VA) and (B) for contrast (TFR-C). Vertical bars represent one standard deviation from the mean.

Satisfaction about the subjective quality of vision achieved with each MCLs was evaluated by means of an ordinal scale, resulting in a mean satisfaction of 3.33 ± 1.33 which corresponded to a value between neutral (3) and satisfied (4). The resulting satisfaction answers were confronted versus the area under the curve for TFR-VA and TFR-C obtained with each lens. The area under the TFR-C was correlated with the general satisfaction r = 0.669 (p =

0.049). No significant correlation ($p > 0.05$) was found for the area under the TFR-VA.

2.7.5. Discussion

The optical modelling with Zemax showed an extended DOF performance of the MCL. Interestingly, the bifocal nature of the lens was not expressly revealed for low spatial frequencies but it turned into a myopic focal shift of about 1.0 D or 1.5 D – depending on the pupil diameter. According to our simulations, a loss of contrast in far vision was expected in comparison to the nacked eye, and the TF-MTF predicted a good tolerance to decentrations. The values of decentration were selected according to the approximated values reported with other commercial CLs (Young et al. 2010). The pupil size independence of our design is one of the advantages of the multiple zone CLs in comparison to aspheric CLs as it has been previously reported with other designs (Bradley et al. 2014). However, one potential drawback of the bifocal CLs versus aspheric designs may be a higher incidence of ghost images, mainly for high addition lenses (Kollbaum et al. 2012). In this study this effect might be minimized due to the low addition of our design combined with the smooth transition between zones in the manufactured lenses (Tilia et al. 2016). Further data analysis would be needed in future studies to determine how exactly the modification of our design affects to the ghost images and how the optical simulations are correlated with the real performance in patients fitted with this design.

We used the Nimo TR1504 in order to measure the power profile of our MCL design. In a previous study (Kim et al. 2015), this instrument has demonstrated to be reliable across a half chord between 0.51 mm and 3.2 mm and to have higher variability up to 0.88 D within 1.0 mm diameter. The reliability of this instrument was not tested in this study and we applied our custom algorithm of zones recognition to one measured profile of each lens. We are aware that this could be a limitation of the current work. Future studies should evaluate the repeatability of the construction and assessment procedures. This will help for instance, to elucidate if the bias in the first zone is due to the manufacture or to the repeatability of Nimo and the custom sofware. With respect to this, although power profiles with this instru-

ment have been previously reported by other authors (Kim et al. 2015; Tilia et al. 2016), to our knowledge none have used an algorithm for automatic recognition of zones. Our custom-made algorithm for transition zone recognition has demonstrated to be useful for computing the mean experimental power along each zone and it use could be recommendable instead of using the **N**imo TR1504 software. In fact, in this way we were able to detect differences between designed and manufactured lenses either in zone diameters and powers. In general, we found that the lenses showed increasing plus power towards the periphery. Differences in power between corresponding zones could be attributable to a positive spherical aberration of the manufactured plus MCLs. In this sense, testing commercial soft CLs for myopia, Wagner et al. also reported a bias between labeled and measured powers (especially for the central, 1mm, zone) in almost all the CLs measured (Wagner et al. 2014). However, in that work the bias was in the opposite direction than in ours which means that plus CLs might induce positive spherical aberration and minus CLs negative spherical aberration.

The theoretical design of the MCLs of this study corresponds to a multizone refractive CLs. Similar designs are currently available on the market such as the Acuvue Bifocal whose visual performance has been evaluated in multiple studies that reported logMAR VA ranging from -0.11 and 0.19 for distance and from 0.12 to 0.14 for near (Kirschen et al. 1999; Situ et al. 2003; Rajagopalan et al. 2006). Recently, Tilia et al. compared the ACUVUE OASYS for Presbyopia (AOP) and a new extended DOF CL design and they reported mean VAs of -0.06 logMAR and -0.08 logMAR at distance and 0.55 logMAR and 0.40 logMAR at near (40 cm), respectively for low presbyopes (Tilia et al. 2016). In our study, we found similar outcomes of VA as it is reflected in Table 2 and in the VA-TFR. It is important to note that mean VA measured with the APP at near was poorer than the corresponding at -2.5 D of defocus in the TFR APP, 0.26 and 0.1 logMAR respectively. This difference was due to the APP for measuring VA used steps of 0.2 logMAR and the TFR APP used 0.1 logMAR steps. The reason for not using 0.1 logMAR steps with the iPad at 40 cm was the limited of resolution (pixels per inch) of the display (Rodríguez-Vallejo 2016).

In terms of other visual skills, MCLs increased the near stereopsis and decreased the far CSF for spatial frequencies over 6 cpd. The improvement of

near stereopsis was related to the improvement of near VA since the random dot stereo-test we used requires non-blurred patterns in both eyes for being correctly fused. Furthermore, the loss in CSF was expected from the comparison between the results shown in Fig. 1 for the nacked-eye and for eye fitted with the MCL.

Another interesting finding is that, even though Zemax simulations predicted a bifocal behavior of our MCLs, experimental TFRs showed smooth extended DOF. This may be due to the non-abrupt transition between near and far zones in the manufactured lenses and to the interaction between the high order aberrations of the eye and the MCLs design (Martin and Roorda 2003).

The general quality of vision achieved with the MCLs abtained a satisfaction grade between neutral and satisfied. The correlations between area under the TFR-VA and TFR-C were computed in order to elucidate if a change in this area might be used in order to predict the satisfaction of the patient depending on the visual performance achieved with the lens. Area under the TFR-VA was not correlated with the satisfaction of the subjects. However, a correlation was found for the area under the TFR-C. This means that, rather than the TFR-VA, the TFR-C could be a metric which might better predict the satisfaction of the patient. This metric might also be useful to evaluate the agreement between the theoretical optical performance and the vision achieved by the patients and to perform changes in the design based in this agreement. These hypothesis should be confirmed in future studies with a higher sample of subjects.

In this study, we have shown an approach that covers all the steps involved in the development of new MCLs. The whole process from the design to the final MCLs fitted to the patient should include appropriate methods for lens characterization. This will ensure that the reproducibility of the manufacturing process is inside the tolerance limits. Furthermore, in this study new iPad applications have been used satisfactory for measuring the visual performance of subjects wearing MCLs.

2.7.6. Acknowledgements

This study was supported by the Ministerio de Economía y Competitividad (Grant DPI2015-71256-R) and by the Generalitat Valenciana (Grant PROMETEOII-2014-072), Spain.

2.7.7. Conflict of Interest

WDF and JAM have proprietary interest in the contact lens design described in this article. MR-V has designed and programmed the APPs used in this study, which currently distributes by the Apple Store with his own developer account.

2.7.8. References

Atchison DA (2006) Optical models for human myopic eyes. Vis Res 46:2236–50.

Benz (2016) G5X p-GMA/HEMA (Hioxifilcon A). http://benzrd.com/benz_g5x.php. Accessed 27 Mar 2016.

Bradley A, Nam J, Xu R, Harman L, Thibos L (2014) Impact of contact lens zone geometry and ocular optics on bifocal retinal image quality. Ophthal Physiol Opt 34:331–45.

Charman WN (2014) Developments in the correction of presbyopia I: spectacle and contact lenses. Ophthal Physiol Opt 34:8–29.

de Carle J (1989) A refractive multizone bifocal. Trans BCLA Conf 12:66–70.

Fernández J, Rodríguez-Vallejo M, Martínez J (2016b) Bridging the gap between lab and clinical practice in assessing multifocal IOLs. In: Cataract Refract. Surg. Today. http://crstodayeurope.com/pdfs/0216CRSTEuro_cs_Fernandez.pdf. Accessed 17 Jul 2016.

Holladay JT, Van Dijk H, Lang A, Portney V, Willis TR, Sun R, Oksman HC (1990) Optical performance of multifocal intraocular lenses. J

Cataract Refract Surg 16:413–22.

Hough T (2006) Correction of presbyopia by contact lenses. In: Douthwaite WA (ed) Contact lens optics and lens design, 3rd ed. Butterworth-Heinemann, Bradford, pp 282–287.

ISO-11979-2 (2014) Ophthalmic implants - Intraocular lenses - Part 2: Optical properties and test methods.

Joannes L, Hough T, Hutsebaut X, Dubois X, Ligot R, Saoul B, Van Donink P, De Coninck K (2010) The reproducibility of a new power mapping instrument based on the phase shifting schlieren method for the measurement of spherical and toric contact lenses. Cont Lens Anterior Eye 33:3–8.

Kim E, Bakaraju RC, Ehrmann K (2015) Reliability of power profiles measured on NIMO TR1504 (Lambda-X) and effects of lens decentration for single vision, bifocal and multifocal contact lenses. J Optom 9:126–136.

Kirschen DG, Hung CC, Nakano TR (1999) Comparison of suppression, stereoacuity, and interocular differences in visual acuity in monovision and Acuvue Bifocal Contact Lenses. Optom Vis Sci 76; 832-7.

Kollbaum PS, Dietmeier BM, Jansen ME, Rickert ME (2012) Quantification of ghosting produced with presbyopic contact lens correction. Eye Contact Lens 38:252–9.

Martin J a, Roorda A (2003) Predicting and assessing visual performance with multizone bifocal contact lenses. Optom Vis Sci 80:812–9.

Plainis S, Ntzilepis G, Atchison DA, Charman WN (2013b) Through-focus performance with multifocal contact lenses: effect of binocularity, pupil diameter and inherent ocular aberrations. Ophthal Physiol Opt 33:42–50.

Plakitsf A, Charman WN (1995) Comparison of the depths of focus with the naked eye and three types of presbyopic contact lens correction. J Br Contact Lens Assoc 18:119–125.

Rajagopalan AS, Bennet ES, Lakshminarayanan V (2006) Visual performance of subjects wearing presbyopic contact lenses. Optom Vis Sci 83:611–615.

Rodríguez-Vallejo M (2016) Comment on: "Effectiveness of a smartphone application for testing near-visual acuity." Eye 30:898–899.

Rodríguez-Vallejo M, Benlloch J, Pons A, Monsoriu JA, Furlan WD (2014a) The effect of Fractal Contact Lenses on peripheral refraction in myopic model eyes. Curr Eye Res 39:1151–60.

Rodríguez-Vallejo M, Llorens-Quintana C, Furlan WD, Monsoriu JA (2016b) Visual acuity and contrast sensitivity screening with a new iPad application. Displays 44:15–20.

Rodríguez-Vallejo M, Remón L, Monsoriu JA, Furlan WD (2015) Designing a new test for contrast sensitivity function measurement with iPad. J Optom 8:101–8.

Rodríguez-Vallejo M, Cuevas V, Furlan WD, Pons A, Monsoriu JA (2014b) Screening visual con iPad. In: XXIII Congreso Internacional Optometría, Contactología y Óptica Oftálmica.

Situ P, Toit R du, Fonn D, Simpson T (2003) Successful monovision contact lens wearers refitted with bifocal contact lenses. Eye Contact Lens 29:181–184.

Tilia D, Bakaraju RC, Chung J, Sha J, Delaney S, Munro A, Thomas V, Ehrmann K, Holden BA (2016) Short-Term Visual Performance of Novel Extended Depth-of-Focus Contact Lenses. Optom Vis Sci 93:1–10.

Toshida H, Takahashi K, Sado K, Kanai A, Murakami A (2008) Bifocal contact lenses: history, types, characteristics, and actual state and problems. Clin Ophthalmol 2:869–77.

Wagner S, Conrad F, Bakaraju RC, Fedtke C, Ehrmann K, Holden BA (2014) Power profiles of single vision and multifocal soft contact lenses. Cont Lens Anterior Eye 38:2–14.

Wolffsohn JS, Jinabhai AN, Kingsnorth A, Sheppard AL, Naroo SA, Shah S, Buckhurst P, Hall LA, Young G (2013) Exploring the optimum step size for defocus curves. J Cataract Refract Surg 39:873–80.

Young G, Schnider C, Hunt C, Efron S (2010) Corneal topography and soft contact lens fit. Optom Vis Sci 87:358–366.

Capítulo 3
Discusión general de los resultados

Los resultados alcanzados en estos tres años de investigación han sido publicados en forma de siete artículos en diversas revistas científicas. En su conjunto, conforman la presente Tesis doctoral centrada en el *diseño*, *caracterización* y *aplicaciones clínicas* de lentes de contacto aperiódicas.

Cada una de estas tres fases conlleva una serie de particularidades retroalimentadas por el resto de etapas del proceso. Por ejemplo, pese a que la primera de las acciones se refiere al *diseño*, este viene enfocado a una *aplicación clínica* particular y podrá sufrir modificaciones según los inconvenientes hallados en los procesos de fabricación detectables a través de la *caracterización*.

Dos diseños aperiódicos han sido llevados a cabo con las *aplicaciones clínicas* principales de ralentización de la progresión de la miopía y compensación de la presbicia. Pese a que ambos diseños se basan en la misma estructura aperiódica denominada Fractal, los tamaños de las zonas varían dependiendo de la aplicación clínica.

El objetivo principal del primer diseño se encuentra dirigido a inducir un error relativo periférico miópico con la menor afectación posible de la visión central. Tras el análisis de trazado de rayos, encontramos que la inducción de error relativo periférico tenía un carácter pupilo-dependiente siendo la situación ideal aquella en la cual la primera zona excedía el diámetro de la pupila en torno a 1 mm. Es por ello que el tamaño de la primera zona terapéutica se inicia a los 4.5 mm de diámetro considerando un tamaño pupilar estándar de 3.5 mm. La segunda de las particularidades del diseño para el control de la miopía es utilizar una γ de 0.324 que asegura una mayor área de la zona terapéutica entre los 4.5 mm y el fin del tamaño de la óptica. La lente de contacto aperiódica también mostró ser sensible al descentramiento disminuyendo el target periférico relativo miópico y la región de la retina periférica donde se encontraba el pico máximo de actuación o potencia dióptrica más negativa. Pese a las limitaciones del diseño en torno a pupilo-dependencia y sensibilidad al descentramiento sus resultados teóricos fueron mejores que los obtenidos con una lente de contacto para el control de la miopía actualmente comercializada con tal propósito, con una mayor inducción de error relativo periférico y un menor compromiso de la visión central.

El segundo de los diseños, cuyo objetivo es la compensación de la presbicia, requiere de un equilibrio entre las zonas con potencia dióptrica para la compensación del error refractivo y las zonas que otorgan una adición dióptrica para aproximar el punto próximo del observador, el cual se encuentra más alejado de la distancia habitual de lectura debido a la pérdida de la capacidad acomodativa. A diferencia de la lente anteriormente descrita para el control de la miopía, ambas zonas compensación y adición se deben encontrar dentro de la región pupilar con el fin de que estas actúen de manera simultánea. Además, con el fin de reducir el área útil para visión próxima cuando el diámetro de pupila se incrementa, la γ de este diseño fue de 0.333. Reduciéndose de esta forma el tamaño de la cuarta zona y concentrando todas las zonas aperiódicas en un diámetro de lente de 4.96 mm a partir del cual la zona óptica restante se encontraba dirigida a la visión lejana.

El análisis de trazado de rayos de este diseño demostró un incremento de la profundidad de foco para frecuencias espaciales bajas con tendencia a un comportamiento bifocal con el incremento de la frecuencia espacial. Podríamos decir por tanto que la lente se comporta como una lente de profundidad de foco extendida la cual posee el pico máximo de visión en la región próxima al valor de la adición de la lente. Esto quiere decir, que para una lente de adición de +1.50D, el pico de eficiencia máxima de la lente se alcanzaría a distancias intermedias (67 cm) y la visión de lejos podría verse ligeramente comprometida en favor de mejorar la visión próxima. Otra de las interesantes características obtenidas de las simulaciones es que pese a tratarse de una lente zonal, la variación del tamaño pupilar de 3.5 mm a 4.5 mm no afectó en gran medida a su comportamiento óptico aunque para 4.5 mm el descentramiento de la lente podría favorecer al foco de visión próxima.

Finalizado el análisis teórico de estos nuevos diseños, se procedió a su fabricación en forma de stock de lentes que posteriormente se utilizarían dentro de los estudios clínicos. El proceso de fabricación de este tipo de lentes zonales es mucho más complejo que el de una lente de contacto monofocal debido a que la superficie óptica de la lente no varía de una manera continua y el torno debe realizar oscilaciones para la fabricación de cada una de las

zonas. Puesto que el fabricante de los prototipos no poseía experiencia previa en la fabricación de este tipo de diseños, fue necesario caracterizar cada uno de los prototipos para reconocer los posibles sesgos con el diseño teórico.

En el caso de la lente para el control de la miopía encontramos una infraestimación del valor dióptrico positivo promedio de las zonas terapéuticas. Pese a que el diseño teórico establecía un valor dióptrico de +2.00 D en las zonas terapéuticas, los prototipos experimentales mostraron un promedio de +1.32 D y una correlación negativa entre el valor positivo de la adición y la potencia negativa de la lente. Esto quiere decir que lentes con una mayor potencia dentro del stock (de 0 a -7.00 D) presentaban una menor adición. Para las lentes de compensación de la presbicia, el stock comprendía potencias entre 0 y +2.00 D con adiciones teóricas de +1.50 D. No obstante, para estas lentes, aunque la potencia para la compensación de la hipermetropía se encontraba próxima a su valor teórico, la adición también fue infra-estimada en aproximadamente hasta las +0.81 D de media.

Los sesgos entre los diseños teóricos y los prototipos pueden originar un comportamiento clínico alejado al esperado en teoría, el cual no podría ser explicable sin un adecuado proceso de caracterización. Esto fue claramente visible en la medida del error relativo periférico en miopes adaptados con los prototipos de lentes para el control de la miopía. Las medidas clínicas del error periférico con el WAM 5500 mostraron un error relativo periférico miópico para el equivalente esférico (componente M) menor al esperado por el análisis de trazado de rayos. Mientras que el trazado de rayos mostró un pico máximo de alrededor de -2.00 D a 30º (para lente descentrada 0.7 mm respecto al centro pupilar), las medidas experimentales mostraron un valor de -1.3 D entre 20º y 25º. Esta hipocorrección es explicable por la infraestimación mostrada en los prototipos experimentales mientras que el desplazamiento del pico máximo se explica por un mayor descentramiento clínico de la lente, 0.83 mm, con respecto a los 0.7 mm simulados en el diseño teórico.

Más allá de estos sesgos, la lente de contacto para el control de la miopía demostró el efecto deseado incrementando el error relativo periférico miópico en los sujetos adaptados con la lente. Además, se analizó el astigmatismo inducido a través de las componentes J_0 y J_{45} en un mapa bidimensional que describió el comportamiento de la lente en regiones más allá del eje horizontal. La transformación de las componentes M, J_0 y J_{45} en las potencias sagital y tangencial a lo largo del meridiano horizontal mostró que pese a la menor adición presentada por la lente en la zona terapéutica, ésta era lo suficiente como para garantizar que las dos focales principales se encontrasen por delante de la retina en la muestra de sujetos cuya miopía media era de -2.62 D.

Para demostrar los efectos clínicos de la lente de contacto para el control de la presbicia nos encontramos con el principal problema de necesitar multitud de test clínicos de medida del rendimiento visual a múltiples distancias. Para solventar esta problemática se decidió desarrollar una serie de aplicaciones para iPad de manera que con un solo dispositivo pudiésemos llegar a realizar todas las pruebas de medida del rendimiento visual necesarias. No obstante, para que estas aplicaciones fuesen extrapolables a cualquier otro iPad, era necesario un análisis de las características de las pantallas y de sus propiedades lumínicas que garanticen una reproducción fiable del contraste en iPads retina no calibrados. Para ello se midió la correlación entre nivel digital y luminancia para cada uno de los canales R, G, B obteniendo las funciones gamma promedio. De acuerdo a la desviación estándar mostrada por los dispositivos en torno a estas curvas se analizaron los niveles de contraste que podían ser utilizados sin necesidad de caracterizar previamente el iPad, concluyendo que un test de sensibilidad al contraste desarrollado con la técnica de bitStealing podría ser utilizado con saltos de -0.1 unidades logarítmicas de contraste hasta un contraste mínimo de -2.2 unidades o con saltos de -0.05 hasta un contraste de -1.7 unidades, sin necesidad de una caracterización previa del iPad.

Posteriormente, se programaron y validaron varias aplicaciones para medir la agudeza visual, sensibilidad al contraste y estereopsis. En el caso del test de medida automatizada de agudeza visual los resultados mostraron una diferencia media de -0.06 logMAR con respecto al considerado como estándar de oro (ETDRS). Ésta sobre-estimación de la agudeza visual con respec-

to al ETDRS en torno a tres letras en un test desarrollado con 5 letras por línea, es explicable por el procedimiento psicofísico automatizado que posee como principal ventaja ser más reproducible que el ETDRS.

Con respecto a la Sensibilidad al Contraste, se programaron dos variantes de un mismo test. Ambas variantes diferían principalmente en el procedimiento psicofísico de medida y los saltos entre los distintos niveles de contraste evaluados. El mejor acuerdo entre el test clínico Functional Acuity Contrast Test (FACT) y la aplicación, se obtuvo cuando se utilizó el mismo procedimiento de medida y los mismos niveles de contraste que el test de referencia. No obstante, en estudios posteriores se demostró que la reproducibilidad de este nuevo sistema de medida era igual e incluso ligeramente inferior al test de referencia por lo que muy posiblemente variando el método psicofísico se podría mejorar la reproducibilidad del test pese a que el acuerdo con el test de referencia podría disminuir.

La validación de la aplicación de estereopsis se llevó a cabo con el TNO para cerca, el cual se fundamenta en el mismo concepto de estereopsis global o puntos aleatorios. Mientras que en lejos la aplicación se comparó con el Howard Dolman, por ser considerado el estándar de referencia aunque este último se basa en estereopsis local o de contornos. El acuerdo con el TNO fue excepcional y la reproducibilidad del test fue mucho mayor que la del test de referencia. No obstante, la estereopsis obtenida con esta aplicación en lejos no puede ser comparada con el Howard Dolman, lo cual es algo previsible ya que ambos test se fundamentan en dos principios diferentes de medida de estereopsis, uno global y el otro local.

Con las aplicaciones de medida del rendimiento visual validadas, la última parte de esta investigación supuso la medida del rendimiento visual en una serie de sujetos présbitas con hipermetropía inferior a las 2 D. La agudeza visual en lejos de los ojos adaptados con los prototipos no se diferenció significativamente con respecto a la no compensación. No obstante, se mostraron pérdidas significativas en la sensibilidad al contraste en visión de lejos para frecuencias espaciales por encima de los 6 cpd. Lo que determina que la visión de los sujetos empeoró ligeramente en visión de lejos afectando a su sensibilidad al contraste pero no a su agudeza visual. Esta pérdida de sensibilidad al contraste en lejos supone un sacrificio de la calidad óptica a dis-

tancia lejana a favor de mejorar de manera significativa la agudeza visual de cerca en hasta dos líneas de agudeza visual, pasando de 0.46 logMAR sin compensación a 0.26 logMAR con la adaptación de los prototipos. Esta mejoría de la calidad óptica en visión próxima supuso también una mejora significativa en la estereopsis a 50 cm. Las curvas de desenfoque de agudeza visual y sensibilidad al contraste mostraron un buen acuerdo con respecto a las simulaciones obtenidas con Zemax, mostrando una profundidad de foco extendida con un pico máximo en torno a -1.00D, próximo al valor de la adición experimental que fue de 0.81 D como había sido calculado a través de trazado de rayos.

Capítulo 4
Conclusiones

Cumplimiento de objetivos

Esta tesis doctoral se cierra con el capítulo de conclusiones finales en el que se repasa el cumplimiento de los objetivos e hipótesis de investigación planteados al inicio del trabajo, se recopilan las principales conclusiones, se exponen las aportaciones más destacadas del trabajo y se plantean futuras líneas de investigación.

A lo largo de la investigación se han cumplido los siguientes objetivos propuestos inicialmente:

1. Diseñar LCs aperiódicas que puedan ser aplicables a la compensación de la presbicia, mejorando el rendimiento visual; o para el control de la progresión de la miopía, induciendo un error relativo periférico miópico.
2. Caracterizar los prototipos fabricados con el fin de determinar el sesgo existente con los diseños teóricos.
3. Evaluar el error relativo periférico inducido en sujetos adaptados con LCs para el control de la miopía.
4. Analizar las capacidades del iPad (hardware) para el desarrollo de test que puedan servir para la medición del rendimiento visual a múltiples distancias con LCs aperiódicas.
5. Programar y validar aplicaciones para iPad que puedan ser utilizadas para la medida de las siguientes habilidades visuales: agudeza visual, sensibilidad al contraste y estereopsis.
6. Evaluar el rendimiento visual en pacientes présbitas adaptados con LCs para la compensación de la presbicia mediante un estudio clínico previo.

En el primer artículo se presenta un nuevo diseño de lente de contacto aperiódica, simulando su rendimiento teórico a través de software de trazado de rayos sobre un modelo de ojo miope. El principal objetivo de este nuevo diseño es inducir un error relativo periférico miópico superior al de las lentes de contacto actualmente comercializadas con objeto de ralentizar la progresión de la miopía. Teniendo además, una menor afectación de la calidad óptica en visión central. Mediante este artículo se cubre parcialmente el ob-

jetivo 1 en torno al diseño de lentes de contacto aperiódicas para el control de la miopía.

En el artículo 2 se evaluaron los prototipos de lentes de contacto aperiódicas para el control de la miopía sobre una muestra de sujetos miopes, siendo la principal variable de medida el error relativo periférico inducido por la lente. En este trabajo se realizó una caracterización previa de los prototipos que posteriormente fueron utilizados para la medida del error relativo periférico. Se encontró un sesgo con respecto a los análisis teóricos que pudo ser explicado en parte gracias al procedimiento de caracterización. Mediante este trabajo se cubren por tanto los objetivos 2 y 3.

En el artículo 3 se analiza la fiabilidad de presentar optotipos de contraste variable en iPads no calibrados. Este trabajo forma parte del análisis previo de este sistema como instrumento de medición del rendimiento visual y derivará en el posterior desarrollo de aplicaciones de medida del rendimiento visual. Con este trabajo se cubre el objetivo 4.

Los artículos 4, 5 y 6 describen los resultados de validación de aplicaciones para la medida de la Sensibilidad al Contraste, Agudeza Visual y Estereopsis. Recogiendo en cada uno de ellos el acuerdo con el estándar de oro o con un test clínico de referencia en el caso de no existir dicho estándar. Estos trabajos recogen también la reproducibilidad de cada una de las aplicaciones y la comparativa con los test de referencia. Estos tres artículos sirven como justificación de cumplimiento de objetivo 5.

El último artículo de esta tesis por compendio de artículos contiene el procedimiento completo de desarrollo de una nueva lente de contacto aperiódica para la compensación de la presbicia. Dentro de este trabajo se muestran las características del diseño teórico a través del modelado en Zemax, la caracterización de los prototipos fabricados y el rendimiento visual alcanzado por los pacientes a través de la adaptación clínica de estos prototipos. Este último artículo engloba el cumplimiento de los objetivos 1, 2 y 6.

Aportaciones realizadas

Tras comprobar el cumplimiento de los objetivos descritos, es momento de realizar un breve resumen sobre las aportaciones más destacadas en torno a las investigaciones realizadas en los últimos tres años.

Dos nuevos prototipos de lentes de contacto para el control de la progresión de la miopía y para la compensación de la presbicia han sido propuestos con el fin de mejorar algunas de las limitaciones de los diseños actuales. En el caso de la lente para el control de la miopía, la principal ventaja que presenta con respecto a la primera lente comercializada con tal propósito, es la inducción de un mayor error relativo periférico miópico y sobre todo sin alterar en gran medida la visión central de los pacientes. En el caso de la lente de contacto para la presbicia, la principal ventaja sobre otras lentes de contacto zonales es la baja pupilo-dependencia para una oscilación natural de la pupila entre 3.5 mm y 4.5 mm, además de la tolerancia al descentramiento que se suele originar en la adaptación de una lente de contacto.

Durante todo el proceso de esta investigación hemos realizado pequeñas aportaciones para la mejora de los procedimientos actuales. Por ejemplo, en el proceso de caracterización de lentes de contacto se desarrolló un algoritmo de reconocimiento de transición entre zonas pudiendo calcular la potencia promedio en cada una de las zonas de la lente de contacto. Esto supone un avance en los procedimientos actuales de caracterización ya que el software actual del NIMO (instrumento de medida) no reconoce automáticamente la transición entre zonas y la adición es calculada a partir de la introducción manual del tamaño de la zona (hasta un límite de cinco zonas). Además, en el proceso de medida del error relativo periférico se desarrolló un software en MATLAB que capturaba cada una de las medidas realizadas con el WAM 5500, descomponiéndolas en notación vectorial y promediándolas para facilitar la medida en un mayor número de puntos en menor tiempo. Esto dio origen a la representación bidimiensional del error relativo periférico, algo que hasta ahora no había sido llevado a cabo en ninguna investigación previa con este instrumento.

El análisis de la validez del iPad para la representación de estímulos de contraste variable sin necesidad de un calibrado previo de la pantalla supone un gran avance para la tele-oftalmología. La cuestión de si es fiable utilizar el

iPad para medir la sensibilidad al contraste sin un calibrado previo ha sido resuelta y esto favorecerá el incremento del desarrollo de aplicaciones móviles para la medida del rendimiento visual. La validación de cada una de estas aplicaciones, demostrando un comportamiento similar al de los test convencionales, e inclusive superior en términos de reproducibilidad en alguno de los casos, supone que estas aplicaciones crezcan en popularidad en el entorno clínico y puedan llegar a utilizarse de una manera masiva gracias a la importante reducción en los costes de este tipo de test frente a los métodos convencionales.

Líneas de investigación futuras

Durante las investigaciones hemos detectado posibles líneas de mejora que pueden dar lugar a la continuación de los estudios iniciados. La primera de ellas es la demostración de que la lente para el control de la miopía no solo genera el efecto óptico deseado sobre la retina, algo demostrado en esta Tesis, sino que realmente produce una ralentización en la progresión de la miopía. Para ello se hace necesario un riguroso ensayo clínico en niños de a partir de unos 8 años de edad frente a un grupo control en el cual se controlen variables como error relativo periférico, horas de porte, cambio en la longitud axial, etc. Además, los resultados clínicos del presente trabajo tanto de esta lente como de la lente para la compensación de la presbicia podrían ser mejorados en un futuro mediante el desarrollo de sistemas de estabilización de la lente, cambio de material, espesores, etc. que terminen minimizando el descentramiento que suele presentar la lente. Es importante también resaltar que el estudio realizado con pacientes, en el caso de la lente de la presbicia, se trata de un estudio clínico previo y que es necesario un ensayo clínico con una muestra mayor de pacientes una vez se alcance una aceptable reproducibilidad en los procesos de fabricación.

Esta Tesis doctoral ha dado lugar a una patente internacional que recoge la invención de la cual el autor de este trabajo es participe (Furlan et al. 2014), y tiene como objetivo proteger la invención durante el desarrollo de los futuros ensayos clínicos, así como la colaboración con empresas del sector interesadas en la tecnología.

El desarrollo de nuevas aplicaciones de medida del rendimiento visual abre igualmente una nueva vía de trabajo centrada en integrar estas aplicaciones con bases de datos que permitan la recogida global de información en múltiples centros clínicos o que puedan ser utilizadas para la autoevaluación del paciente con su dispositivo móvil y el seguimiento remoto por parte del profesional de la visión (Fernández et al. 2016d; Fernández et al. 2016f). Prueba de ello es el gran interés despertado en la comunidad oftalmológica internacional por la aplicación "Multifocal Lens Analyzer" diseñada y programada por el autor de esta Tesis y que fue clasificada por la revista "*Cataract & Refractive Surgery Today Europe*" como una de las 5 invenciones destacadas en su especial "*Eyes for innovation, profiles of physician-innovators in ophthalmology*" (Fernández et al. 2016b). Esta nueva aplicación permite medir las curvas de desenfoque de manera automatizada en términos de agudeza visual y sensibilidad al contraste (Salvestrini et al. 2016). Siendo el primer instrumento clínico disponible para tal propósito, el cual servirá para entender de mejor forma como complicaciones durante la cirugía (Fernández et al. 2016a), parámetros biométricos oculares (Fernández et al. 2016c), diferentes tipos de intervención quirúrgica (Fernández et al. 2015c), etc. pueden afectar al rendimiento visual de pacientes sometidos a procedimientos para la compensación de la presbicia (Fernández et al. 2015a; Fernández et al. 2015b). Además, la inclusión de esta aplicación en los futuros ensayos clínicos con la lente aperiódica para la compensación de la presbicia podría ayudar a mejorar los procedimientos en la refracción del paciente adaptado con este tipo de lentes, ya que la sobre-refracción con lentes de contacto multifocales suele ser especialmente compleja.

Bibliografía General

Alexander KR, Barnes C, Fishman GA, Pokorny J, Smith VC (2004) Contrast sensitivity deficits in inferred magnocellular and parvocellular pathways in retinitis pigmentosa. Invest Ophthalmol Vis Sci 45:4510–4519.

Alexander KR, McAnany JJ (2010) Determinants of contrast sensitivity for the Tumbling E and Landolt C. Optom Vis Sci 87:28–36.

American Academy of Ophthalmology (2010) Preferred Practice Pattern Guidelines. Comprehensive Adult Medical Eye Evaluation. American Academy of Ophthalmology, San Francisco CA.

American National Standard (1992) Ophthalmics-Instruments- General-Purpose Clinical Visual Acuity Charts. ANSI Z80.21-1992(R1998).

American Optometric Association (1994a) Comprehensive Adult Eye and Vision Examination. In: Optom. Clin. Pract. Guidel.

American Optometric Association (1994b) Pediatric eye and vision examination. In: Optom. Clin. Pract. Guidel.

AMETEK Ultra Precision Technologies (2016) Optoform 40. http://www.sterlingint.com/lathes/optoform-40/. Accessed 28 Sep 2016.

AMO-Wavefront Sciences (2014) ClearWave. http://www.lumetrics.com/documents/ClearWave_new.pdf. Accessed 28 Sep 2016.

Ansari E, Morgan J, Snowden R (2002) Psychophysical characterisation of early functional loss in glaucoma and ocular hypertension. Br J Ophthalmol 86:1131–1135.

Anstice NS, Phillips JR (2011) Effect of dual-focus soft contact lens wear on axial myopia progression in children. Ophthalmology 118:1152–61.

Armstrong RA, Davies LN, Dunne MCM, Gilmartin B (2011) Statistical guidelines for clinical studies of human vision. Ophthalmic Physiol Opt 31:123–36.

Arumugam B, Hung LF, To CH, Holden B, Smith EL (2014) The effects of simultaneous dual focus lenses on refractive development in infant monkeys. Invest Ophthalmol Vis Sci 55:7423–7432.

Arumugam B, Hung LF, To CH, Sankaridurg P, Smith EL (2016) The effects of the relative strength of simultaneous competing defocus signals on emmetropization in infant rhesus monkeys. Invest Ophthalmol Vis Sci 57:3949.

Aslam TM, Murray IJ, Lai MY, Linton E, Tahir HJ, Parry NR (2013) An assessment of a modern touch-screen tablet computer with reference to core physical characteristics necessary for clinical vision testing. J R Soc Interface 10:20130239.

Atchison DA (2006) Optical models for human myopic eyes. Vis Res 46:2236–50.

Atchison DA, Li SM, Li H, Li SY, Liu LR, Kang MT, Meng B, Sun YY, Zhan SY, Mitchell P, Wang N (2015) Relative peripheral hyperopia does not predict development and progression of myopia in children. Invest Ophthalmol Vis Sci 56:6162–6170.

Atchison DA, Pritchard N, Schmid KL (2006) Peripheral refraction along the horizontal and vertical visual fields in myopia. Vis Res 46:1450–8.

Atchison DA, Pritchard N, White SD, Griffiths AM (2005) Influence of age on peripheral refraction. Vis Res 45:715–20.

Atchison D, Scott D, Charman W (2007) Measuring ocular aberrations in the peripheral visual field using Hartmann-Shack aberrometry. J Opt Soc Am A 24:2963–2973.

Bakaraju RC, Ehrmann K, Papas E, Ho A (2008) Finite schematic eye models and their accuracy to in-vivo data. Vis Res 48:1681–94.

Beck RW, Ruchman MC, Savino PJ, Schatz NJ (1984) Contrast sensitivity measurements in acute and resolved optic neuritis. Br J Ophthalmol 68:756–9.

Benavente-Pérez A, Nour A, Troilo D (2014) Axial eye growth and refractive error development can be modified by exposing the peripheral retina to relative myopic or hyperopic defocus. Invest Ophthalmol Vis Sci 55:6765–73.

Benz (2016) G5X p-GMA/HEMA (Hioxifilcon A). http://benzrd.com/benz_g5x.php. Accessed 27 Mar 2016.

Bernell A division of vision training products (2014) Howard-Dolman type test. http://www.bernell.com/product/HDTEST/126. Accessed 11 Sep 2014.

Berntsen DA, Kramer CE (2013) Peripheral defocus with spherical and multifocal soft contact lenses. Optom Vis Sci 90:1215–1224.

Black JM, Jacobs RJ, Phillips G, Chen L, Tan E, Tran A, Thompson B (2013) An assessment of the iPad as a testing platform for distance visual acuity in adults. BMJ Open 20; 3(6).

Bland JM, Altman DG (1999) Statistical methods in medical research. Stat Methods Med Res 8:135–160.

Bogfjellmo L-G, Bex PJ, Falkenberg HK (2014) The development of global motion discrimination in school aged children. J Vis 14:19.

Bradley A, Nam J, Xu R, Harman L, Thibos L (2014) Impact of contact lens zone geometry and ocular optics on bifocal retinal image quality. Ophthal Physiol Opt 34:331–45.

Buehren T, Iskander DR, Collins MJ, Davis B (2007) Potential higher-order aberration cues for sphero-cylindrical refractive error development. Optom Vis Sci 84:163–174.

Bühren J, Terzi E, Bach M, Wesemann W, Kohnen T (2006) Measuring contrast sensitivity under different lighting conditions: comparison of three tests. Optom Vis Sci 83:290–8.

Bunce C (2009) Correlation, agreement, and Bland-Altman analysis: statistical analysis of method comparison studies. Am J Ophthalmol 148:4–6.

Calatayud A, Antonio J, Serra M, Furlan WD (2013) Diseño y caracterización experimental de nuevas lentes difractivas basadas en geometrías aperiódicas. Tesis Doctoral. Universitat Politècnica de València.

Calossi A (2007) Corneal asphericity and spherical aberration. J Refract Surg 23:505–514.

Calver R, Radhakrishnan H, Osuobeni E, O'Leary D (2007) Peripheral refraction for distance and near vision in emmetropes and myopes. Ophthalmic Physiol Opt 27:584–93.

Carstensen B (2010) Comparing methods of measurement: Extending the LoA by regression. Stat Med 29:401–10.

Carstensen B, Simpson J, Gurrin LC (2008) Statistical models for assessing agreement in method comparison studies with replicate measurements. Int J Biostat 4:Article 16.

Charman WN (2014) Developments in the correction of presbyopia I: spectacle and contact lenses. Ophthal Physiol Opt 34:8–29.

Charman WN (2011) Keeping the world in focus: how might this be achieved? Optom Vis Sci 88:373–376.

Charman WN, Radhakrishnan H (2010) Peripheral refraction and the development of refractive error: a review. Ophthalmic Physiol Opt 30:321–38.

Chauhan T, Perales E, Xiao K, Hird E, Karatzas D, Wuerger S (2014) The achromatic locus: Effect of navigation direction in color space. J Vis 14:25,1-11.

Chu CH, Kee CS (2015) Effects of optically imposed astigmatism on early eye growth in chicks. PLoS One 10:e0117729.

Chung K, Mohidin N, O'Leary DJ (2002) Undercorrection of myopia enhances rather than inhibits myopia progression. Vis Res 42:2555–9.

Chylack LT, Padhye N, Khu PM, Wehner C, Wolfe J, McCarthy D, Rosner B, Friend J (1993) Loss of contrast sensitivity in diabetic patients with LOCS II classified cataracts. Br J Ophthalmol 77:7–11.

Ciner EB, Schmidt PP, Orel-Bixler D, Dobson V, Maguire M, Cyert L, Moore B, Schultz J (1998) Vision screening of preschool children: evaluating the past, looking toward the future. Optom Vis Sci 75:571–84.

Cinta Puell Marín M (2006) Las ametropías esféricas. In: Óptica Fisiológica. El sistema óptico del ojo y la visión binocular. E-Prints Complutense, Madrid, p 50.

Consilium Ophthalmologicum Universale (1984) Visual acuity measurement standard. Visual Functions Committee, International Council of Ophthalmology.

Cox I (1990) Theoretical calculation of the longitudinal spherical aberration of rigid and soft contact lenses. Optom Vis Sci 67:277–82.

Davies LN, Mallen EA (2009) Influence of accommodation and refractive status on the peripheral refractive profile. Br J Ophthalmol 93:1186–90.

de Carle J (1989) A refractive multizone bifocal. Trans BCLA Conf 12:66–70.

De Fez D, Luque MJ, García-Domene MC, Camps V, Piñero D (2016) Colorimetric characterization of mobile devices. Optom Vis Sci 93:1–9.

Diether S, Wildsoet CF (2005) Stimulus requirements for the decoding of myopic and hyperopic defocus under single and competing defocus conditions in the chicken. Inves Opthal Vis Sci 46:2242–52.

Dorr M, Lesmes LA, Lu ZL, Bex PJ (2013) Rapid and reliable assessment of the contrast sensitivity function on an iPad. Inves Opthal Vis Sci 54:7266–7273.

Douthwaite WA (2006) Contact lens optics design. Heinemann, Butterworth.

Efron S, Efron N, Morgan PB (2008) Repeatability and reliability of ocular aberration measurements in contact lens wear. Cont Lens Anterior Eye 31:81–8.

Ehrenstein WH, Ehrenstein A (1999) Psychophysical Methods. In: Modern techniques in neuroscience research. Springer, p 1214.

Ehsaei A, Mallen EA, Chisholm CM, Pacey IE (2011) Cross-sectional sample of peripheral refraction in four meridians in myopes and emmetropes. Invest Ophthalmol Vis Sci 52:7574–7585.

Elliott DB, Situ P (1998) Visual acuity versus letter contrast sensitivity in early cataract. Vis Res 38:2047–2052.

Faria-Ribeiro M, Queirós A, Lopes-Ferreira D, Jorge J, González-Méijome JM (2013) Peripheral refraction and retinal contour in stable and progressive myopia. Optom Vis Sci 90:9–15.

Fedtke C, Ehrmann K, Falk D, Bakaraju RC, Holden BA (2014) The BHVI-EyeMapper: Peripheral Refraction and Aberration Profiles. Optom Vis Sci 91:1199–1207.

Fedtke C, Ehrmann K, Holden BA (2009) A review of peripheral refraction techniques. Optom Vis Sci 86:429–46.

Feng X, Zhang X, Jia Y (2015) Improvement in fusion and stereopsis following surgery for intermittent exotropia. J Pediatr Ophthalmol Strabismus 52:52–57.

Fernandes PR, Neves HI, Lopes-Ferreira DP, Jorge JM, González-Meijome JM (2013) Adaptation to Multifocal and Monovision Contact Lens Correction. Optom Vis Sci 90:228–235.

Fernández J, Martínez J, Rodríguez-Vallejo M (2016a) Capítulo 22. Complicaciones durante la irrigación/aspiración. In: Monografía SECOIR. Complicaciones en la cirugía del cristalino. pp 199–205.

Fernández J, Martínez J, Rodríguez-Vallejo M (2015a) Capítulo 27-2-4. Plataforma Supracor. In: Monografía SECOIR. Óptica para el cirujano faco-refractivo. pp 347–350.

Fernández J, Martínez J, Rodríguez-Vallejo M (2015b) Capítulo 20. Bases ópticas de las lentes acomodativas. In: Monografía SECOIR. Óptica para el cirujano faco-refractivo. pp 261–266.

Fernández J, Martínez J, Rodríguez-Vallejo M (2015c) Zero Phaco: the evolution of femtosecond laser-assissted cataract. In: XXXIII Congress ESCRS.

Fernández J, Rodríguez-Vallejo M, Martínez J (2016b) Bridging the gap between lab and clinical practice in assessing multifocal IOLs. In: Cataract Refract. Surg. Today. http://crstodayeurope.com/pdfs/0216CRSTEuro_cs_Fernandez.pdf. Accessed 17 Jul 2016.

Fernández J, Rodríguez-Vallejo M, Martínez J, Tauste A (2016c) Impact of corneal spherical aberration and tear break-up time on contrast sensitivity and visual acuity defocus curves in patients implanted with MIOLs. In: XXXIV Congress ESCRS.

Fernández J, Rodríguez-Vallejo M, Martínez J, Tauste A, Piñero D (2016d) Corneal Thickness After SMILE Affects Scheimpflug-based Dynamic Tonometry. J Refract Surg. Accepted for publish. doi:10.3928/1081597X-20160816-02

Fernández J, Tauste A, Rodríguez-Vallejo M (2016e) Eye Injuries in Sports Practice: Mini-Review. Adv Ophthalmol Vis Syst 4:11–14.

Fernández J, Valero A, Martínez J, Piñero DP, Rodríguez-Vallejo M (2016f) Short-term outcomes of small-incision lenticule extraction (SMILE) for low, medium, and high myopia. Eur J Ophthalmol Ahead of print.

Ferree C, Rand G, Hardy C (1931) Refraction for the peripheral field of vision. Arch Ophthalmol 5:717–731.

Ferris FL, Bailey I (1996) Standardizing the measurement of visual acuity for clinical research studies: Guidelines from the Eye Care Technology Forum. Ophthalmology 103:181–182.

Fischer RF, Tadic B (2000) Tolerancing and producibility. In: Professional M-H (ed) Optical System Design, First Edit. pp 366–388

Flitcroft D (2013) Is myopia a failure of homeostasis? Exp Eye Res 114:16–24.

Franco S, Silva AC, Carvalho AS, Macedo AS, Lira M (2010) Comparison of the VCTS-6500 and the CSV-1000 tests for visual contrast sensitivity testing. Neurotoxicology 31:758–61.

Fricke TR, Siderov J, Faa M (1997) Stereopsis, stereotests, and their relation to vision screening and clinical practice. Clin Exp Optom 80:165–172.

Friendly DS (1978) Preschool visual acuity screening tests. Trans Am Ophthalmol Soc 76:383–480.

Furlan WD, Andrés P, Saavedra G, Pons A, Monsoriu JA, Calatayud A, Remón L, Giménez F, Rojas JL, Larra E, Salazar PJ, Rodríguez-Vallejo M (2013) Mejoras en el objeto de la Patente principal nº 201031316 por "Lente oftálmica multifocal y procedimiento para su obtención".

Furlan WD, Andrés Bou P, Pons Martí A, Saavedra Tortosa G, Monsoriu Serra JA, Giménez Palomares F, Remón Martí L, Catalayud Catalayud A, Rodríguez-Vallejo M, Rojas JL, Larra E, Salazar PJ (2014) Multifocal, hybrid diffractive-refractive ophthalmic lens, use of the lens and method for the production thereof. Patent WO 2014198972 A1.

Furlan WD, García J, Muñoz L (2009) Refracción ocular, acomodación y ametropías. In: Fundamentos de optometría, 2ª Edición. Universitat de València, pp 23–25.

Furlan WD, Remón L, Llorens C, Rodríguez-Vallejo M, Monsoriu JA (2016) Comparison of two different devices to assess intraocular lenses. Optik (Stuttg) 127:10108–10114.

Furlan WD, Saavedra G, Monsoriu JA (2007) White-light imaging with fractal zone plates. Opt Lett 32:2109–11.

Furlan WD, Saavedra G, Pons A, Bou PA, Monsoriu JA, Calatayud A, Remón L, Giménez F, Rojas JL, Larra E, Salazar P (2012a) Multifocal ophthalmic lens and method for obtaining same. ES Patent 070559. 2011. WO 2012/028755 A1.

Furlan WD, Saavedra G, Pons A, Bou PA, Monsoriu JA, Calatayud A, Remón L, Giménez F, Rojas JL, Larra E, Salazar P, Rodríguez-Vallejo M (2012b) Multifocal ophthalmic lens and method for obtaining same. Improvements. ES Patent P201330862.

Gantz L, Bedell HE (2011) Variation of stereothreshold with random-dot stereogram density. Optom Vis Sci 88:1066–71.

Garner L (1977) Front surface topography of spherical flexible contact lenses on the eye. Aust J Optom 60:40–45.

Ginsburg AP (1996) Next generation contrast sensitivity testing. In: Fuctional assessment of low vision. St Louis: Mosby Year Book Inc, pp 77–88.

Gonza L, Blanco L, Carlos J, Fern S, Sanz O, Mun MA (2008) Axial length, corneal radius, and age of myopia onset. Optom Vis Sci 85:89–96.

González-Méijome JM, Faria-Ribeiro MA, Lopes-Ferreira DP, Fernandes P, Carracedo G, Queiros A (2015) Changes in peripheral refractive profile after orthokeratology for different degrees of myopia. Curr Eye Res 41:199–207.

González-Méijome JM, Peixoto-de-Matos SC, Faria-Ribeiro M, Lopes-Ferreira DP, Jorge J, Legerton J, Queiros A (2016) Strategies to regulate myopia progression with contact lenses: a review. Eye Contact Lens 42:24–34.

Gu X-J, Hu M, Li B, Hu X-T (2014) The role of contrast adaptation in saccadic suppression in humans. PLoS One 9:e86542.

Gwiazda J (2009) Treatment options for myopia. Optom Vis Sci 86:624–628.

Hartwig A, Charman WN, Radhakrishnan H (2016) Baseline peripheral refractive error and changes in axial refraction during one year in a young adult population. J Optom 9:32–39.

He JC (2014) Theoretical model of the contributions of corneal asphericity and anterior chamber depth to peripheral wavefront aberrations. Ophthalmic Physiol Opt 34:321–330.

Hess RF, Ding R, Clavagnier S, Liu C, Guo C, Viner C, Barrett BT, Radia K, Zhou J (2016) A robust and reliable test to measure stereopsis in the clinic. Invest Ophthalmol Vis Sci 57:798–804.

Hitchcock EM, Dick RB, Krieg EF (2004) Visual contrast sensitivity testing: a comparison of two F.A.C.T. test types. Neurotoxicol Teratol 26:271–7.

Hitchings RA, Powell DJ, Arden GB, Carter RM (1981) Contrast sensitivity gratings in glaucoma family screening. Br J Ophthalmol 65:515–7.

Ho W-C, Wong O-Y, Chan Y-C, Wong S-W, Kee C-S, Chan HH-L (2012) Sign-dependent changes in retinal electrical activity with positive and

negative defocus in the human eye. Vis Res 52:47–53.

Holladay JT, Van Dijk H, Lang A, Portney V, Willis TR, Sun R, Oksman HC (1990) Optical performance of multifocal intraocular lenses. J Cataract Refract Surg 16:413–22.

Holmes JM, Beck RW, Repka MX, Leske DA, Kraker RT, Blair RC, Moke PS, Birch EE, Saunders RA, Hertle RW, Quinn GE, Simons KA, Miller JM (2001) The amblyopia treatment study visual acuity testing protocol. Arch Ophthalmol 119:1345–53.

Holmes JM, Birch EE, Leske DA, Flu VL, Mohney BG (2009) New tests of distance stereoacuity and their role in evaluating intermittent exotropia. Ophthalmology 114:1215–1220.

Hong XIN, Himebaugh N, Thibos LN (2001) On-Eye evaluation of optical performance of rigid and soft contact lenses. Optom Vis Sci 78:872–880.

Horner DG, Soni PS, Vyas N, Himebaugh NL (2000) Longitudinal changes in corneal asphericity in myopia. Optom Vis Sci 77:198–203.

Hough T (2006) Correction of presbyopia by contact lenses. In: Douthwaite WA (ed) Contact lens optics and lens design, 3rd ed. Butterworth-Heinemann, Bradford, pp 282–287.

Huang J, Wen D, Wang Q, McAlinden C, Flitcroft I, Chen H, Saw SM, Chen H, Bao F, Zhao Y, Hu L, Li X, Gao R, Lu W, Du Y, Jinag Z, Yu A, Lian H, Jiang Q, Yu Y, Qu J (2016) Efficacy comparison of 16 interventions for myopia control in children. Ophthalmology 123:697–708.

Ip JM, Huynh SC, Kifley A, Rose KA, Morgan IG, Varma R, Mitchell P (2007) Variation of the contribution from axial length and other oculometric parameters to refraction by age and ethnicity. Invest Ophthalmol Vis Sci 48:4846–4853.

ISO-11979-2 (2014) Ophthalmic implants - Intraocular lenses - Part 2: Optical properties and test methods.

Jennings JA, Charman WN (1978) Optical image quality in the peripheral retina. Am J Optom Physiol Opt 55:582–90.

Joannes L, Hough T, Hutsebaut X, Dubois X, Ligot R, Saoul B, Van Donink P, De Coninck K (2010) The reproducibility of a new power mapping instrument based on the phase shifting schlieren method for the measurement of spherical and toric contact lenses. Cont Lens Anterior Eye 33:3–8.

Kang P, Fan Y, Oh K, Trac K, Zhang F, Swarbrick HA (2013) The effect of multifocal soft contact lenses on peripheral refraction. Optom Vis Sci 90:658–66.

Kang P, Swarbrick H (2013) Time course of the effects of orthokeratology on peripheral refraction and corneal topography. Ophthal Physiol Opt 33:277–82.

Kee CS, Hung LF, Qiao-Grider Y, Roorda A, Smith EL (2004) Effects of optically imposed astigmatism on emmetropization in infant monkeys. Invest Ophthalmol Vis Sci 45:1647–1659.

Kemper AR, Margolis PA, Downs SM, Bordley WC (1999) A systematic review of vision screening tests for the detection of amblyopia. Pediatrics 104:1220–1222.

Kim CY, Chung SH, Kim T, Cho YJ, Yoon G, Seo KY (2007) Comparison of higher-order aberration and contrast sensitivity in monofocal and multifocal intraocular lenses. Yonsei Med J 48:627–633.

Kim E, Bakaraju RC, Ehrmann K (2015) Reliability of power profiles measured on NIMO TR1504 (Lambda-X) and effects of lens decentration for single vision, bifocal and multifocal contact lenses. J Optom 9:126–136.

Kirschen DG, Hung CC, Nakano TR (1999) Comparison of suppression, stereoacuity, and interocular differences in visual acuity in monovision and Acuvue Bifocal Contact Lenses. Optom Vis Sci 76; 832-7.

Kollbaum PS, Dietmeier BM, Jansen ME, Rickert ME (2012) Quantification of ghosting produced with presbyopic contact lens correction. Eye Contact Lens 38:252–9.

Kollbaum PS, Jansen ME, Kollbaum EJ, Bullimore MA (2014) Validation of an iPad Test of Letter Contrast Sensitivity. Optom Vis Sci 91:291–6.

Kollbaum PS, Jansen ME, Tan J, Meyer DM, Rickert ME (2013) Vision

performance with a contact lens designed to slow myopia progression. Optom Vis Sci 90:205–14.

Lahav K, Levkovitch-Verbin H, Belkin M, Glovinsky Y, Polat U (2011) Reduced mesopic and photopic foveal contrast sensitivity in glaucoma. Arch Ophthalmol 129:16–22.

Lambda-X (2014) NIMO TR1504. http://www.lambda-x.com/documents/LX-TR1504.pdf. Accessed 28 Sep 2016.

Landis JR, Koch GG (1977) The measurement of observer agreement for categorical data. Biometrics 33:159–174.

Lee SY, Koo NK (2005) Change of stereoacuity with aging in normal eyes. Korean J Ophthalmol 19:136–9.

Leek MR (2001) Adaptive procedures in psychophysical research. Percept Psychophys 63:1279–92.

Legras R, Chateau N, Charman WN (2004) A method for simulation of foveal vision during wear of corrective lenses. Optom Vis Sci 81:729–38.

Leising KJ, Wolf JE, Ruprecht CM (2013) Visual discrimination learning with an iPad-equipped apparatus. Behav Process 93:140–147.

Leone JF, Mitchell P, Kifley A, Rose KA (2014) Normative visual acuity in infants and preschool-aged children in Sydney. Acta Ophthalmol 92: e521-9.

Lesmes LA, Lu ZL, Baek J, Albright TD (2010) Bayesian adaptive estimation of the contrast sensitivity function: the quick CSF method. J Vis 10:1–21.

Lin TP, Rigby H, Adler JS, Hentz JG, Balcer LJ, Galetta SL, Devick S, Cronin R, Adler CH (2015) Abnormal visual contrast acuity in parkinson's disease. J Park Dis 5:125–130.

Lindberg C, Fishman G, Anderson R, Vasquez V (1981) Contrast sensitivity in retinitis pigmentosa. Br J Ophthalmol 65:855–858.

Liou H, Brennan N (1997) Anatomically accurate, finite model eye for optical modeling. J Opt Soc Am A Opt Image Sci Vis 14:1684–95.

Llorens-Quintana C, Vela JE, Rodríguez-Vallejo M, Monsoriu JA, Walter D Furlan (2014) Medida adaptable de la estereopsis de lejos y cerca con StereoTAB. Comparativa con Howard Dolman. In: Gené A, Bueno-Gimeno I, Sañudo F (eds) Temas actuales en Optometría. Ediciones MC. Montserrat Cruz, pp 323–326.

Long GM, Penn DL (1987) Normative contrast sensitivity functions: the problem of comparison. Am J Optom Physiol Opt 64:131–5.

Lundström L, Mira-Agudelo A, Artal P (2009) Peripheral optical errors and their change with accommodation differ between emmetropic and myopic eyes. J Vis 9:1–11.

Maldonado-Codina C, Efron N (2003) Hydrogel Lenses – Materials and Manufacture : A Review. Optom Pract 4:101–115.

Maldonado-Codina C, Efron N (2005) Impact of manufacturing technology and material composition on the surface characteristics of hydrogel contact lenses. Clin Exp Optom 88:396–404.

Malo J, Luque MJ (2014) COLORLAB: A color processing tool-box for Matlab. http://www.uv.es/vista/. Accessed 5 May 2014.

Marcos S (2010) Ocular ageing: improving the quality of sight for cataract and presbyopia sufferers. LYCHNOS (Notebooks Fund Gen CSIC) 2:60–65.

Martin JA, Roorda A (2003) Predicting and assessing visual performance with multizone bifocal contact lenses. Optom Vis Sci 80:812–9.

McAlinden C, Khadka J, Pesudovs K (2011) Statistical methods for conducting agreement (comparison of clinical tests) and precision (repeatability or reproducibility) studies in optometry and ophthalmology. Ophthalmic Physiol Opt 31:330–8.

Monsoriu JA, Saavedra G, Furlan WD (2004) Fractal zone plates with variable lacunarity. Opt Express 12:4227–34.

Murdoch IE, Morris SS, Cousens SN (1998) People and eyes: statistical approaches in ophthalmology. Br J Ophthalmol 82:971–3.

Mutti DO, Sholtz RI, Friedman NE, Zadnik K (2000) Peripheral refraction

and ocular shape in children. Invest Ophthalmol Vis Sci 41:1022–30.

National Eye Institute (2014) Corrective lenses statistics. In: Glas. Crafter. http://www.statisticbrain.com/corrective-lenses-statistics/. Accessed 24 Jul 2016.

Navarro R, Palos F, González L (2007) Adaptive model of the gradient index of the human lens. I. Formulation and model of aging ex vivo lenses. J Opt Soc Am A 24:2175–85.

Navarro R, Santamaria J (1985) Accommodation-dependent model of the human eye with aspherics. J Opt Soc Am A 2:1273–1281.

Norton T, Corliss D, Bailey J (2002) The psychophysical measurement of visual function. MA: Butterworth-Heinemann, Burlington.

Optocraft (2014) SHSOphthalmic omniSpect. http://www.optocraft.de/products/SHSOmnispect/index.en.php. Accessed 28 Sep 2016.

Owsley C (2003) Contrast sensitivity. Ophthalmol Clin North Am 16:171–178.

Pageau M, de Guise D, Saint-Amour D (2015) Random-dot stereopsis in microstrabismic children: stimulus size matters. Optom Vis Sci 92:208–216.

Peli E (1990) Contrast in complex images. J Opt Soc Am A 7:2032–40.

Pelli DG, Robson JG, Wilkins AJ (1988) The design of a new letter chart for measuring contrast sensitivity. Clin Vis Sci 2:187–199.

Perera C, Chakrabarti R, Islam FMA, Crowston J (2015) The Eye Phone Study: reliability and accuracy of assessing Snellen visual acuity using smartphone technology. Eye 29:888–894.

Pesudovs K, Hazel C, Doran R, Eliot D (2004) The usefulness of Vistech and FACT contrast sensitivity charts for cataract and refractive surgery outcomes research. Br J Ophthalmol 88:11–16.

PhasePhocus (2014) Phase Phocus Lens Profiler. http://www.phasefocus.com/wp-content/uploads/2014/07/Phase-Focus-Lens-Profiler-System.pdf. Accessed 28 Sep 2016.

Phillips J (2008) Contact lens and method. US Patent 20080218687 A1.

Plainis S, Atchison DA, Charman WN (2013a) Power profiles of multifocal contact lenses and their interpretation. Optom Vis Sci 90:1066–1077.

Plainis S, Charman WN (1998) On-eye power characteristics of soft contact lenses. Optom Vis Sci 75:44–54.

Plainis S, Ntzilepis G, Atchison DA, Charman WN (2013b) Through-focus performance with multifocal contact lenses: effect of binocularity, pupil diameter and inherent ocular aberrations. Ophthal Physiol Opt 33:42–50.

Plakitsf A, Charman WN (1995) Comparison of the depths of focus with the naked eye and three types of presbyopic contact lens correction. J Br Contact Lens Assoc 18:119–125.

Pomerance GN, Evans DW (1994) Test-retest reliability of the CSV-1000 contrast test and its relationship to glaucoma therapy. Invest Ophthalmol Vis Sci 35:3357–3361.

Queirós A, Lopes-Ferreira D, González-Méijome JM (2016) Astigmatic peripheral defocus with different contact lenses: review and meta-analysis. Curr Eye Res Feb 2:1–11.

Quevedo L, Pérez A, Cardona G, Fornieles A, Rodríguez Vallejo M (2012) Diferencias de género en agudeza visual dinánima. Gac Optom y Óptica Oftálmica 38–45.

Radhakrishnan H, Allen PM, Calver RI, Theagarayan B, Price H, Rae S, Sailoganathan A, O'Leary DJ (2013) Peripheral refractive changes associated with myopia progression. Investig Ophthalmol Vis Sci 54:1573–1581.

Rae SM, Price HC (2009) The effect of soft contact lens wear and time from blink on wavefront aberration measurement variation. Clin Exp Optom 92:274–82.

Rajagopalan AS, Bennet ES, Lakshminarayanan V (2006) Visual performance of subjects wearing presbyopic contact lenses. Optom Vis Sci 83:611–615.

Remón L (2012) Diseño, fabricación y control de lentes intraoculares multifocales. Tesis Doctoral. Universitat Politècnica de València.

Remón L, Benlloch J, Rodríguez-Vallejo M, Monsoriu JA, Furlan WD (2012) Reliability and repeatability of intraocular lenses optical characterization by the Kaleo system. In: European Academy of Optometrists Congress.

Remón L, Rodríguez-Vallejo M, Benlloch J, Pons A, Monsoriu JA, Furlan WD (2014) Lente de contacto fractal para el control de la progresión de la miopía. In: XIII Congreso Internacional de Optometría, Contactología y Óptica Oftálmica. Madrid.

Rempt F, Hoogerheide J, Hoogenboom WP (1971) Peripheral retinoscopy and the skiagram. Ophthalmologica 162:1–10.

Rice ML, Leske D a, Holmes JM (2004) Comparison of the amblyopia treatment study HOTV and electronic-early treatment of diabetic retinopathy study visual acuity protocols in children aged 5 to 12 years. Am J Ophthalmol 137:278–82.

Rodríguez-Vallejo M (2015) Comment on: "The Eye Phone Study: reliability and accuracy of assessing Snellen visual acuity using smartphone technology." Eye 29:1627.

Rodríguez-Vallejo M (2016) Comment on: "Effectiveness of a smartphone application for testing near-visual acuity." Eye 30:898–899.

Rodríguez-Vallejo M (2014a) Caracterización bidimensional del error refractivo periférico. In: Gené A, Bueno-Gimeno I, Sañudo F (eds) Temas actuales en Optometría. Ediciones MC. Montserrat Cruz, pp 319–322.

Rodríguez-Vallejo M (2009a) Software libre en terapia visual "Los picapiedra sobre ruedas", un videojuego de entrenamiento y evaluación de la motilidad ocular. Ver y Oir 26:12–17.

Rodríguez-Vallejo M (2009b) Influencia de las aberraciones de alto orden en el rendimiento visual con lentes de contacto. Ver y Oir 233:82–90.

Rodríguez-Vallejo M (2014b) ClinicCSF. Contrast sensitivity test for tablets. http://www.test-eye.com. Accessed 2 Oct 2016.

Rodríguez-Vallejo M, Benlloch J, Monsoriu JA, Furlan WD (2013a)

Medición psicofísica de la función visual en Screening sanitario con iPad 3ª generación. In: V Congreso Español de Metrología.

Rodríguez-Vallejo M, Benlloch J, Pons A, Monsoriu JA, Furlan WD (2014a) The effect of Fractal Contact Lenses on peripheral refraction in myopic model eyes. Curr Eye Res 39:1151–60.

Rodríguez-Vallejo M, Benlloch J, Remón L, Pons A, Furlán W, Monsoriu JA (2013b) Validación de métodos de medida de la curva de sensibilidad al contraste con la aplicación ClinicCSF para iPad. In: Gené A, Bueno-Gimeno I, Sañudo F (eds) Temas actuales en Optometría. Ediciones MC. Montserrat Cruz, pp 145–151

Rodríguez-Vallejo M, Bernabeu Juárez A, García Pérez S, Leal Pino L (2010a) Evaluación de los movimientos oculares sacádicos mediante un videojuego de entrenamiento de la motilidad ocular: "Los Picapiedra sobre ruedas." Gac. Optom. y Óptica Oftálmica; pp 28-32.

Rodríguez-Vallejo M, Cuevas V, Furlan W, Pons A, Monsoriu JA (2014b) Screening visual con iPad. In: XXIII Congreso Internacional Optometría, Contactología y Óptica Oftálmica.

Rodríguez-Vallejo M, Neydenova K, Monsoriu JA, Ferrando V, Furlan WD (2016a) Two-dimensional relative peripheral refractive error induced by Fractal Contact Lenses for myopia control. arXiv:1609.06987 [physics.med-ph].

Rodríguez-Vallejo M, Jiménez Jiménez R (2010) Influencia de la agudeza visual en el tiempo de reacción. Evaluación en árbitros de fútbol mediante el software "Visual Sport Performance." In: XXI Congreso Internacional de Optometría, Contactología y Óptica Oftálmica.

Rodríguez-Vallejo M, Llorens-Quintana C, Furlan WD, Monsoriu JA (2016b) Visual acuity and contrast sensitivity screening with a new iPad application. Displays 44:15–20.

Rodríguez-Vallejo M, Llorens-Quintana C, Juan A, Furlan WD (2016c) Design, characterization and visual performance of a new Multifocal Contact Lens. arXiv:1609.06712 [physics.med-ph].

Rodríguez-Vallejo M, Llorens-Quintana C, Monsoriu JA, Furlan W (2016d) Reproducibilidad de pantallas iPad retina en la evaluación de la

sensibilidad al contraste. In: XXIV Congreso Internacional de Optometría, Contactología y Óptica Oftálmica.

Rodríguez-Vallejo M, Llorens-Quintana C, Monsoriu JA, Furlan W (2016e) Diseño, caracterización y rendimiento visual con nuevos diseños de lentes de contacto multifocales. In: XXIV Congreso Internacional de Optometría, Contactología y Óptica Oftálmica.

Rodríguez-Vallejo M, Llorens-Quintana C, Montagud D, Furlan WD, Monsoriu JA (2016f) Fast and reliable stereopsis measurement at multiple distances with iPad. arXiv:1609.06669 [cs.CV].

Rodríguez-Vallejo M, Martínez Verdú FM (2008) Habililidades visuales en el árbitro asistente de fútbol. Ver y oir 25:208–214.

Rodríguez-Vallejo M, Monsoriu JA, Furlan WD (2016g) Inter-display Reproducibility of Contrast Sensitivity Measurement with iPad. Optom Vis Sci Aug 24:[Epub ahead of print].

Rodríguez-Vallejo M, Montalban R, Jiménez Jiménez R (2010b) trabajo: Evaluación de la curva de sensibilidad al contraste espacial acromática mediante el software "Clinic CSFs." In: XXI Congreso Internacional de Optometría, Contactología y Óptica Oftálmica.

Rodríguez-Vallejo M, Remón L, Monsoriu JA, Furlan WD (2015) Designing a new test for contrast sensitivity function measurement with iPad. J Optom 8:101–108.

Rojo P, Royo S, Caum J, Ramírez J, Madariaga I (2015) Generalized ray tracing method for the calculation of the peripheral refraction induced by an ophthalmic lens. Opt Eng 54:25106–25113.

Rosén R, Jaeken B, Lindskoog Petterson A, Artal P, Unsbo P, Lundström L (2012a) Evaluating the peripheral optical effect of multifocal contact lenses. Ophthalmic Physiol Opt 32:527–34.

Rosén R, Lundström L, Unsbo P (2012b) Sign-dependent sensitivity to peripheral defocus for myopes due to aberrations. Inves Opthal Vis Sci 53:7176–82.

Ross J, Clarke D, Bron A (1985) Effect of age on contrast sensitivity function: uniocular and binocular findings. Br J Ophthalmol 69:51–56.

Rucker JC, Sheliga BM, FitzGibbon EJ, Miles FA, Phil D, Leigh RJ (2006) Contrast sensitivity, first-order motion and initial ocular following in demyelinating optic neuropathy. J Neurol 253:1203–1209.

Rutstein RP, Corliss DA (2000) Distance stereopsis as a screening device. Optom Vis Sci 77:135–9.

Rutstein RP, Fullard RJ, Wilson JA, Gordon A (2015) Aniseikonia induced by cataract surgery and its effect on binocular vision. Optom Vis Sci 92:201–207.

Saavedra G, Furlan W, Monsoriu JA (2003) Fractal zone plates. Opt Lett 28:971–3.

Saladin JJ (2005) Stereopsis from a performance perspective. Optom Vis Sci 82:186–205.

Salvestrini P, Rodríguez-Vallejo M, Martínez J, Hueso E, Fernández J (2016) Método automatizado de medida de curvas de desenfoque de agudeza visual y sensibilidad al contraste con iPad. In: XXIV Congreso Internacinonal de Optometría, Contactología y Óptica Oftálmica.

Sankaridurg P, Donovan L, Varnas S, Ho A, Chen X, Martinez A, Fisher S, Lin Z, Smith EL, Ge J, Holden B (2010) Spectacle lenses designed to reduce progression of myopia: 12-month results. Optom Vis Sci 87:631–41.

Sankaridurg P, Holden B, Smith EL, Naduvilath T, Chen X, de la Jara PL, Martinez A, Kwan J, Ho A, Frick K, Ge J (2011) Decrease in rate of myopia progression with a contact lens designed to reduce relative peripheral hyperopia: one-year results. Invest Ophthalmol Vis Sci 52:9362–7.

Santodomingo J, Morgan P (2014) Lentes de contacto adaptadas en España en 2013: comparación con otros países. Gac. Optom. y Óptica Oftálmica 489:1–9.

Santodomingo-Rubido J, Villa-Collar C, Gilmartin B, Gutiérrez-Ortega R (2012) Myopia control with orthokeratology contact lenses in Spain: refractive and biometric changes. Invest Ophthalmol Vis Sci 53:5060–5.

Schwiegerling JT (1995) Chapter 2: The design and development of

schematic eye models. In: Visual performance prediction using schematic eye models. Ph.D. Thesis. p 17.

Seidemann A, Schaeffel F, Guirao A, Lopez-gil N, Artal P, Photorefractor A (2002) Peripheral refractive errors in myopic , emmetropic , and hyperopic young subjects. J Opt Soc Am A 19:2363–2373.

Shah N, Laidlaw DA, Rashid S, Hysi P (2012) Validation of printed and computerised crowded Kay picture logMAR tests against gold standard ETDRS acuity test chart measurements in adult and amblyopic paediatric subjects. Eye 26:593–600.

Sheppard AL, Davies LN (2010) Clinical evaluation of the Grand Seiko Auto Ref/Keratometer WAM-5500. Ophthal Physiol Opt 30:143–51.

Simons K (1981) A comparison of the Frisby, Random-Dot E, TNO, and Randot circles stereotests in screening and office use. Arch Ophthalmol 99:446–52.

Situ P, Toit R du, Fonn D, Simpson T (2003) Successful monovision contact lens wearers refitted with bifocal contact lenses. Eye Contact Lens 29:181–184.

Smith EL (2013) Optical treatment strategies to slow myopia progression: Effects of the visual extent of the optical treatment zone. Exp Eye Res 114:77–88.

Smith EL (2012) The Charles F. Prentice award lecture 2010: A case for peripheral optical treatment strategies for myopia. Optom Vis Sci 88:1029–1044.

Smith EL, Kee C, Ramamirtham R, Qiao-Grider Y, Hung LF (2005) Peripheral vision can influence eye growth and refractive development in infant monkeys. Invest Ophthalmol Vis Sci 46:3965–3972.

Sokol S, Moskowitz A, Skarf B, Evans R, Molitch M, Senior B (1985) Contrast sensitivity in diabetics with and without background retinopathy. Arch Ophthalmol 103:51–54.

Statistics Netherlands [CBS] (2013) More than 6 in 10 people wear glasses or contact lenses. In: Web Mag. http://www.cbs.nl/en-GB/menu/themas/gezondheid-welzijn/publicaties/artikelen/archief/2013/2013-3849-wm.htm.

Accessed 28 Sep 2016.

StereoOptical Co. Inc. (2014) Optec functional vision analyzer. http://www.stereooptical.com/. Accessed 5 May 2014.

Stewart CE, Hussey A, Davies N, Moseley MJ (2006) Comparison of logMAR ETDRS chart and a new computerised staircased procedure for assessment of the visual acuity of children. Ophthal Physiol Opt 26:597–601.

Suryakumar R, Allison RS (2015) Accommodation and pupil responses to random-dot stereograms. J Optom 9:40–6.

Tabernero J, Schaeffel F (2009) Fast scanning photoretinoscope for measuring peripheral refraction as a function of accommodation. J Opt Soc Am A Opt Image Sci Vis 26:2206–10.

Tabernero J, Vazquez D, Seidemann A, Uttenweiler D, Schaeffel F (2009) Effects of myopic spectacle correction and radial refractive gradient spectacles on peripheral refraction. Vis Res 49:2176–86.

Tahir HJ, Murray IJ, Parry NR, Aslam TM (2014) Optimisation and assessment of three modern touch screen tablet computers for clinical vision testing. PLoS One 9:e95074.

Tarutta E, Chua W-H, Young T, Goldschmidt E, Saw S-M, Rose KA, Smith EL, Mutti DO, Ashby R, Stone RA, Wildsoet C, Howland HC, Fischer AJ, Stell WK, Reichenbach A, Frost M, Gentle A, Zhu X, Summers-Rada J, Barathi V, Jiang L, McFadden S, Guggenheim JA, Hammond C, Schippert R, To C-H, Gwiazda J, Marcos S, Collins M, Charman WN, Artal P, Tabernero J, Atchison DA, Troilo D, Norton TT, Wallman J (2011) Myopia: Why study the mechanisms of myopia? Novel approaches to risk factors signalling eye growth- How could basic biology be translated into clinical insights? Where are genetic and proteomic approaches leading? How does visual function contribute to an. Optom Vis Sci 88:404–447.

Thibos LN, Bradley A, Liu T, López-Gil N (2013) Spherical aberration and the sign of defocus. Optom Vis Sci 90:1284–91.

Thibos LN, Wheeler W, Horner D (1997) Power vectors: an application of Fourier analysis to the description and statistical analysis of refractive

error. Optom Vis Sci 74:367–75.

Ticak A, Walline JJ (2013) Peripheral optics with bifocal soft and corneal reshaping contact lenses. Optom Vis Sci 90:3–8.

Tilia D, Bakaraju RC, Chung J, Sha J, Delaney S, Munro A, Thomas V, Ehrmann K, Holden BA (2016) Short-term visual performance of novel extended depth-of-focus contact lenses. Optom Vis Sci 93:1–10.

To L, Woods RL, Goldstein RB, Peli E (2013) Psychophysical contrast calibration. Vision Res 90:15–24.

To L, Woods RL, Peli E (2009) 17.3: Visual calibration of displays for accurate contrast reproduction. SID Symp Dig Tech Pap 40:216–219.

Tong L, Saw SM, Tan D, Chia KS, Chan WY, Carkeet A, Chua WH, Hong CY (2002) Sensitivity and specificity of visual acuity screening for refractive errors in school children. Optom Vis Sci 79:650–657.

Toshida H, Takahashi K, Sado K, Kanai A, Murakami A (2008) Bifocal contact lenses: history, types, characteristics, and actual state and problems. Clin Ophthalmol 2:869–77.

Tranoudis I, Efron N (2004) Parameter stability of soft contact lenses made from different materials. Cont Lens Anterior Eye 27:115–31.

Troilo D, Gottlieb MD, Wallman J (1987) Visual deprivation causes myopia in chicks with optic nerve section. Curr Eye Res 6:993–9.

Turnbull PR, Munro OJ, Phillips JR (2016) Contact lens methods for clinical myopia control. Optom Vis Sci 93:1–7.

Tyler CW (1997) Colour bit-stealing to enhance the luminance resolution of digital displays on a single pixel basis. Spat Vis 10:369–377.

UNE-EN ISO 18369-2 (2013) Óptica oftálmica. Lentes de contacto. Parte 2: Tolerancias. (ISO 18369-2:2012).

van Doorn LL, Evans BJ, Edgar DF, Fortuin MF (2014) Manufacturer changes lead to clinically important differences between two editions of the TNO stereotest. Ophthal Physiol Opt 34:243–9.

Varón C, Gil MA, Alba-Bueno F, Cardona G, Vega F, Millán MS, Buil JA (2014) Stereo-Acuity in patients implanted with multifocal intraocular

lenses: Is the choice of stereotest relevant? Curr Eye Res 39:711–719.

Vasudevan B, Flores M, Gaib S (2014) Objective and subjective visual performance of multifocal contact lenses: pilot study. Cont Lens Anterior Eye 37:168–74.

VectorVision (2014a) CSV-1000. http://www.vectorvision.com. Accessed 5 May 2014.

VectorVision (2014b) Contrast Sensitivity Values for the CSV-1000E in Log Units. http://www.vectorvision.com/. Accessed 5 May 2014.

Vitale S, Ellwein L, Cotch MF, Ferris FL, Sperduto R (2014) Prevalence of refractive error in the United States. Epidemiology 126:1999–2004.

Wagner S, Conrad F, Bakaraju RC, Fedtke C, Ehrmann K, Holden BA (2014) Power profiles of single vision and multifocal soft contact lenses. Cont Lens Anterior Eye 38:2–14.

Walline JJ (2016) Myopia control: A review. Eye Contact Lens 42:3–8.

Walline JJ, Greiner KL, McVey ME, Jones-Jordan LA (2013) Multifocal contact lens myopia control. Optom Vis Sci 90:1207–14.

Wallman J, Gottlieb MD, Rajaram V, Fugate-Wentzek LA (1987) Local retinal regions control local eye growth and myopia. Science 237:73–7.

Wallman J, Winawer J (2004) Homeostasis of eye growth and the question of myopia. Neuron 43:447–68.

Wang J, Hatt SR, O'Connor AR, Drover JR, Adams R, Birch EE, Holmes JM (2010) The final version of the distance Randot Stereotest: normative data, reliability, and validity. J AAPOS 14:142–146.

Wang J, Jiao S, Ruggeri M, Shousha MA, Shousha MA, Chen Q (2009) In situ visualization of tears on contact lens using ultra high resolution optical coherence tomography. Eye Contact Lens 35:44–9.

Wang YZ, Thibos LN, Lopez N, Salmon T, Bradley A (1996) Subjective refraction of the peripheral field using contrast detection acuity. J Am Optom Assoc 67:584–9.

Watson AB, Yellott JI (2012) A unified formula for light-adapted pupil size. J Vis 12:1–16.

Westheimer G (2013) Clinical evaluation of stereopsis. Vis Res 90:38–42.

Whatham A, Zimmermann F, Lazon P, Jara D (2009) Influence of accommodation on off-axis refractive errors in myopic eyes. J Vis 9:1–13.

Wolffsohn JS, Calossi A, Cho P, Gifford K, Jones L, Li M, Lipener C, Logan NS, Malet F, Matos S, Meijome JMG, Nichols JJ, Orr JB, Santodomingo-Rubido J, Schaefer T, Thite N, van der Worp E, Zvirgzdina M (2016) Global trends in myopia management attitudes and strategies in clinical practice. Cont Lens Anterior Eye 39:106–116.

Wolffsohn JS, Jinabhai AN, Kingsnorth A, Sheppard AL, Naroo SA, Shah S, Buckhurst P, Hall LA, Young G (2013) Exploring the optimum step size for defocus curves. J Cataract Refract Surg 39:873–80.

Woods RL, Tregear SJ, Mitchell RA (1998) Screening for ophthalmic disease in older subjects using visual acuity and contrast sensitivity. Ophthalmology 105:2318–2326.

Yamaguchi T, Ohnuma K, Konomi K, Satake Y, Shimazaki J, Negishi K (2013) Peripheral optical quality and myopia progression in children. Graefes Arch Clin Exp Ophthalmol 19770614.

Young G, Schnider C, Hunt C, Efron S (2010) Corneal topography and soft contact lens fit. Optom Vis Sci 87:358–366.

Zemax R (2013) Zemax 13. Optical Design Program. Surface Types. 345–346.

Zhang Z-T, Zhang S-C, Huang X-G, Liang L-Y (2013) A pilot trial of the iPad tablet computer as a portable device for visual acuity testing. J Telemed Telecare 19:55–9.

Zhao LQ, Zhu H (2011) Contrast sensitivity after zyoptix tissue saving LASIK and standard LASIK for myopia with 6-month followup. J Ophthalmol 2011:839371.

Zheleznyak L, Barbot A, Ghosh A, Yoon G (2016) Optical and neural resolution in peripheral vision. J Vis 16:1–11.

Zhou Y, Huang C, Xu P, Tao L, Qiu Z, Li X, Lu Z-L (2006) Perceptual learning improves contrast sensitivity and visual acuity in adults with anisometropic amblyopia. Vis Res 46:739–50.